

AD-A111 650

OHIO STATE UNIV RESEARCH FOUNDATION COLUMBUS

F/G 12/1

PREDICTING THE TRANSVERSE CONDUCTIVITY OF UNIDIRECTIONAL AND BI--ETC(U)

MAR 81 R H ZIMMERMAN

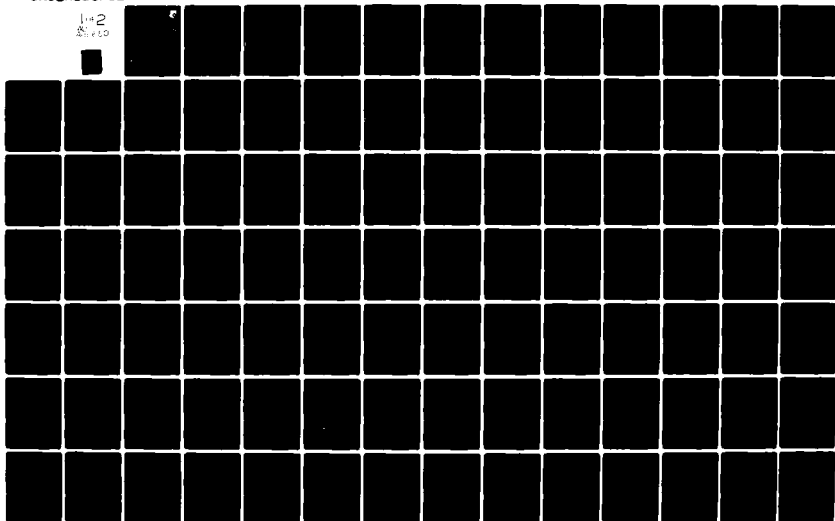
APOSR-78-3640

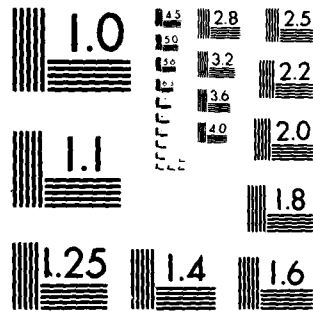
UNCLASSIFIED

AFWAL-TR-80-3155

NL

1-2  
2-10



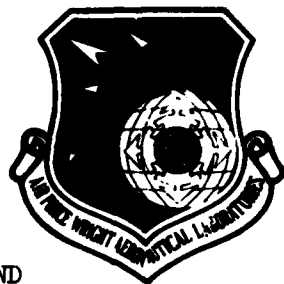


MICROCOPY RESOLUTION TEST CHART  
NATIONAL BUREAU OF STANDARDS 1963-A

ADA111650

LEVEL

2



AFWAL-TR-80-3155

PREDICTING THE TRANSVERSE CONDUCTIVITY OF UNIDIRECTIONAL AND  
BIDIRECTIONAL FILAMENTARY COMPOSITES

The Ohio State University  
Research Foundation  
1314 Kinnear Road  
Columbus, Ohio 43212

October 20, 1980

TECHNICAL REPORT AFWAL-TR-80-3155

Interim Report for Period June 10, 1978 - September 10, 1980

Approved for public release;  
distribution unlimited.

DTIC  
SELECTED  
MAR 4 1982  
H

ONE FILE COPY

FLIGHT DYNAMICS LABORATORY  
AIR FORCE WRIGHT AERONAUTICAL LABORATORIES  
AIR FORCE SYSTEMS COMMAND  
WRIGHT-PATTERSON AIR FORCE BASE, OHIO 45433

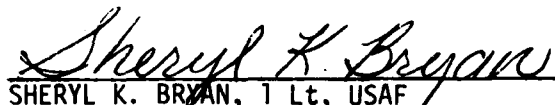
82 03 124

# NOTICE

When Government drawings, specifications, or other data are used for any purpose other than in connection with a definitely related Government procurement operation, the United States Government thereby incurs no responsibility nor any obligation whatsoever; and the fact that the government may have formulated, furnished, or in any way supplied the said drawings, specifications, or other data, is not to be regarded by implication or otherwise as in any manner licensing the holder or any other person or corporation, or conveying any rights or permission to manufacture use, or sell any patented invention that may in any way be related thereto.

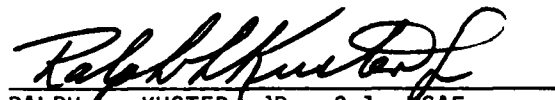
This report has been reviewed by the Office of Public Affairs (ASD/PA) and is releasable to the National Technical Information Service (NTIS). At NTIS, it will be available to the general public, including foreign nations.

This technical report has been reviewed and is approved for publication.

  
SHERYL K. BRYAN, 1 Lt, USAF  
Project Engineer  
Design & Analysis Methods Group

  
FREDERICK A. PICCHIONI, Lt Col, USAF  
Ch, Analysis & Optimization Branch

FOR THE COMMANDER

  
RALPH L. KUSTER, JR., Col, USAF  
Chief, Structures & Dynamics Div.

"If your address has changed, if you wish to be removed from our mailing list, or if the addressee is no longer employed by your organization please notify AFWAL/FIBR, W-PAFB, OH 45433 to help us maintain a current mailing list".

Copies of this report should not be returned unless return is required by security considerations, contractual obligations, or notice on a specific document.

REPORT DOCUMENTATION PAGE		READ INSTRUCTIONS BEFORE COMPLETING FORM
1. REPORT NUMBER AFWAL-TR-80-3155	2. GOVT ACCESSION NO.	3. RECIPIENT'S CATALOG NUMBER
4. TITLE (and Subtitle) PREDICTING THE TRANSVERSE CONDUCTIVITY OF UNIDIRECTIONAL AND BIDIRECTIONAL FILAMENTARY COMPOSITES		5. TYPE OF REPORT & PERIOD COVERED Interim 6/10/78 - 9/10/80
		6. PERFORMING ORG. REPORT NUMBER 761108/711129
7. AUTHOR(s)  Richard H. Zimmerman		8. <del>CONTRACT</del> OR GRANT NUMBER(s)  AFOSR 78-3640
9. PERFORMING ORGANIZATION NAME AND ADDRESS The Ohio State University 1314 Kinnear Road Research Foundation, Columbus, Ohio 43212		10. PROGRAM ELEMENT, PROJECT, TASK AREA & WORK UNIT NUMBERS Proj.No.2307 Task 2307N1 Work Unit 2307N112
11. CONTROLLING OFFICE NAME AND ADDRESS Department of the Air Force Air Force Office of Scientific Research Bolling Air Force Base, Washington D.C. 20332		12. REPORT DATE March 1981
14. MONITORING AGENCY NAME & ADDRESS (if different from Controlling Office) Flight Dynamics Laboratory (AFFDL/FBRA Air Force Wright Aeronautical Laboratories(AFSC) Wright-Patterson Air Force Base, Ohio 45433		13. NUMBER OF PAGES 178
		15. SECURITY CLASS. (of this report)  Unclassified
16. DISTRIBUTION STATEMENT (of this Report)    "Approved for public release; distribution unlimited."		15a. DECLASSIFICATION/DOWNGRADING SCHEDULE
17. DISTRIBUTION STATEMENT (of the abstract entered in Block 20, if different from Report)		
18. SUPPLEMENTARY NOTES		
19. KEY WORDS (Continue on reverse side if necessary and identify by block number) Unidirectional composites, Bidirectional composites, Two-phase conduction, Composite Material, One-Dimensional Conduction, Composites, Conductivity, Transverse Conductivity, Filamentary Composites, Conduction, Fiber-Matrix Systems, Models, Conduction Models, Rayleigh Equation		
20. ABSTRACT (Continue on reverse side if necessary and identify by block number) This Phase II report of the grant AFOSR 78-3640 presents studies of analytical models capable of predicting the transverse conductivity of unidirectional and bidirectional filamentary composites to an accuracy of several per cent. The models are based on adaptations of the Rayleigh solution and one-dimensional conduction analysis. Values of the conductivity defined by Han and Cosner (by numerical methods) and presented in the Phase I report of this grant study are used as the basis for judging the validity of the models. The adaptations can be used to predict, within several per cent, the transverse (continued) →		

Unclassified

SECURITY CLASSIFICATION OF THIS PAGE(When Data Entered)

Block 20 (Abstract) continued...

conductivity of a variety of types of fiber-matrix systems, while retaining the ability to isolate first-order effects of the principal variables in a relatively direct manner

SECURITY CLASSIFICATION OF THIS PAGE(When Data Entered)

## FOREWORD

The financial support of the U.S. Air Force Office of Scientific Research by a grant (AFOSR 78-3640) through The Ohio State University Research Foundation is acknowledged with appreciation. The grant study is administered under the direction of Mr. Nelson Wolf, AFFDL/FBRA Wright-Patterson Air Force Base.

Professor Lit S. Han, Mechanical Engineering, The Ohio State University, is the Supervisor of the grant study. His invitation to become involved in this research and his willingness always to support and encourage the work are gratefully acknowledged. Two students who contributed extensively to the work are William Boyee, Captain, U.S. Army Reserve, and Joseph Fletcher, 1st Lieutenant, U.S. Air Force.

Accession For	
NTIS GRA&I	<input checked="checked" type="checkbox"/>
DTIC TAB	<input type="checkbox"/>
Unannounced	<input type="checkbox"/>
Justification	<input type="checkbox"/>
By _____	
Distribution/	
Availability Codes	
A _____	
Dist _____	
A	

DTIC  
COPY  
INSPECTED  
2

# TABLE OF CONTENTS

<u>Section</u>	<u>Title</u>	<u>Page</u>
I	Introduction . . . . .	1
	Objective Of Phase II Study . . . . .	1
	Need for Simplified, Approximate Models . . . . .	2
	Key Dependency Upon Phase I Results . . . . .	3
	Perspective on the Transverse Conductivity of Filamentary Composites. . . . .	4
	Principal Variables and Idealizations . . . . .	4
	Tow and Matrix Conductivities . . . . .	7
	Bounds on Transverse Conductivity . . . . .	9
	Representative Levels of Longitudinal Bulk Conductivity. . . . .	13
II	Use of Modified Rayleigh Equations to Estimate the Transverse Conductivity of Unidirectional, Filamentary Composite Materials . . . . .	17
	The Rayleigh Equation . . . . .	18
	Adaptation to the Square Array . . . . .	19
	Hexagonal Array . . . . .	34
	Rectangular Array . . . . .	40
	Staggered Regular Array . . . . .	56
III	Use of One-Dimensional Conduction Models to Estimate the Transverse Conductivity of Unidirectional, Filamentary Composite Materials . . . . .	77
	Square Array . . . . .	77
	Rectangular Array . . . . .	91
	Staggered Regular Array . . . . .	95
IV	Adaptation of Conduction Models for Unidirectional Fibers to A Bidirectional Packing Geometry. . . . .	103
V	Conclusions. . . . .	113



## TABLE OF CONTENTS

<u>Appendices</u>	<u>Title</u>	<u>Page</u>
A	Use of Approximate Analysis of A Two-Phase Composite Material to Identify the Major Factors Influencing Its Transverse Conductivity. . . . .	117
B	Approximate Analysis of the Effects of Fiber Packing and Fiber Cross-Sectional Configuration on the Conductivity of A Tow-Matrix Series Path. . . .	139

# List of Illustrations

<u>Figure Number</u>	<u>Title</u>	<u>Page</u>
I-1	Influence of Tow Packing Density and Packing Geometry on the Bulk Conductivity of a Composite Material . . . . .	5
I-2	Impact of the Tow-to-Matrix Conductivity Ratio on the Bulk Conductivity of a Composite Material .	6
I-3	Representative Conductivities of Tow and Matrix Materials . . . . .	8
I-4	Spread between the Upper and Lower Bounds on the Transverse Conductivity for a Tow Volume Ratio $v_t$ of Two Thirds . . . . .	14
I-5	Representative Ranges on the Longitudinal Conductivity for Conventional Composite Materials. Unidirectional Tow . . . . .	15
II-1	Composite having Circular Fibers in a Square Array . . . . .	19
II-2	Validity of the Rayleigh Equation for Unidirectional Fibers Embedded in a Square Array. . . . .	23
II-3	Comparative Accuracy of the Rayleigh and the Modified Rayleigh Equations for a Square Array . .	27
II-4	Anisotropy of a Filamentary Composite having a Square Fiber Array . . . . .	31
II-5	Accuracy of Equation II-11 as a Direct Means of Estimating Effects of Tow Conductivity and Tow Volume Ratio on the Transverse-to-Longitudinal Conductivity Ratio . . . . .	33
II-6	The Hexagonal Packing Array. . . . .	34
II-7	Illustrating the Hexagonal Fiber Packing Geometry Yields a Lower Transverse Conductivity than a Square Array . . . . .	35
II-8	Comparison of the Accurate Values of the Transverse Conductivity for an Hexagonal Array . .	39

# List of Illustrations (Cont'd)

<u>Figure Number</u>	<u>Title</u>	<u>Page</u>
II-9	Comparative Results Obtained by Use of the Rayleigh Equations for the Hexagonal Array. . . .	41
II-10	Tow-Matrix System Having Constant-Diameter Filaments Embedded in a Rectangular Array . . . .	42
II-11	Interrelationship of Fiber Diagonal Angle and the Minimum Matrix Gap for the Han-Cosner Rectangular Array Data . . . . .	45
II-12	Influence of Fiber Diagonal Angle on the Transverse Conductivity of a Rectangular Array. .	54
II-13	Validity of the Semi-Empirical $C_9$ Equations for the Rectangular Array . . . . .	57
II-14	Influence of Tow Volume Ratio and Packing Angle on the Transverse Conductivity of Fibers Embedded in an In-Line Rectangular Array . . . .	58
II-15	Staggered Regular Array . . . . .	59
II-16	Influence of Fiber Diagonal Angle on the Transverse Conductivity of a Staggered Array. . .	60
II-17	Variation in the Fiber Spacing Ratios with the Fiber Diagonal Angle for the Staggered Regular Array . . . . .	62
II-18	Extent to which the Rayleigh Parameter $mv_t$ Correlates the Staggered Array Conductivity . . .	73
II-19	Correlation of Transverse Conductivity for the Staggered Array by Use of a Packing Parameter . .	74
III-1	Tow-Matrix System having Unidirectional Fibers Embedded in a Square Array. . . . .	78
III-2	Conceptual Validity of the One-Dimensional Model for Parallel, Circular Fibers Embedded in a Square Array . . . . .	81
III-3	Validity of One-Dimensional Conduction Analysis for Fibers Embedded in a Square Array . . . . .	83

# List of Illustrations

<u>Figure Number</u>	<u>Title</u>	<u>Page</u>
III-4	Agreement of Revised One-Dimensional Model for a Circular Fiber with the Han-Cosner Data . . .	86
III-5	Test of the Approximate Model . . . . .	92
III-6	Test of the Approximate Model Equation III-22 . . .	93
IV-1	A Bidirectional Packing Pattern Consisting of Alternating Orthogonal Rows of Filamentary Tow Embedded in a Matrix . . . . .	104
A-1.	Illustrating the Model in This Approximate Analysis to Indicate Principal Variables. Tow Embedded in Rectangular Array. . . . .	118
A-2.	Use of Approximate Model to Determine the Effect of Fiber Diagonal Angle on the Transverse Conductivity of Square Fibers in A Rectangular Array. . . . .	130
A-3	A Comparison of the Results by the Approximate Model with the Rayleigh-Maxwell Solution . . . . .	135
A-4	A Comparison of the Asymptotic Solutions ( $\bar{k} \gg 1$ ) for the Approximate Model with the Rayleigh-Maxwell Solutions for Spheres and Cylinders. . . . .	136
B-1	Schematic of Filamentary Composite Material, Consisting of Continuous Parallel Tow of Arbitrary Cross-Section Embedded in a Matrix. . .	140
B-2	Representative Conductivities for A Tow-Matrix Series Path Having Tow of Uniform Thickness. . . .	144
B-3	Wedge-Type Filamentary Tow. . . . .	145
B-4	Conductivities of the Tow-Matrix Series path for Various Wedge Configurations. . . . .	146
B-5	Illustrating the Influence of the Wedge Taper on the Tow-Matrix Series Conductivity for Equal Tow Volume Ratio $v'_t$ . . . . .	147

List of Illustrations (Cont'd)

<u>Figure Number</u>	<u>Title</u>	<u>Page</u>
B-6	Transverse Relative Conductivities of the Tow-Matrix Series Path for Circular, Octagonal and Rectangular Tow. . . . .	149
B-7	Representative Values of the Conductivity for A Tow-Matrix Series Path. Isotropic Tow. . .	154
B-8	Illustrating the Anisotropic Conductivity Characteristics of the Tow-Matrix Element. Ratio of the Series Tow-Matrix Conductivity to the Parallel Tow-Matrix Conductivity. . . . .	155

# List of Tables

<u>Table</u>	<u>Title</u>	<u>Page</u>
II-1	Han-Cosner Values of the Bulk Transverse Conductivity for a Tow-Matrix System having Circular Filaments Unidirectionally Embedded in a Square Array . . . . .	20
II-2	Deviation between the Han-Cosner Data and the Rayleigh Equation for the In-Line Transverse Conductivity of a Tow-Matrix System Consisting of Circular, Parallel Fibers Embedded in a Square Array. . . . .	24
II-3	The Ratio of the Asymptotic Transverse Conductivity Defined by the Modified Rayleigh Equations to the Corresponding Accurate Value. Square Array. . . . .	29
II-4	Han-Cosner Transverse Conductivities for a Tow-Matrix System having Circular Filaments Unidirectionally Embedded in an Hexagonal Array. . . . .	37
II-5	Geometrical Characteristics of the Rectangular Array Under the Conditions of Maximum Packing . . . . .	43
II-6	Han-Cosner Values of the Bulk Transverse Conductivity for a Tow-Matrix System Having Circular Filaments Unidirectionally Embedded in a Rectangular Array . . . . .	40
II-7	Han-Cosner Values of the Bulk Transverse Conductivity for a Tow-Matrix System Consisting of Circular Filaments Unidirectionally Embedded in a Staggered Array . . . . .	04
III-1	Comparison of Zinsmeister-Purohit Transverse Conductivity Data for Square Fibers in a Square Array with the Approximate Equation Based on One-Dimensional Analysis. . . . .	30
III-2	Ratio $k_{eq}/k_{H-C}$ for Model Equation (III-13). Circular Fiber in Square Array. . . . .	88
III-3	Ratio $k_{eq}/k_{H-C}$ for Model Equation (III-14). Circular Fiber in Square Array. . . . .	89

# List of Tables

<u>Table</u>	<u>Title</u>	<u>Page</u>
III-4	Ratio $k_{eq}/k_{H-C}$ for Model Equation (III-12) with $F_1$ by Equation (III-15) and $F_2 = 1.06$ . . . .	89
III-5	Ratio $k_{eq}/k_{H-C}$ for Model Equations (III-16) and (III-17) . . . . .	90
III-6	Accuracy of Equation (III-31) for the Hexagonal Array . . . . .	97
IV-1	Accurate Bulk Conductivities of a Filamentary Composite having Alternating Orthogonal Layers of Equally Spaced Circular, Isotropic Fibers. . . . .	105
IV-2	Same Tow-Matrix System as for Table IV-1, Except $y = 2x = 2z$ . . . . .	106

## SUMMARY

Using the transverse conductivity data for various idealized fiber-matrix systems developed by Han and Cosner [1] in Phase I of this grant study as the basis for judging validity, this Phase II study modifies and adapts several simplified analytical models --- ones which allow comparatively direct interpretation of the effects of key material properties --- such that they predict the transverse conductivity of uni- and bidirectional filamentary composites with reasonably good accuracy.

Both the two-dimensional Rayleigh solution and one-dimensional conduction analysis are used to form the functional framework of the models. In these models, the primary variables are organized in a rather simple, direct manner and are grouped in ways which enhance generalization of the results. Modifications of the models are introduced to produce working relationships which replicate the accurate Han-Cosner data (for a variety of fiber patterns) to within several per cent -- usually less. For the first time, therefore, because of the availability of extensive transverse conductivity data (the Phase I results), it is possible to rather comprehensively assess the ability of both the Rayleigh solution and one-dimensional conduction methods to predict the conductivity of filamentary composites.

The two-phase, two-dimensional Rayleigh solution shows remarkable capacity to be adapted to the accurate prediction of transverse conductivities, especially when modified on the basis of relative packing density. Modified Rayleigh equations for unidirectional fibers are also found to be applicable to models for bidirectional fiber systems.

Though one-dimensional conduction analysis has been used extensively over the years to estimate conduction in multi-phase materials and though it has been applied a number of times to composites, information allowing assessment of its ability to predict transverse conductivities has been --- with two limited exceptions --- rather sparse. The Phase I results of this grant study allowed comprehensive



testing of the validity of this approach. The one-dimensional models are found to be quite good. They provide a reasonable basis to estimate the conductivity of rather complex geometrical patterns. Again, the relative fiber packing density is found to be helpful in extending their usefulness. Though not more accurate than a modified Rayleigh equation, adjusted models based on one-dimensional conduction have an advantage in that there is greater potential for application when developing models for special fiber patterns, packing geometries and sectional configurations. This approach is also shown to work well for bidirectional fiber systems.

The overall results of this study suggest that models for most any idealized fiber-matrix assemblage could be organized functionally by adaptation of models for unidirectional fiber systems, and that these models should be capable of estimating transverse conductivities to within approximately ten per cent for conventional composites and to within roughly twenty per cent for a wide variety of tow (reinforcement) configurations.

## NOMENCLATURE

### Variable

a	Maximum width of tow element (perpendicular to direction of transverse conductivity); also a term in the parameter $(\bar{k}_t - a)/(\bar{k}_t + a)$
a'	Length of tow element (perpendicular to plane of width and depth dimensions)
A	Maximum depth of tow element (parallel to direction of transverse conductivity)
AR	Aspect ratio of bidirectional fiber system (ratio of width or length to depth)
c	Width spacing of tow element (center-to-center distance)
c'	Length spacing of tow-element (center-to-center distance)
C	Depth spacing of tow element (center-to-center distance); also an angle adjustment factor
D	Diameter
F	Adjustment Factor
I	Integer value
k	Bulk transverse conductivity
$\bar{k}$	Bulk transverse conductivity ratio $k/k_m$

$k_{lg}$	Bulk longitudinal conductivity
$\bar{k}_{lg}$	Bulk longitudinal conductivity ratio $k_{lg}/k_m$
$k_m$	Matrix conductivity (assumed to be isotropic)
$k_{m-t}$	Conductivity of series matrix-tow path
$k_t$	Tow (reinforcing element) conductivity in transverse direction
$\bar{k}_t$	Tow conductivity ratio (transverse) $k_t/k_m$
$k_{t-lg}$	Tow conductivity in longitudinal direction
$\bar{k}_{t-lg}$	Tow conductivity ratio $k_{t-lg}/k_m$ in longitudinal direction
$\ell$	Diagonal spacing ratio $D/L$
$L$	Diagonal spacing of tow element (center-to-center distance); also length spacing ratio of tow $a'/c'$
$m$	Tow transverse conductivity parameter $(\bar{k}_t - 1)/(\bar{k}_t + 1)$
$M$	Tow transverse conductivity parameter $[1 - (\bar{k}_t)^{-1}]$
$n$	Number of types or parameter in general or tow transverse conductivity parameter $(\bar{k}_t - 1)/(\bar{k}_t + 2)$
$P$	Tow conductivity parameter $(\bar{k}_t - 1)$
$q$	Conduction heat rate
$r$	Width aspect ratio of tow $a/A$

$r'$	Length aspect ratio of tow $a'/A$
$R$	Transverse aspect ratio of tow array $c/C$
$R'$	Longitudinal aspect ratio of array $c'/C$
$\bar{R}$	$R/r$
$\bar{R}'$	$R'/r$
$s$	Width spacing ratio of tow $a/c$
$S$	Depth spacing ratio of tow $A/C$
	Longitudinal spacing ratio $D/z$
$t$	Area taper ratio of tow (cross section)
$T$	Temperature or parameter
Theta ( $\theta$ )	Diagonal angle of tow elements (in transverse plane)
$v$	Volume fraction of any component
$v_t$	Volume fraction occupied by tow
$v_{\max}$	Maximum volume fraction
$\bar{v}$	Relative volume $v_t/v_{\max}$
$V$	Volume

$x, y, z$	Conduction path coordinates
$X$	Transverse resistance parameter $M_S (v_t/r \tan \theta)^{1/2}$ and normalized coordinate $2x/A$
$Y$	Bulk transverse conductivity parameter $(\bar{k} - 1)/M_S v_t$

<u>Subscript</u>	<u>Refers to</u>
e	Effective
l	Layer
lg	Longitudinal direction
m	Matrix
sq	Square array
S	Direction of depth spacing ratio
t	Tow
tr	Transverse direction

## SECTION I

### Introduction

This study is Phase II of the grant project "Heat Conduction in Composite Materials" sponsored by the U.S. Air Force Office of Scientific Research. Its dependent relationship to the completed Phase I of this grant study is explained subsequently in this Section.

#### Objective of Phase II Study

This study (Phase II) seeks to determine the ability of simplified analytical models to predict (to an accuracy of several per cent) the transverse conductivity of uni- and bidirectional fiber-matrix assemblages.

The use of simplified models to estimate the conductivities of multi-phase materials is, in no way, new. Many publications over the past roughly one hundred years dealing with the conductivity (and similar properties) of heterogeneous media have employed this approach. And, especially throughout the past two decades, this approach has been used to estimate bulk conductivities of a variety of types of filamentary composite materials, e.g. [3], [11], [12], [18], [23], [24].

The emphasis in this study centers on assessment of the ability of several particular models to predict bulk conductivities of unidirectional filamentary composites, to adapt and refine the usefulness of these methods through adjustments (and alteration), and, in instances, to develop models. Value is placed on working relationships which allow isolation of the first-order effects in a relatively uncomplicated manner, while retaining their ability to estimate conductivity to an accuracy of several per cent. With few exceptions, this study centers on the adaptation and elaboration of prior contributions in an effort to provide useful, direct means for assessing the influences of key design variables on the bulk conductivity of composite materials.

### Need for Simplified, Approximate Models

Analytical models for predicting the bulk transverse conductivity of composite materials --- which models are comparatively simple and direct in use, yet essentially valid in concept and accuracy --- are important for a variety of reasons.

In the preliminary design of systems employing composite materials and where heat conduction is a matter of importance, analytical models which highlight the functional interrelation of the principal design variables in comparatively direct ways, which stem from a reasonably sound physical model and which rely on secondary parameters (adjustment factors) to provide acceptable levels of precision ---- usually are valuable as working relationships (design equations). Such relationships expedite the investigative, preliminary design process by allowing the concept designer to observe directly first-order effects on the conductivity of composite materials as the conditions of the design investigation are varied. The criticality of various design regions can be assessed more readily. Time and other expenses involved in evaluating conduction processes can be reduced.

Analytical models, if valid in concept, organize the variables involved in a complex conduction process and show their orders of importance. Models can indicate approximate groupings of variables to generalize data, assist in estimating conductivities beyond the range of available information, and allow design of experiments which enhance the range of applicability of the test results. They simplify interpolation and extropalation of any set of conductivity data. Models allow specific estimates of the influences of various factors, e.g. fiber weave, fiber shape, packing configuration, and so forth. Models enable the designer to become better able to select designs which yield the type of conducting material desired ---- be it need for the composite to serve as a conductor, a semi-conductor or an insulator.

In short, comparatively simple, approximate models which estimate bulk transverse conductivities of composites at reasonable levels of accuracy facilitate both the understanding of the key variables



involved and the preliminary design process.

#### Key Dependency Upon Phase I Results

This study draws heavily upon a number of important prior results on conduction in heterogeneous materials --- those which relate, for example, to model concepts, to classical solutions, analog methods, numerical methods, bounds, effects of fiber geometry, and so forth. Prior contributions used extensively in this Phase II study are the classical two-dimensional Rayleigh solution, one-dimensional conduction analyses and those few literature sources providing accurate values of the bulk conductivity along with the corresponding component properties and geometrical properties of the fiber-matrix system. It is in the latter category that Phase I of this grant study serves almost exclusively as the source of accurate conductivity information.

In Phase I, Han and Cosner [1] determined (by numerical analysis) accurate values of the transverse conductivity for idealized models of filamentary composites having various types of unidirectional and bidirectional fiber packing geometries. For the first time, therefore, extensive data on conductivity --- for various idealized fiber-matrix assemblages and for a comprehensive range of values on both the fiber volume fraction and the fiber-to-matrix conductivity ratio --- became available. The analytical methods and both the scope and accuracy of the results highlight their studies.

Without both the qualitative consistency and quantitative breadth of the Phase I results, the Phase II study --- the subject of this report --- would have been far more limited, especially with respect to conclusions about the ability of simplified models to predict transverse conductivities at reasonable levels of accuracy. Prior to the completion of the Han-Cosner studies, the literature contained few conductivity data providing also the needed corresponding specifics about packing geometry, fiber shape, fiber content and component properties. Thus, without the Phase I results, both the Phase II testing of the validity of simplified models and the Phase II determination of the adjustments and alterations to the models necessary to render accurate results

would not have been possible.

#### Perspective on the Transverse Conductivity of Filamentary Composites

Usually, the bulk transverse conductivity of a wide variety of combinations of reinforcing material and matrix material (as used in composites) falls in the general numerical range of  $1/5$  to 5 times the matrix conductivity. The variables influencing the transverse conductivity are many; their influences can be appreciable. For example, typical effects of the packing density and packing configuration on the transverse conductivity of filamentary tow (fiber reinforcing elements) embedded in a continuous matrix are illustrated in Figure I-1. Here, for a tow (fiber) conductivity six (6) times that of the matrix conductivity (i.e. glass or ceramic fibers, for example, in a resinous matrix), the bulk transverse conductivity is seen to be fairly sensitive to the packing density and packing array angle of the fibers. The range on possible values of transverse conductivity is always bounded (discussed later in this Section), with the upper bound being the bulk conductivity when the matrix and tow components are in parallel paths and the lower bound being the conductivity when the same two components are in a series path.

The tow-to-matrix conductivity ratio  $k_t/k_m$  for the many types of composites (also reviewed later in this Section) has an extensive numerical range. Its impact on the bulk transverse conductivity is illustrated in Figure I-2. Large departures of the tow conductivity from that of the matrix magnify the influences of the geometrical features of the tow-matrix system (packing density, packing configuration, fiber shape) on the transverse conductivity.

#### Principal Variables and Idealizations

The principal variables affecting the transverse conductivity of filamentary composites are the volume fraction of the tow (the packing density), the void volume fraction, the conductivity of the tow in a particular direction, the conductivity of the matrix in a particular direction, the tow cross-sectional configuration and its packing

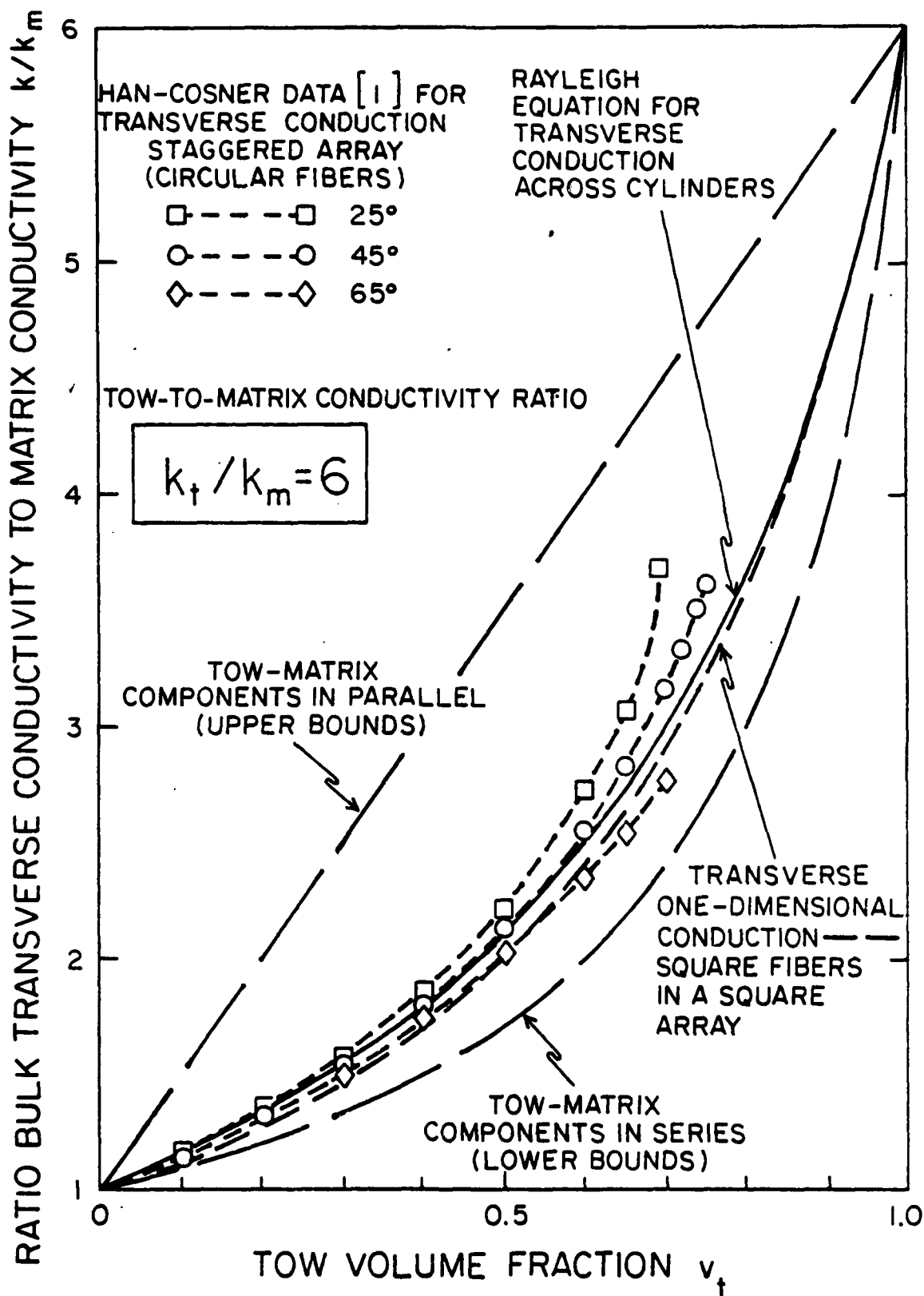


Figure I-1. Illustrating the Influence of Tow Packing Density and Packing Geometry on the Bulk Conductivity of A Composite Material. Isotropic Tow and Matrix.

- (a) Transverse one-dimensional conduction (circular fibers in a square array)
- (b) Rayleigh equation for unidirectional cylinders
- (c) Same as (a), except square fibers

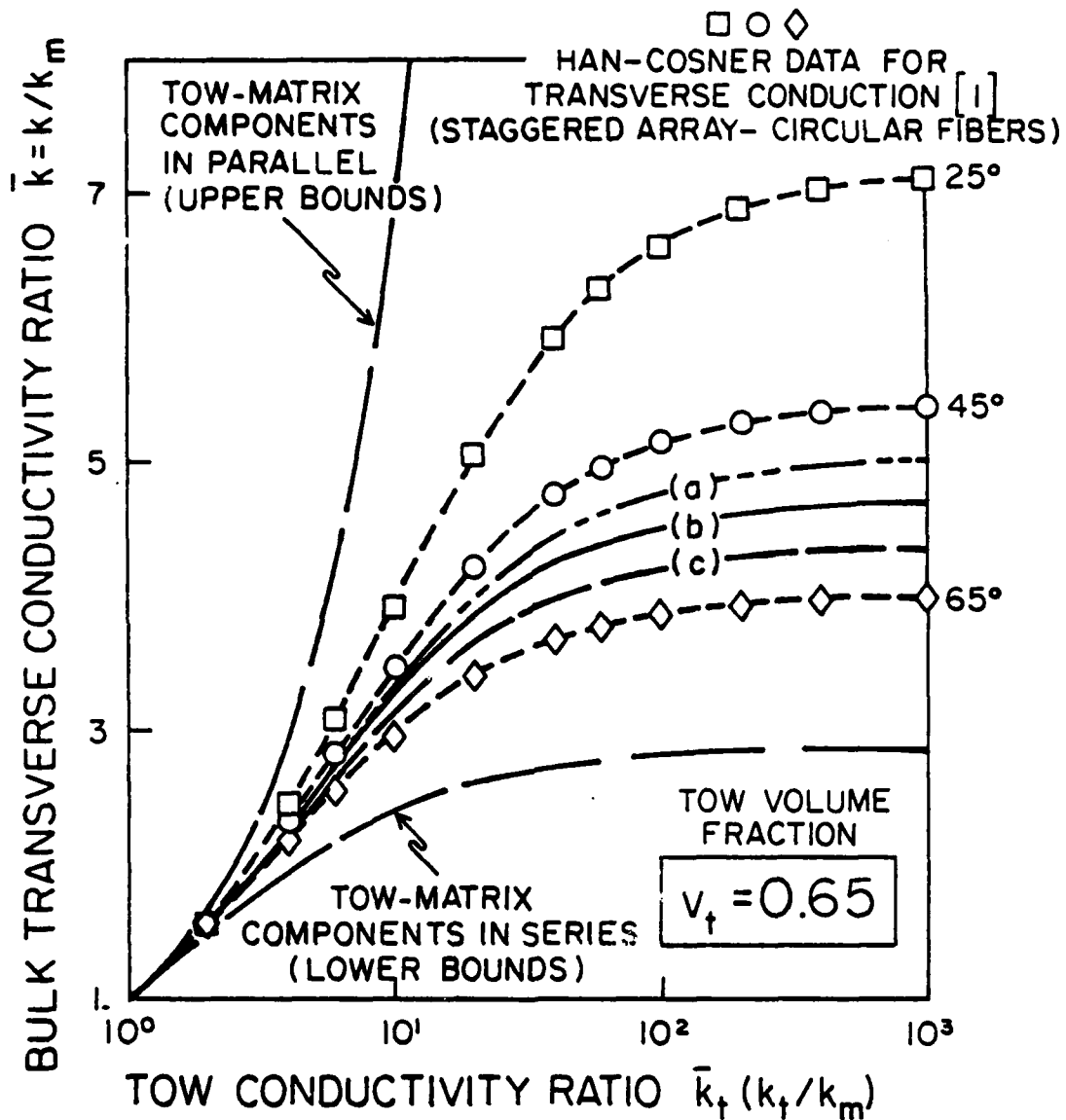


Figure I-2. Illustrating the Impact of the Tow-to-Matrix Conductivity Ratio on the Bulk Conductivity of A Composite Material. Isotropic Tow and Matrix.

orientation, the transverse array, the tow weave, heterogeneities in the component materials, interfacial resistances, organizational structure of a layer and a ply, and the number of types of both tow material and matrix material.

For the most part, this study (Phase II) considers conventional composites having a single type of reinforcing element (tow) embedded in a continuous matrix. The following idealizations are applied to the tow-matrix system. The tow is filamentary, continuous and unidirectional (the latter always, except for two bidirectional assemblages), homogeneous and orthotropic (or isotropic) --- organic, metallic or ceramic. The matrix is homogeneous and isotropic --- organic, metallic or ceramic. There are no imperfections such as voids, interfacial resistances and delaminations. The thickness of each layer (or ply) is large in comparison to the thickness of a single tow element.

#### Tow and Matrix Conductivities

Representative values of the tow and matrix conductivities (at normal temperatures and as summarized from an extensive review of the literature) are shown in Figure I-3. The thermal conductivity of the tow (reinforcing element) ranges from roughly 0.01 to 100 B/h·f·R (approximately 0.02 to 200 W/m·K). The lowest levels for tow materials are in the conductivity region of insulators, the mid-level values in the range of semi-conductors and the highest levels in range of conductors. Matrix materials have conductivities ranging from approximately 0.1 to 100 B/h·f·R. Thus, the tow-to-matrix conductivity ratio ( $\bar{k}_t = k_t/k_m$ ) for a two-phase system --- which parameter along with the volume fraction of the tow  $v_t$  are the premier factors in the determination of transverse conductivity --- has a potential range for these particular materials of approximately  $10^{-4}$  to  $10^3$ . The usual combinations of tow and matrix materials reduce the range on  $\bar{k}_t$  to roughly  $10^{-2}$  to  $10^3$ .

For resin matrices, typical values of the conductivity ratio  $\bar{k}_t$

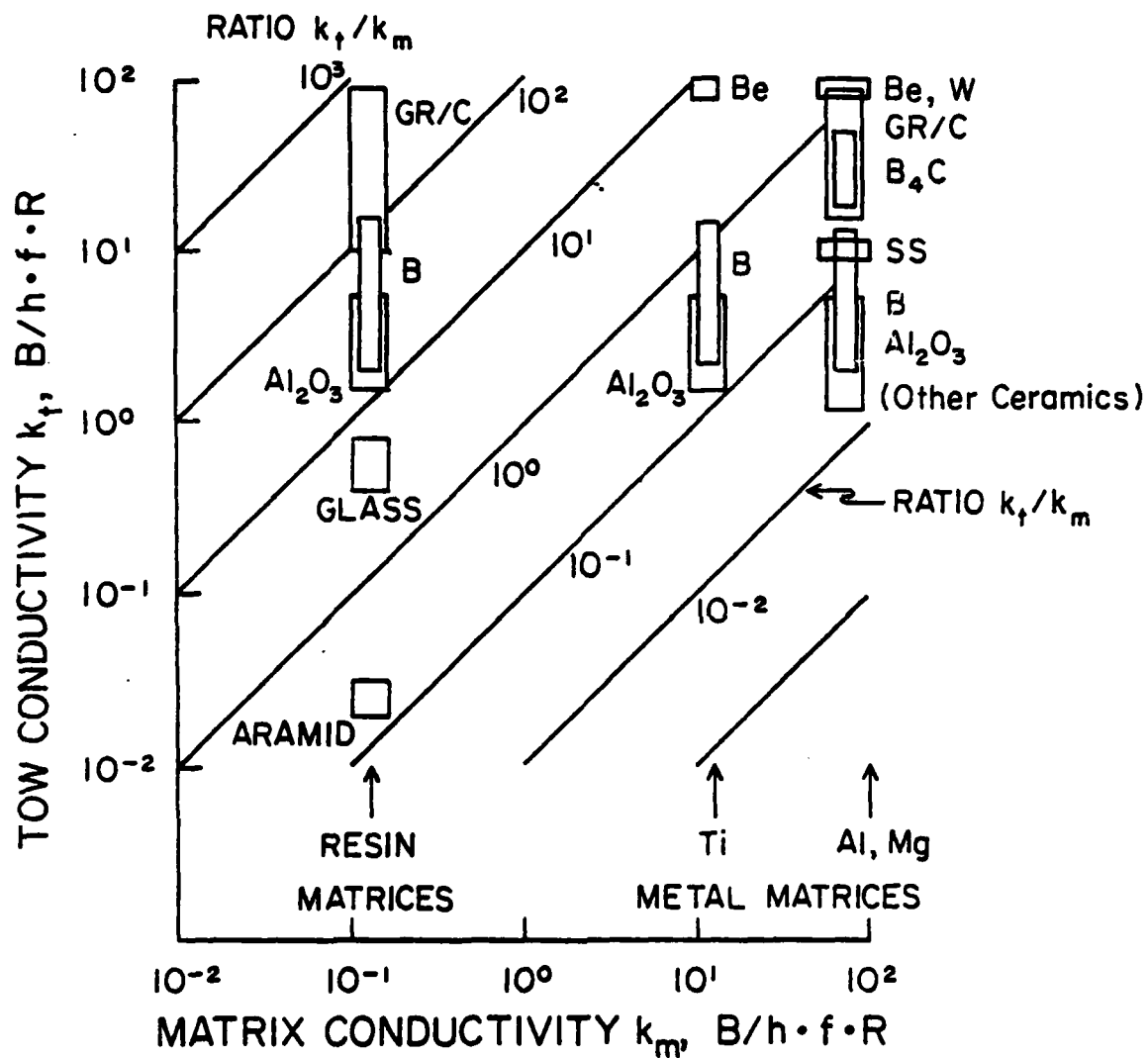


Figure I-3. Representative Conductivities of Tow and Matrix Materials. Temperature Range Approximately 0-200° F.

range from 1/5 for aramid tow elements to well over 500 for graphite tow (Figure I-3). Ceramic elements in a resin binder have values of the conductivity ratio  $\bar{k}_t$  generally in the range from 4-5 to 40-50. For metal matrices, the conductivity ratio  $\bar{k}_t$  ranges from approximately 0.01 to 10.

The conductivity ratio  $\bar{k}_t$  is a central factor in the prediction of transverse conductivities. Always, the bulk transverse conductivity has a value between the conductivities of the tow and matrix components, and, the extent to which the bulk transverse conductivity of a composite departs from the matrix conductivity is determined in large measure by the conductivity ratio of the components  $\bar{k}_t$ .

The conductivity ratio of the components  $\bar{k}_t$  expresses itself in the bulk conductivity relationships in three principal forms: (i)  $(\bar{k}_t-1)$ , (ii)  $(\bar{k}_t-1)/\bar{k}_t$  and (iii)  $(\bar{k}_t-1)/(\bar{k}_t+1)$ . Form (i) is associated with longitudinal conductivity relationship, i.e. when the tow and matrix components are in parallel;  $(\bar{k}_t-1)$  is an index to the extent to which the tow could shift the bulk longitudinal conductivity away from that of the matrix. Forms (ii) and (iii) express themselves when the tow and matrix components are in series. They index the extent to which the resistance of a tow-matrix series path is altered when a portion of the matrix is replaced with tow. As seen from the range of conductivities (Figure I-3), actual values of form (i) can range from approximately -1 to well over 500, form (ii) from roughly -50 to unity and form (iii) from about -1 to +1.

#### Bounds on Transverse Conductivity

Over the years, in the study of electrostatic, electromagnetic, mechanical and thermal properties of heterogeneous media, considerable attention has been given to definition of the maximum possible numerical range on the value of a property, once the value of that same property and its concentration are specified for each component in the multi-phase medium. In particular, many of these studies identify upper and lower bounds for the transverse conductivity of a filamentary composite material in terms of the volume fractions and

conductivities of both the binder (matrix) and the reinforcing component (tow). Given the latter constraints ( $v_t$ ,  $v_m$ ,  $k_t$  and  $k_m$ ), the range of possible values of transverse conductivity --- for all fiber shapes and for all fiber packing configurations --- is set by these bounds.

This subject of bounds on conductivity in composite materials has been researched extensively at advanced levels of analysis [2]. In all instances, it is shown that the spread between the bound levels for filament-reinforced materials can be appreciable --- that geometrical factors are especially important, except when the volumetric level of the reinforcing component ( $v_t$ ) is low. Thus, these studies (coupled with several studies reported in the literature which show specific influences of fiber shape and packing geometry), no doubt, contributed to highlighting the need for exact assessment of the transverse conductivity of various specific fiber packing arrays (such as completed by Han and Cosner [1] in Phase I of this grant project).

As is well known and set forth in the literature many times, the absolute upper and absolute lower bounds on the conductivity of a two-phase medium occur when the two components are organized to form a unidirectional laminate (layers of tow and matrix). Then, the longitudinal conductivity defines the absolute upper bounds (tow and matrix in parallel) and the transverse conductivity defines the absolute lower bounds (tow and matrix in series). These specific bounds (in terms of the ratio of the transverse conductivity  $k$  to the matrix conductivity  $k_m$ , i.e.  $\bar{k} = k/k_m$ ) are

$$(\bar{k})^+ = 1 + (\bar{k}_{t-lg} - 1) v_t \quad (I-1)$$

and

$$(\bar{k})^- = [1 - v_t + v_t / \bar{k}_{t-tr}]^{-1} = (1 - M_{tr} v_t)^{-1} \quad (I-2)$$

where  $\bar{k}_t$  is the ratio of the tow conductivity  $k_t$  in the particular direction to the matrix conductivity  $k_m$ . The spread as defined by these bounds is appreciable. For example, with  $\bar{k}_{t-lg} = \bar{k}_{t-tr} = 10$  and  $v_t = 0.5$ ,  $\bar{k}^+$  and  $\bar{k}^-$  are 5.5 and 1.8, respectively.

Hashin [3] has shown that for cylinders unidirectionally embedded in a matrix and randomly distributed, the upper and lower bounds on the transverse conductivity are constrained only by the cylinder volume



fraction  $v$  and the cylinder and matrix conductivities. These bounds (in rearranged form) are

$$(\bar{k})^+ = \bar{k}_t(1 + \bar{k}_t v') / (\bar{k}_t + v') \text{ where } v' = v_t / (2 - v_t) \quad (I-3)$$

$$(\bar{k})^- = (1 + m v_t) / (1 - m v_t) \text{ where } m = (\bar{k}_t - 1) / (\bar{k}_t + 1) \quad (I-4)$$

They provide an indication of the maximum spread in the transverse conductivity of filamentary composites (given  $v_t$  and  $\bar{k}_t$ ) which could result from all possible choices of both the cross-sectional configuration of the fibers and the geometrical pattern with which the fibers are embedded in the matrix. This spread also can be appreciable for filamentary composites. A tow-volume fraction  $v_t$  of  $2/3$  and a transverse tow-to-matrix conductivity ratio  $\bar{k}_t$  of 50 are not unusual. For this condition, equations (I-3) and (I-4) show that the transverse conductivity could range from roughly 5 to roughly 25 times the matrix conductivity, depending upon the geometrical patterns of the fiber shape and its array. With  $\bar{k}_t = 10$  and  $v_t = 0.5$ , for which the parallel and series path levels (the absolute bounds) are 5.5 and 1.8, the Hashin bounds are 4.2 and 2.4.

Nomura and Chou [4] have shown somewhat tighter bounds on a random transverse distribution of continuous, unidirectional fibers. Rearranging and adapting their relationships to the variable forms used in this study,

$$(\bar{k})^+ = \left\{ [1 + (\bar{k}_t - 1)v_t]^2 + \bar{k}_t \right\} / (1 + \bar{k}_t) \quad (I-5)$$

$$(\bar{k})^- = \bar{k}_t(1 + \bar{k}_t) / \left\{ [\bar{k}_t - v_t(\bar{k}_t - 1)]^2 + \bar{k}_t \right\}$$

For  $\bar{k}_t = 10$  and  $v_t = 0.5$ , the Nomura-Chou bounds are 3.7 and 2.7.

Several studies on bounds include effects of geometry and, thereby, shrink the bound spread. Beran and Silmutzer [6] applied the Beran and Miller methods [5] to specific filamentary composites (where geometrical parameters are included in addition to primary parameters  $v_t$  and  $\bar{k}_t$ ). Elsayed and McCoy [7] extended the latter study to include a greater number of geometrical factors. (Hale [8] presents an excellent summary of these studies). The closure in the Hashin bounds produced by the Beran-Silmutzer method is typically 20 to 35 per cent for circular fibers.

The Elsayed-McCoy methods appear to shrink the Beran-Silnutzer spread by another roughly 25 to 50 per cent. Thus, though the contraction can be significant, the residual spread usually remains appreciable. Further, the range in choice of the geometrical parameters used by the latter two methods is sufficient to result in uncertainty on the extent to which the Hashin bounds are contracted for particular fiber matrix systems.

Donea [9] applied variational principles to Hashin's methods to develop specific bounds for the transverse conductivity of filamentary composites when the fibers are circular in cross-section and when they are embedded (i) in a square array, (ii) in an hexagonal array and (iii) in a random array. These bounds (re-expressed here in terms of the maximum possible volume fraction) are

$$(\bar{k})^+ = v_{\max} \bar{k} + (1-v_{\max}) \quad (1-7)$$

$$(\bar{k})^- = \bar{k} / [v_{\max} + (1-v_{\max})\bar{k}] \quad (1-8)$$

where

$$\bar{k} = [1 + m(v_t/v_{\max})] / [1 - m(v_t/v_{\max})] \quad (1-9)$$

$$m = (\bar{k}_t - 1) / (\bar{k}_t + 1)$$

The maximum volume fraction  $v_{\max}$  for the square array is  $\pi/4$ ; for the hexagonal array, it is  $\pi/2(3)^{1/2} = 0.907$ . The Donea bounds for the random array are the same as the Hashin bounds, equations (I-3) and (I-4).

The Donea bound spread is greatest for the random array and least for the hexagonal array, since it can be shown that for a given tow volume ratio  $v_t$ , the minimum distance between fibers will be greatest for the hexagonal array, some less for the square array and can be least for a random array.

The bounds on the transverse conductivity for square fibers in a rectangular array has been shown by Elrod [9] to be (re-expressed into the parameter forms used in this study)

$$(\bar{k})^- = 1 - s + s (1 - MS)^{-1} \quad (I-10)$$

$$(\bar{k})^+ = [1 - S + S (1 + Ps)^{-1}]^{-1} \quad (I-11)$$

Where (with reference to Figure B-1)  $s$  and  $S$  are the width spacing ratio ( $a/c$ ) and depth spacing ratio ( $A/C$ ), respectively, and  $M$  and  $P$  are tow conductivity parameters,  $M = 1 - \bar{k}_t^{-1}$  and  $P = \bar{k}_t - 1$ .

Spreads in both the Hashin bounds and the Nomura-Chou bounds for a random transverse array, in the Donea bounds for the square and hexagonal arrays and in the Elrod bounds for square fibers in a square array are illustrated in Figure I-4 for unidirectional fiber systems having a fiber volume content  $v_t = 2/3$ . With circular fibers and a fiber conductivity 40 times the matrix conductivity ( $\bar{k}_t = 40$ ) and  $v_t = 2/3$ , the ratio of the upper to lower bounds is roughly 1.3, 2.3, 3.4 and 4.6 for the Donea bounds for the hexagonal array, for the Donea bounds for the square array, the Nomura-Chou bounds for the random array and the Hashin bounds for the random array, respectively. Thus, clearly, there is potential for the transverse conductivity of composite materials to be influenced appreciably by the geometrical features of the tow-matrix system, i.e. the sectional shape of the reinforcing elements, their orientation and their packing configuration.

#### Representative Levels of Longitudinal Bulk Conductivity

Although this study focuses on the transverse bulk conductivity of composites, the longitudinal bulk conductivity (tow and matrix components in parallel conduction paths) enters the study when considering both the anisotropy of composites and bidirectional fiber patterns.

For the idealized unidirectional, tow-matrix systems considered in this study (no imperfections --- as described earlier in this Section), the longitudinal bulk conductivity  $k_{lg}$  is defined by application of the

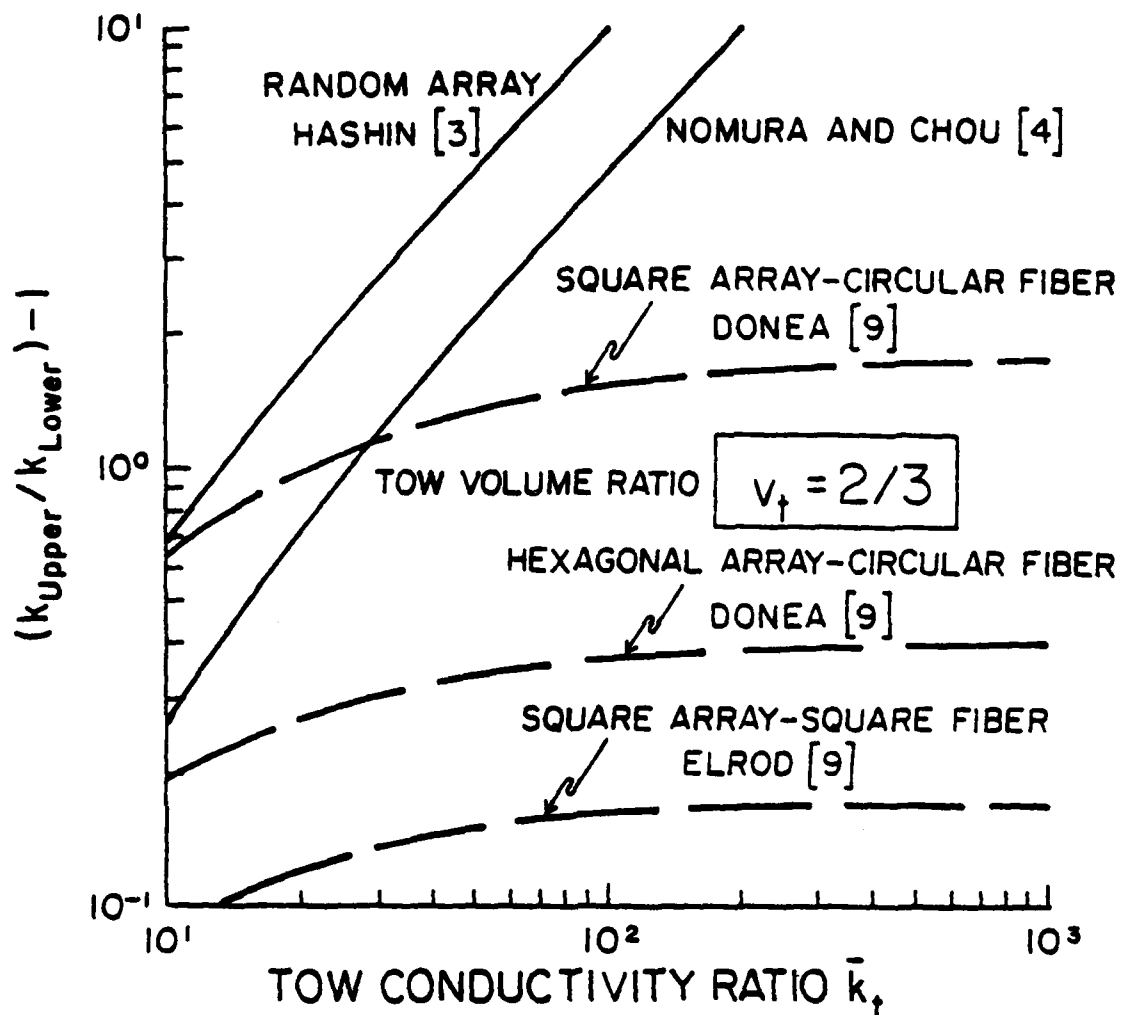


Figure I-4. Illustrating the Spread between the Upper and Lower Bounds on the Transverse Conductivity for a Tow Volume Ratio  $v_t$  of Two Thirds.

conduction equation to the tow and matrix components in parallel. This yields the familiar equation  $k_{lg} = v_m k_m + v_t k_{t-lg}$ , which here is expressed on a relative basis as

$$\bar{k}_{lg} = 1 + (\bar{k}_{t-lg} - 1)v_t \quad (I-12)$$

where  $\bar{k}_{lg} = k_{lg}/k_m$ ,  $\bar{k}_{t-lg} = k_{t-lg}/k_m$  and  $v_t$  is the volume fraction of the tow component.

Representative values of the longitudinal relative conductivity  $\bar{k}_{lg}$  (evaluated by equation I-12 using tow conductivity ranges taken from Figure I-3) are shown in Figure I-5 for a number of tow-matrix combinations. For the tow volume ratio  $v_t$  in the general range of 1/3 to 2/3 (i.e. the reinforcement volume being from one half to twice the volume of the matrix), the longitudinal conductivity of aramid tow in a resin base is approximately 1/2 to 3/4 of the matrix conductivity. In contrast, for graphite fibers in a resin matrix, the longitudinal conductivity can be well over 100 times that of the matrix. The tow, depending upon the type and amount, could shift the bulk conductivity, for example, from that of a near-insulator to that of a semi-conductor or even to that of a conductor.

The ratio of the longitudinal conduction in the reinforcing elements to the corresponding conduction in the matrix is  $k_t v_t / k_m v_m = \bar{k}_t (v_t / v_m)$ . For mid-range levels of tow content and for graphite or metal or ceramic tow in a resinous matrix (for which  $\bar{k}_t$  could range from roughly 10 to 700), the longitudinal conduction occurs almost entirely within the reinforcing elements. However, for inorganic tow elements embedded in metal matrices, the tow longitudinal conduction might be only one tenth to twice that in the matrix. Aramid tow embedded in a resin base at mid-range levels of tow content results in the tow longitudinal conduction being in the range of one tenth to two fifths of that in the matrix.

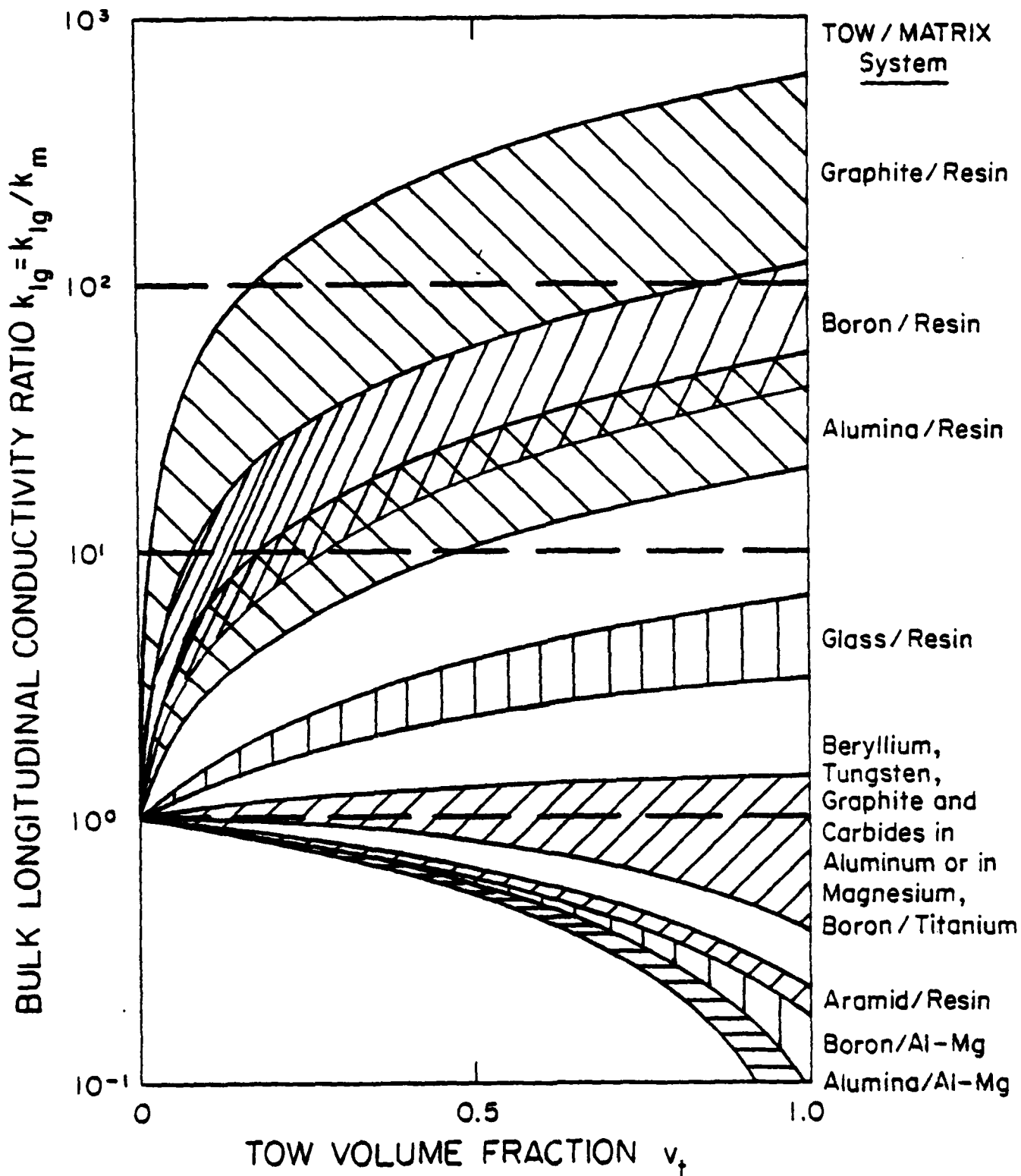


Figure I-5. Representative Ranges on the Longitudinal Conductivity for Conventional Composite Materials. Unidirectional Tow.

## SECTION II

### Use of Modified Rayleigh Equations to Estimate the Transverse Conductivity of Unidirectional, Filamentary Composite Materials

As the various transverse conductivity studies progressed throughout both Phase I and Phase II of this research effort, it became apparent that the Rayleigh solution for a two-phase, two-dimensional system is quite capable of describing first-order effects of both the tow volume fraction  $v_t$  and the tow conductivity ratio  $\bar{k}_t$  on the transverse conductivity of filamentary composites. Further, it became increasingly clear that the Rayleigh equation provides a comparatively simple, direct means to estimate the transverse conductivity of a unidirectional, filamentary composite material, that this relationship isolates the principal variables in an uncomplicated manner, and that this basic expression has excellent potential for adjustment and modification to improve its accuracy and to extend its applicability to a variety of fiber-matrix assemblages.

In this Section II, the Rayleigh equation for a two-phase, two-dimensional system is both adjusted and modified to improve its accuracy and to expand its usefulness. Adjustment factors are introduced which improve its ability to replicate the accurate Han-Cosner data [1]. Further, the concept of relative packing density is applied to this relationship to extend its application to different fiber arrays.

In short, the Rayleigh equation has been found especially capable both of serving as the framework to functionally organize the key variables and in submitting to modifications and adjustments which yield comparatively direct, accurate relationships for the description of the transverse conductivity of both uni- and bi-directional composites.

### The Rayleigh Equation

In 1892, Rayleigh [10] derived an expression for the transverse conductivity of a two-phase, two dimensional system consisting of long, solid cylinders of uniform diameter (isotropic and homogeneous) unidirectionally embedded at a "dilute" level (low volume fraction  $v$ ) in a continuous, isotropic, homogeneous matrix. This well-known expression as applied to the transverse conductivity  $k$  of a unidirectional tow(t)-matrix(m) system is

$$(k - k_m)/(k + k_m) = v_t(k_t - k_m)/(k_t + k_m) \quad (\text{II-1})$$

Or, in a form more directly useful when applied to a filamentary composite, the ratio of the bulk transverse conductivity  $k$  to the matrix conductivity  $k_m$  is

$$\bar{k} = (1 + mv_t)/(1 - mv_t) \quad (\text{II-2})$$

where

$$m \equiv (\bar{k}_t - 1)/(\bar{k}_t + 1)$$

$$\bar{k}_t \equiv k_t/k_m$$

$k_t \equiv$  conductivity  $k$  of the tow (fiber) in the transverse direction

$k_m \equiv$  conductivity  $k$  of the isotropic matrix

$\bar{k} \equiv k/k_m$ , the transverse relative conductivity, where  $k$  is the bulk transverse conductivity of the tow-matrix system

$v_t \equiv$  tow volume ratio, the fraction of the system's volume occupied by fibers

This same basic equation has been developed in various ways (e.g. Hashin [3], Kerner [11], Halpin and Tsai [12] from Hermans [13] and Hill [14], Behrens [15]). For circular fibers, the Halpin-Tsai equation [12] and the Rayleigh equation are equivalent. The modified versions of the Halpin-Tsai equation by Neilsen [16] and by Chow [17] have been examined.

In the following parts of this Section, the Rayleigh equation (II-2) is modified and adapted semiempirically to the accurate data [1].



### Adaptation to The Square Array

#### a. Accurate Values of the Bulk Transverse Conductivity.

The in-line transverse conductivities of a filamentary composite having unidirectional, circular fibers embedded in a matrix in a square array, Figure II-1, have been investigated a number of times over the years using classical analysis, analogs, models and exact numerical methods (e.g. [10], [12], [18], [19].

The Han-Cosner transverse (in-line) conductivities for fibers in this array [1] (and as obtained by exact numerical methods) provide, by far, the most extensive and accurate set of analytical data. Hence, their results are used as the basis for modifying and improving the accuracy of the Rayleigh equation for the square array. The Han-Cosner data for uniform diameter filaments (transversely isotropic and homogeneous) embedded in a square array within an isotropic, homogeneous matrix (no voids and no interfacial resistances) are summarized in Table II-1.

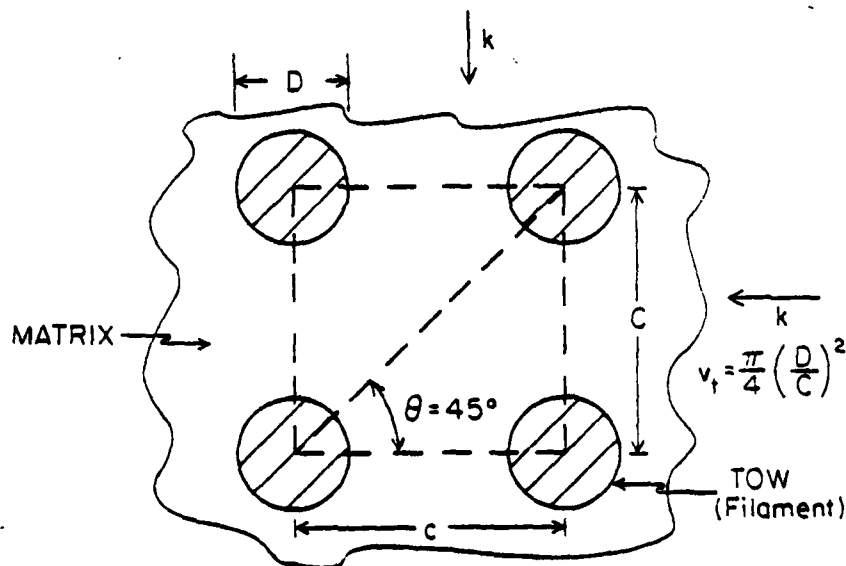


Figure II-1. Illustrating a Filamentary Composite having Unidirectional, Circular Fibers in A Square Array.

Table II-1. Han-Cosner Values of the Bulk Transverse (In-Line) Relative Conductivity ( $\bar{k} = k/k_m$ ) for A Tow-Matrix System Having Circular Filaments (Uniform Diameter)  $m$  Unidirectionally Embedded in A Square Array. Homogeneous Tow, Transversely Isotropic. Homogeneous Matrix, Isotropic. No Voids. No Interfacial Resistances. [1]. (See Footnote).

Tow-to-Matrix Conductivity Ratio $\bar{k}_t$	Tow Volume Ratio $v_t$					
	0.10	0.20	0.30	0.40	0.50	
0.10	0.8487	0.7187	0.6053	0.5049	0.4140	
0.20	0.8750	0.7647	0.6664	0.5778	0.4968	
0.40	0.9178	0.8421	0.7721	0.7070	0.6460	
0.60	0.9512	0.9048	0.8604	0.8181	0.7775	
1.00	1.0000	1.0000	1.0000	1.0000	1.0000	
2.00	1.0690	1.1429	1.2223	1.3080	1.4010	
4.00	1.1277	1.2728	1.4395	1.6339	1.8657	
6.00	1.1538	1.3334	1.5463	1.8045	2.1283	
10.00	1.1782	1.3915	1.6520	1.9806	2.4155	
20.00	1.1990	1.4421	1.7472	2.1459	2.7011	
40.00	1.2102	1.4701	1.8011	2.2426	2.8763	
60.00	1.2142	1.4799	1.8202	2.2773	2.9408	
100.00	1.2174	1.4880	1.8359	2.3061	2.9948	
200.00	1.2198	1.4941	1.8479	2.3283	3.0368	
400.00	1.2210	1.4972	1.8540	2.3396	3.0583	
600.00	1.2214	1.4982	1.8561	2.3434	3.0656	
1000.00	1.2217	1.4991	1.8577	2.3464	3.0714	
2000.00	1.2220	1.4997	1.8590	2.3487	3.0758	
	0.60	0.65	0.70	0.72	0.74	0.75
0.10	0.3292	0.2879	0.2462	0.2290	0.2113	0.2021
0.20	0.4212	0.3846	0.3483	0.3337	0.3190	0.3115
0.40	0.5885	0.5607	0.5335	0.5227	0.5119	0.5066
0.60	0.7386	0.7196	0.7009	0.6935	0.6862	0.6826
1.00	1.0000	1.0000	1.0000	1.0000	1.0000	1.0000
2.00	1.5028	1.5576	1.6154	1.6394	1.6641	1.6767
4.00	2.1510	2.3224	2.5207	2.6097	2.7055	2.7563
6.00	2.5561	2.8318	3.1729	3.3350	3.5171	3.6172
10.00	3.0372	3.4732	4.0611	4.3641	4.7264	4.9373
20.00	3.5618	4.2231	5.2125	5.7774	6.5166	6.9857
40.00	3.9093	4.7525	6.1118	6.9514	8.1362	8.9491
60.00	4.0426	4.9629	6.4919	7.4679	8.8919	9.9046
100.00	4.1567	5.1465	6.8350	7.9449	9.6151	10.8440
200.00	4.2470	5.2942	7.1191	8.3479	10.2470	11.6850
400.00	4.2938	5.3716	7.2708	8.5664	10.5970	12.1610
600.00	4.3097	5.3979	7.3230	8.6419	10.7190	12.3290
1000.00	4.3224	5.4191	7.3653	8.7034	10.8190	12.4660
2000.00	4.3321	5.4352	7.3973	8.7501	10.8960	12.5720

Note: Values of the transverse conductivity determined by Han and Cosner appear in [1] in graphical form only. The data tabulated in this Table II-1 (and in Tables II-4, II-6, II-7, IV-1 and IV-2 of this report) were prepared during this study using computer programs developed earlier by Han and Cosner, but not contained in [1].

The tow-volume ratio  $v_t$  for these data covers the range 0 - 0.75 ( $v_{t-\max} = \pi/4$ ). The range on the tow conductivity ratio  $\bar{k}_t$  ( $k_t/k_m$ ) is 0.10 to 2000. They conducted an error-spread study of the results and concluded that, for this particular model and its idealizations, the results are accurate to approximately 0.02 per cent for  $v_t \leq 0.6$ , to approximately 0.1 per cent at  $v_t = 0.7$ , to about 0.5 per cent at  $v_t = 0.725$ , to within 0.8 per cent at  $v_t = 0.74$  and 1.5 per cent at  $v_t = 0.75$ .

The Han-Cosner data for  $\bar{k}_t < 1$  were determined only over the more limited range on  $\bar{k}_t$  from 0.10 to unity. However, in this study, it has been found that the Rayleigh equation has a reciprocity characteristic. (If for a given tow volume ratio  $v_t$ , one substitutes into equation (I-2) the reciprocal of the tow conductivity ratio, the form of the Rayleigh solution is such that it defines the reciprocal of the bulk conductivity.) To a high level of accuracy, the Han-Cosner data (Table II-1) exhibit this same reciprocity feature. For example, with  $v_t = 0.7$  and  $\bar{k}_t = 10$ , Table II-1 shows a bulk transverse (in-line) conductivity  $\bar{k} = k/k_m = 4.061$ , and  $\bar{k}^{-1} = 0.2462$ . With  $v_t = 0.7$ , but  $\bar{k}_t = 0.10$ , from Table II-1, the transverse (in-line) conductivity is shown to be 0.2462. Thus, though it is not possible to test the reciprocity of the Han-Cosner data beyond the range  $0.1 < \bar{k}_t < 1$ , the application of this method to data in Table II-1 for  $\bar{k}_t$  up to 2000 very likely will yield quite accurate results over an equivalent reciprocal range on  $\bar{k}_t$ .

b. Modification of the Rayleigh Equation.

The Rayleigh equation (II-2) indicates the transverse relative conductivity  $\bar{k}$  to be a function only of the variable group  $mv_t$  (hereafter referred to as the Rayleigh parameter). The validity of the Rayleigh equation for the square array is illustrated in Figure II-2, where it is compared against a portion of the accurate Han-Cosner data (Table II-1). Clearly, the Rayleigh solution has "first-order" qualitative soundness. The Rayleigh parameter serves in a major way to correlate the data from Table II-1. Its form is essentially correct. Quantitatively, it is quite accurate for the conditions it was developed, i.e. "dilute" concentrations of the discontinuous phase --- which correspond to low values of the tow volume ratio  $v_t$ . However, it is quite inaccurate at high values of the Rayleigh parameter  $mv_t$ . (The maximum possible value of the Rayleigh parameter for the square array is  $\pi/4$ , since  $m_{\max} \rightarrow 1$  at large values of  $\bar{k}_t$ .) And, since filamentary composites have actual values of the Rayleigh parameter up to the vicinity of  $3/4$ , it is readily evident equation (II-2) could be appreciably in error if used to predict an in-line transverse conductivity of a densely-packed fiber-matrix system for which the fiber conductivity departs significantly from that of the matrix. The trend on the extent to which the Rayleigh equation (II-2) differs from the numerical solutions (Table II-1) is shown in Table II-2.

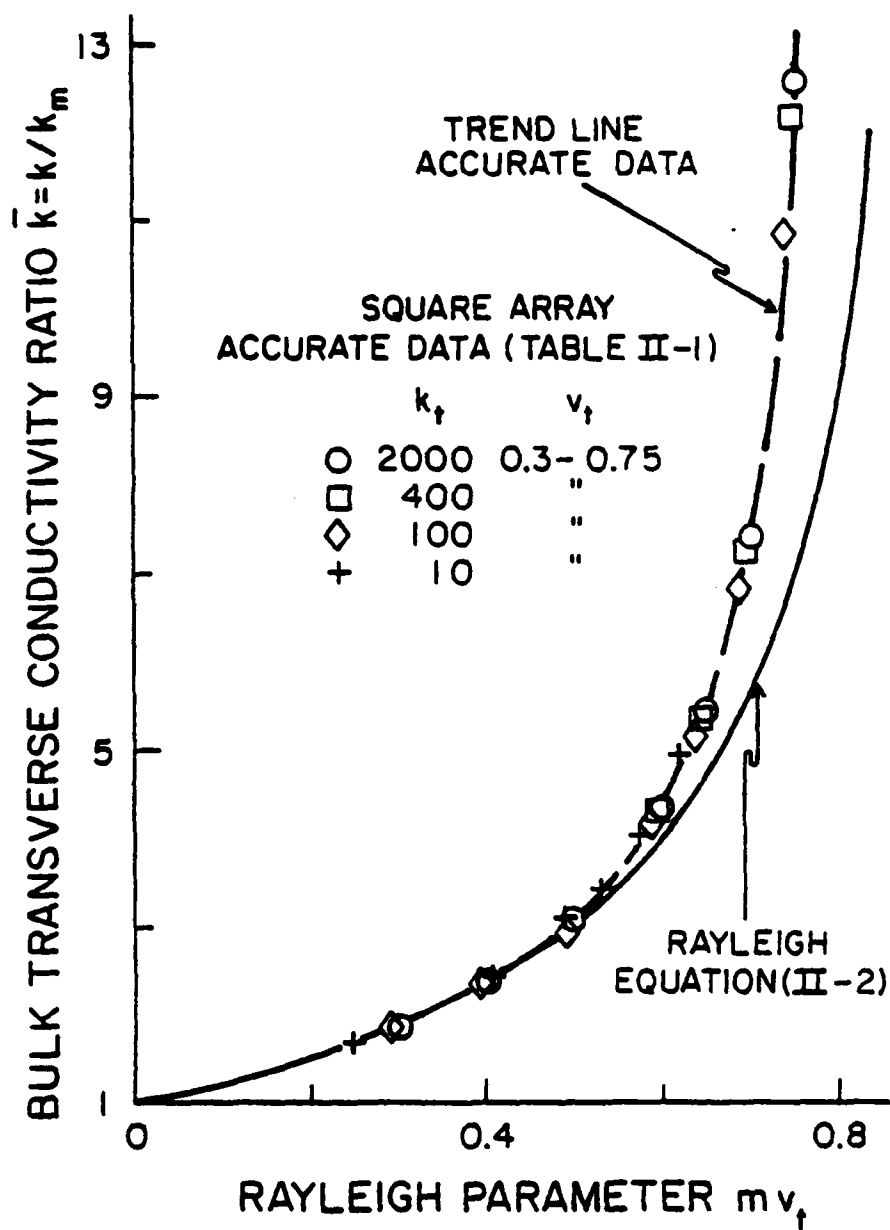


Figure II-2. Illustrating the Validity in Principle of the Rayleigh Equation for Unidirectional Fibers Embedded in A Square Array.

Table II-2. Deviation between the Han-Cosner Data (Table II-1) and the Rayleigh Equation (II-1) for the In-Line Transverse Conductivity of a Tow-Matrix System Consisting of Circular, Parallel Fibers Embedded in A Square Array.  $(k_{H-C} - k_{Ra})/k_{Ra}$  is shown as A Percentage.

Tow-Volume Ratio $v_t$	Tow Conductivity Ratio $\bar{k}_t$			
	$10^{-1}$	$1$	$10$	$1000$
0.3	-	-	-	-
0.5	-1	-	1	3
0.6	-4	-	4	8
0.7	-10	-	10	31
0.75	-18	-	18	79

Thus, though the Rayleigh equation (II-1) is seen to be qualitatively correct (Figure II-2), modification is needed to improve its accuracy. The form of the modification which will be applied is shown by the following parallel reasoning. For spheres embedded in a cubical array, Rayleigh [10] showed that at low concentrations, the conductivity is given by

$$\bar{k} = (1 + 2nv)/(1 - nv) \text{ where } n = (\bar{k}_t - 1)/(\bar{k}_t + 2)$$

For larger volume fractions of spherical bodies, Rayleigh introduced a second-order correction term which revised the previous expression to the form

$$\bar{k} = (1 + 2nv - T_1)/(1 - nv - T_1)$$

where

$$T_1 = \text{constant } v^{10/3} (\bar{k}_t - 1)/(\bar{k}_t + 4/3)$$

Meridith and Tobias [20] modified this latter expression to further improve its validity at higher volume fractions. Their equation for spheres in a continuous matrix is of the form

$$\bar{k} = [1 + 2nv(1 - T_2)]/[1 - nv(1 + T_3)]$$

where

$$T_2 = 0.2045 f(\bar{k}_t) v^{4/3} + 1.0665 f'(\bar{k}_t) v^{7/3}$$

$$T_3 = 0.409 f(\bar{k}_t) v^{4/3} + 0.906 f'(\bar{k}_t) v^{7/3}$$

$$f(\bar{k}_t) = (\bar{k}_t + 2)/(\bar{k}_t + 4/3)$$

$$f'(\bar{k}_t) = (\bar{k}_t - 1)/(\bar{k}_t + 4/3)$$

Examination of the comparative magnitudes of the terms  $T_2$  and  $T_3$  show that, to a good approximation, the Meridith-Tobias equation can be reduced to the form

$$\bar{k} = [1 + 2nv(1 - f)]/[1 - nv(1 + f)]$$

where  $f$  is assigned the functional form

$$f = v^x (e + gv)$$

with  $e$  and  $g$  being functions of  $\bar{k}_t$ . By applying this reasoning to the two-dimensional case, it is to be expected, therefore, that second-order modifications of the Rayleigh equation for unidirectional cylinders should be essentially of similar functional form.

If the form of the modification of the Rayleigh equation is taken to be equation (II-2) with an adjustment factor  $F$ , i.e. if one lets

$$\bar{k} = (1 + Fmv_t)/(1 - Fmv_t) \quad (\text{II-3})$$

then, from the previous examination of the term  $f$ , it follows that the adjustment factor  $F$  should be related to  $f$  by

$$(F - 1)/F = fmv_t \doteq F - 1$$

Thus, this parallel reasoning suggests the term  $F$  has the form

$$F - 1 \doteq mv_t^y [e_1 F(\bar{k}_t) + g_1 F'(\bar{k}_t) v_t]$$

Therefore, starting with the modified form of the Rayleigh equation (II-3), using the Han-Cosner accurate data (Table II-1) to establish accurate values of  $F = F(\bar{k}_t, v_t)$  for the square array, and being guided by the previously indicated functional form for the adjustment

factor  $F$ , nine semi-empirical equations (to describe  $F$ ) were developed and studied for accuracy. The two equations for the adjustment factor  $F$  judged to be most useful --- in descending order of accuracy --- are:

$$F_i = 1 + 0.314v_t^4 \left[ 1 + 11.2v_t \right] (1/2)(5v_t - 1)(2v_t - 1)^2 \left[ f(\bar{k}_t) \right] \quad (\text{II-4})$$

$$f(\bar{k}_t) = [\bar{k}_t(\bar{k}_t - 5/2) + 3/2] / [\bar{k}_t(\bar{k}_t + 5/2) - 3/2] \text{ for } \bar{k}_t > 1$$

$$F_{ii} = 1 + 0.535v_t^5 (\bar{k}_t - a) / (\bar{k}_t + a) \text{ for } \bar{k}_t > 1 \quad (\text{II-5})$$

$$a = 2.25 \text{ for } \bar{k}_t \geq 2, a = 5/3 \text{ for } \bar{k}_t \leq 2, a = \bar{k}_t \text{ for } 1 < \bar{k}_t < 2$$

For  $\bar{k}_t < 1$ , these same equations apply, except that  $\bar{k}_t$  in  $F_i$  and  $F_{ii}$  is to be introduced as  $\bar{k}_t^{-1}$ . (The actual value of  $\bar{k}_t$  is to be used in the term  $m = (\bar{k}_t - 1) / (\bar{k}_t + 1)$  in the Rayleigh parameter  $mv_t$ .)

The ability of equation (II-3) and its companion equation (II-4) or (II-5) to replicate the accurate Han-Cosner data for the square array (Table II-1) generally is within one half of one per cent. Based on equation (II-4) for  $F_i$ , equation (II-3) yields values of the in-line transverse conductivity for a square array within  $\pm 0.2$  per cent for all values of the tow conductivity ratio  $\bar{k}_t$  in Table II-1 and for values of the tow volume ratio  $v_t \leq 0.72$ . At  $v_t = 0.74$  and  $\bar{k}_t \geq 100$ , the accuracy of this method is about  $\pm 0.5$  per cent. With  $v_t$  in the range  $0.74 - 0.75$  and high value of  $\bar{k}_t$ , differences of one to two per cent exist between the Han-Cosner data and the modified Rayleigh equation (II-3) based on  $F_i$ . The adjustment factor  $F_{ii}$ , equation (II-5), used with equation (II-3) describe the accurate data to  $\pm 0.4$  per cent except at high  $\bar{k}_t$  with  $v_t > 0.7$  (where differences up to several per cent can exist).

In summary, for the approximate overall range on the tow conductivity ratio  $\bar{k}_t$  for filamentary composites,  $1/50 \leq \bar{k}_t \leq 750$ , and for fiber content levels  $v_t \leq 0.72$ , the modified Rayleigh equation replicates the in-line transverse conductivities for a square array (Table II-1) to  $\pm 0.2$  per cent based on the  $F_i$ , equation (II-4), and to  $\pm 0.5$  per cent using the  $F_{ii}$ , equation (II-5).

A comparison of the results obtained by use of the modified Rayleigh equation (based on  $F_{ii}$ ) is illustrated in Figure II-3.



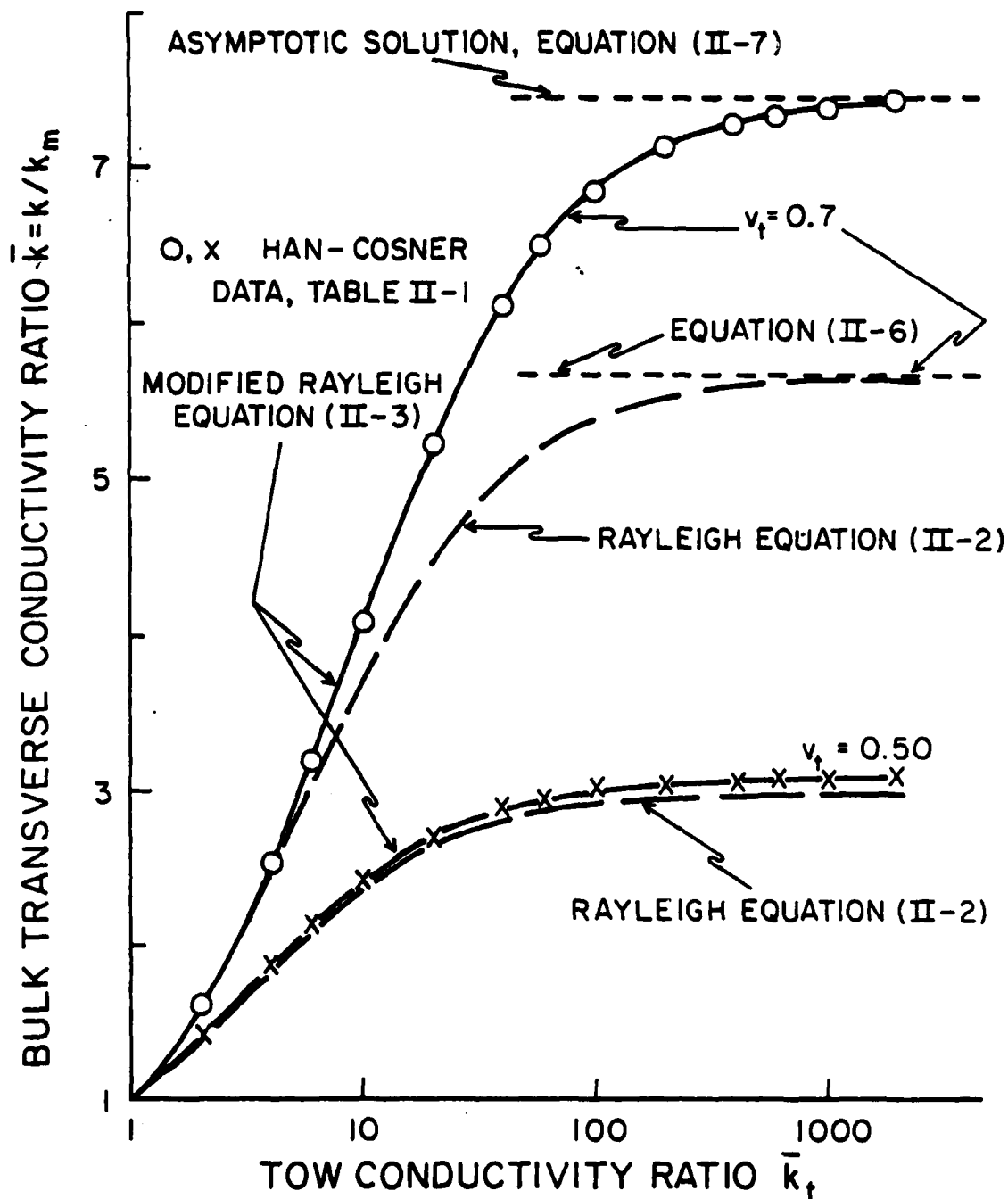


Figure II-3. Illustrating the Comparative Accuracy of the Rayleigh and the Modified Rayleigh Equations for Fibers Embedded in a Square Array.

For very high (and very low) values of the tow conductivity ratio  $\bar{k}_t$ , the Rayleigh equation (II-2) yields the asymptotic solutions

$$\bar{k} = (1 + v_t)/(1 - v_t) \text{ for } \bar{k}_t \gg 1 \quad (\text{II-6})$$

$$\bar{k} = (1 - v_t)/(1 + v_t) \text{ for } \bar{k}_t \ll 1$$

The modified Rayleigh equation (II-3) for very high (and very low) values of  $\bar{k}_t$  is

$$\bar{k} = (1 + Fv_t)/(1 - Fv_t) \text{ for } \bar{k}_t \gg 1 \quad (\text{II-7})$$

$$\bar{k} = (1 - Fv_t)/(1 + Fv_t) \text{ for } \bar{k}_t \ll 1$$

The accuracy of these asymptotic solutions is summarized in Table II-3. The ratio of the transverse conductivity (for  $\bar{k}_t \gg 1$ ) as defined both by the Rayleigh equation (II-2) and the modified Rayleigh equation (II-3) (for both adjustment factors  $F_i$  and  $F_{ii}$ ) is compared with the corresponding transverse conductivity defined by the Han-Cosner accurate data (the latter when extrapolated to an infinite value of  $\bar{k}_t$ ). For the tow volume fraction  $v_t \leq 0.72$ , the maximum error for the unadjusted Rayleigh equation is 30 per cent, for the modified Rayleigh equation using  $F_i$  about 0.2 per cent and for the modified equation using  $F_{ii}$  about 0.5 per cent. Differences of several per cent exist with  $v_t$  in the range 0.74 - 0.75.

### c. Transverse-to-Longitudinal Conductivity of A Square Array

For the combinations of tow and matrix materials used in filamentary composite materials, the longitudinal conductivity could be three orders of magnitude higher than the transverse conductivity. The material is, therefore, highly anisotropic.

Since the longitudinal conduction occurs in two parallel, continuous paths for the idealized model (no voids, no heterogeneities, no interfacial resistances), the longitudinal conductivity is defined by

$$\bar{k}_{lg} = 1 + (\bar{k}_{t-lg} - 1) v_t \quad (\text{II-8})$$

where

$$\bar{k}_{lg} \equiv k_{\text{bulk - longitudinal}} / k_{\text{matrix}}$$

$$\bar{k}_{t-lg} \equiv k_{\text{tow(fiber) - longitudinal}} / k_{\text{matrix}}$$

$$v_t \equiv \text{tow volume fraction}$$

Table II-3. The Ratio of the Asymptotic Transverse Conductivity ( $\bar{k}_t \gg 1$ ) Defined by the Modified Rayleigh Equations to the Corresponding Accurate Value (Table II-1). Square Array.

$v_t$	Rayleigh Equation (II-2)	Modified Rayleigh Equation (II-3)	
		$\frac{F_i}{F_{ii}}$	$\frac{F_{ii}}{F_{ii}}$
0.1	1.0	1.0	1.0
0.2	1.0	1.0	1.0
0.3	0.998	1.0	0.999
0.4	0.992	1.0	0.998
0.5	0.974	1.0	0.996
0.6	0.921	0.999	0.998
0.65	0.865	1.001	1.002
0.70	0.763	1.003	1.001
0.72	0.698	1.001	0.993
0.74	0.610	0.990	0.968
0.75	0.553	0.975	0.941

In this study, the matrix is assumed to be isotropic. However, the tow sometimes needs to be treated orthotropically, since its longitudinal and transverse conductivities can differ by a ratio of three or more.

The anisotropy of this particular tow-matrix system (as defined by the ratio of the bulk transverse conductivity to its bulk longitudinal conductivity) can be obtained directly from the Han-Cosner data for the square array (Table II-1) and equation (II-8). This ratio  $k/k_{lg}$  is always less than unity (except in the unusual situation where the fiber conductivity transversely happens to exceed the fiber conductivity longitudinally), since the tow-matrix system is discontinuous in the transverse plane.

The general pattern on the ratio of the transverse conductivity to the longitudinal conductivity (both on a bulk basis) for the square array is shown in Figure II-4 for various values of the tow volume ratio  $v_t$  and for the entire range of tow conductivity ratio  $\bar{k}_t$  likely to be encountered in fiber composites. The anisotropy is not especially sensitive to tow volume ratio in the general range  $0.2 < v_t < 0.7$  (Figure II-4). The tow-to-matrix conductivity ratio  $\bar{k}_t$  is the influential parameter. With  $\bar{k}_t > 1$ , the tow-matrix system could have a bulk longitudinal conductivity two to three orders of magnitude higher than its bulk transverse conductivity. Thus, since a composite material can have longitudinal conductivity levels comparable to materials classified as "conductors", the corresponding bulk transverse conductivity could be near the range of conductivities classified as "insulators". For a tow-to-matrix conductivity ratio  $\bar{k}_t < 1$ , the anisotropy is seen to be much less (than for  $\bar{k}_t > 1$ ), since now the higher-conductivity component (the matrix) is continuous in both directions.

The modified Rayleigh equation (II-3) and the longitudinal equation (II-8) are useful in estimating transverse-to-longitudinal conductivity ratios. For  $\bar{k}_t < 1$ , a condition of minimum  $k/k_{lg}$  either does not exist or involves tow volume levels of no practical concern.

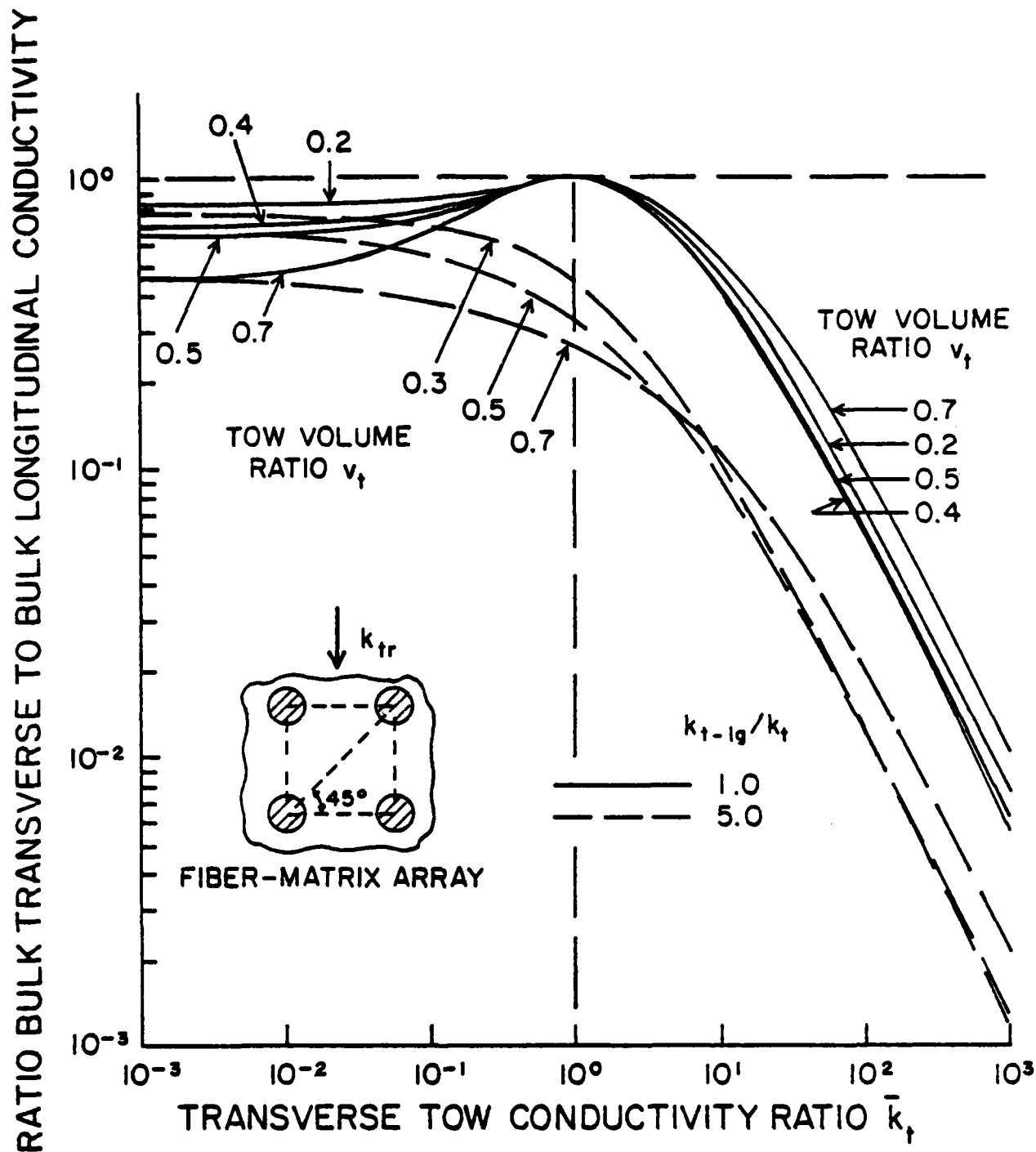


Figure II-4. The Anisotropy of A Filamentary Composite having A Square Fiber Array --- As Defined by the Ratio of the Bulk Transverse Conductivity (Table II-1) and the Longitudinal Conductivity (Equation II-8).

However, for  $\bar{k}_t > 1$ , this conductivity ratio  $k/k_{lg}$  has minimum values in the general range  $v_t = 0.4-0.5$  (which are relatively insensitive to the tow volume ratio  $v_t$ ). The adjustment factor  $F_i$  (or  $F_{ii}$ ) has values between 1.0-1.02 for this volume ratio range. Hence, its variation in this region can be ignored, and the condition of minimum transverse-to-longitudinal conductivity ratio is given by

$$Fm v_t = -1 + (2)^{1/2} [1 - m/(\bar{k}_{t-lg} - 1)]^{1/2} \quad (II-9)$$

where  $m = (\bar{k}_t - 1)/(\bar{k}_t + 1)$  in the transverse direction. Or, for isotropic tow, the minimum condition is defined by

$$Fm v_t = -1 + [2\bar{k}_t/(\bar{k}_t + 1)]^{1/2} \quad (II-10)$$

For the special case of isotropic tow with  $\bar{k}_t \gg 1$ ,  $Fm v_t = (2)^{1/2} - 1 = 0.414$ ,  $m = 1$  and  $F = 1.01$  (equation II-4). Therefore,  $v_t = 0.41$  for the condition of minimum  $k/k_{lg}$ . It follows that at the minimum condition, the transverse conductivity is  $\bar{k} = (1 + Fm v_t)/(1 - Fm v_t) = (2)^{1/2}/[2 - (2)^{1/2}] = 2.41$ . Also, for  $\bar{k}_t \gg 1$ ,  $\bar{k}_{lg} = 1 + (\bar{k}_t - 1)v_t \doteq \bar{k}_t v_t$ . Thus,  $(k/k_{lg})_{min} \doteq 2.41/0.41 \bar{k}_t \doteq 5.9/\bar{k}_t$ . The actual values of  $k/k_{lg}$  for  $\bar{k}_t \gg 1$  are seen in Figure II-4 to agree with this result.

A semi-empirical relationship for the ratio of the transverse to longitudinal conductivities  $k/k_{lg}$  (as developed from the Rayleigh and longitudinal conduction equations) is

$$(k/k_{lg})[(k_{t-lg}/k_t)(\bar{k}_t + 4)(v_t)(1 - v_t)/(1 + v_t)] \doteq 1 \quad (II-11)$$

where  $k_{t-lg}$ ,  $k_t$  and  $\bar{k}_t$  are the longitudinal conductivity of the tow, the transverse conductivity of the tow and the ratio of the transverse tow conductivity to the matrix conductivity, respectively. Its usefulness is in its separation of variables, thereby allowing direct estimates of their influences on the conductivity ratio  $k/k_{lg}$ . For the square array, Figure II-5 illustrates that equation (II-11) is accurate to  $\pm 20$  per cent for all  $\bar{k}_t \geq 2$  and  $0.2 \leq v_t \leq 0.7$ . Its accuracy is  $\pm 10$  per cent for  $\bar{k}_t \geq 3$  and  $0.3 \leq v_t \leq 0.6$ .

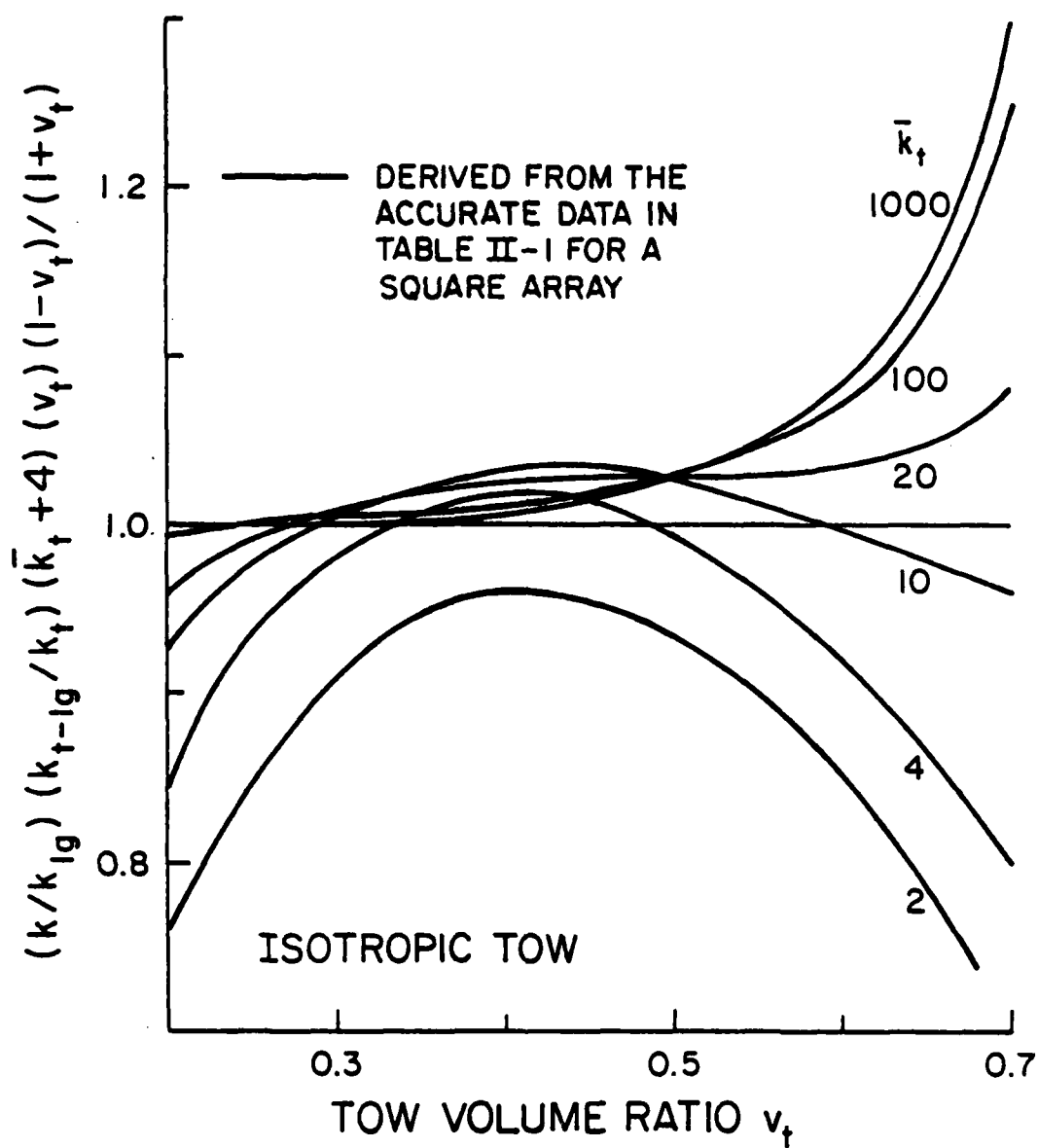


Figure II-5. Illustrating the Accuracy of Equation II-11 as A Direct Means of Estimating Effects of Tow Conductivity and Tow Volume Ratio on the Transverse-to-Longitudinal Conductivity Ratio. Square Array.

## The Hexagonal Array

### a. Hexagonal Packing Array Versus the Square Packing Array.

The staggered array having a fiber-diagonal angle of 30 or 60 degrees forms an hexagonal transverse array (Figure II-6).

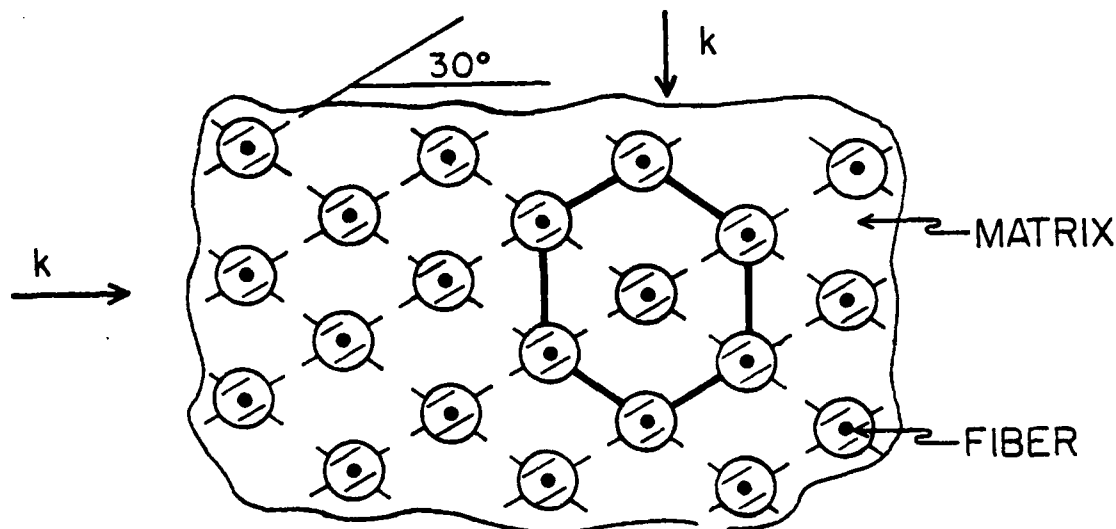


Figure II-6. Illustrating the Hexagonal Packing Array.

A tow-matrix system having uniform-diameter, unidirectional filaments packed in this array is isotropic transversely in the principal in-line fiber directions, if both the tow and matrix are isotropic transversely. However, for the same system bulk characteristics (equal tow volume ratio  $v_t$  and equal tow-to-matrix conductivity ratio  $\bar{k}_t$ ), the square packing geometry yields a higher transverse conductivity. This characteristic (first indicated by shear-modules studies of various packing geometries, e.g. [21] [22]) is likewise exhibited by the conductivity data developed by Han and Cosner [1]. Though the difference in the transverse conductivity between that for the square array and the hexagonal array is small (under two per cent) when the tow-volume ratio  $v_t < 1/2$ , the difference can become appreciable under high-density packing (tow-volume ratios in the range  $2/3$  to  $3/4$ )--- see Figure II-7.



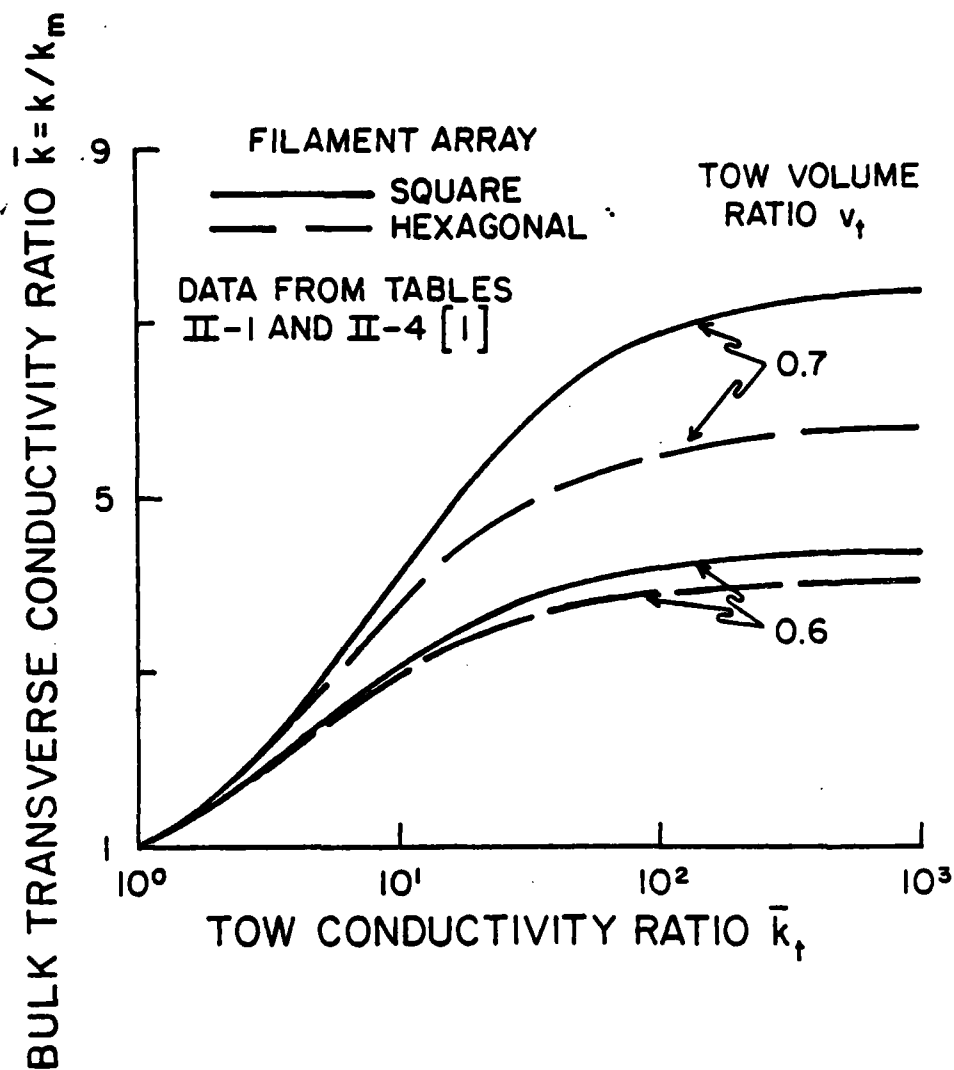


Figure II-7. Illustrating the Hexagonal Fiber Packing Geometry Yields A Lower Transverse Conductivity than a Square Array (for Equal Tow Volume Ratios and Equal Tow Conductivity Ratios).

For example, if  $\bar{k}_t = 100$  and  $v_t = 0.7$ , the transverse conductivities for the square array and the hexagonal array are 0.8 and 5.5 times the matrix conductivity, respectively (Figure II-7).

The hexagonal array (versus the square array for equivalent tow-volume ratios) has a lower fiber packing density. The in-line center-to-center distance between fibers packed hexagonally is  $2^{0.5}/3^{0.25} = 1.075$  times the corresponding in-line distance in a square array. The reciprocal of the square of this distance is an index of the relative packing density, i.e.  $(3)^{1/2}/2$ . (For maximum packing density, the tow-volume ratios are  $v_{t-sq} = \pi/4$  and  $v_{t-hex} = (\pi/2)/(3)^{1/2} = 0.907$ ; the ratio of the two being  $(3)^{1/2}/2$ .) Thus, under the condition of high density packing, the thermal resistance of the matrix gap between fibers could be altered appreciably by change from an hexagonal to a square packing array.

#### b. Transverse Conductivity Data

Calculated values of the transverse conductivity for the hexagonal array have been determined by Han and Cosner [1]. They evaluated this array for fiber angles of both 30 and 60 degrees, thereby generating two sets of data for the hexagonal array. The two sets agree, except for minor differences at the highest tow volume ratio (and then only by roughly 1/4 of one per cent). The Han-Cosner data for the hexagonal array (Table II-4) cover the same range on the tow conductivity ratio,  $\bar{k}_t = k_t/k_m$  from 0.1 to 2000, as for the square array (Table II-1). The maximum tow volume ratio  $v_t$  for the hexagonal array is 0.87, which, relative to its limit of 0.907, is at the same approximate level as the maximum tow volume ratio  $v_t$  of 0.75 for the square array (limit of  $\pi/4$ ).

The transverse conductivity for a tow conductivity ratio  $\bar{k}_t < 0.1$  can be estimated from this same set of data (Table II-4) by the reciprocity procedure. For example, if  $\bar{k}_t = 0.01$  and  $v_t = 0.6$ , then for  $\bar{k}_t = 100$  and  $v_t = 0.6$ ,  $\bar{k} = 3.88$ . Thus,  $\bar{k}$  for  $\bar{k}_t = 0.01$  would be estimated to be  $3.88^{-1} = 0.258$ .

Table II-4. Han-Cosner Transverse Relative Conductivities ( $\bar{k} = k/k_m$ ) for A Tow-Matrix System having Circular Filaments (Uniform Diameter) Unidirectionally Embedded in An Hexagonal Array. Homogeneous Tow, Transversely Isotropic. Homogeneous Matrix, Isotropic. No Voids, No Interfacial Resistances. [1]. See Footnote to Table II-1.

Tow-to-Matrix Conductivity Ratio $\bar{k}_t$	Tow Volume Ratio $v_t$			
	0.10	0.20	0.30	0.40
0.10	0.8487	0.7188	0.6058	0.5068
0.20	0.8750	0.7647	0.6667	0.5789
0.40	0.9178	0.8421	0.7721	0.7073
0.60	0.9512	0.9048	0.8605	0.8182
1.00	1.0000	1.0000	1.0000	1.0000
2.00	1.0690	1.1429	1.2222	1.3077
4.00	1.1277	1.2727	1.4390	1.6317
6.00	1.1538	1.3333	1.5455	1.8002
10.00	1.1782	1.3913	1.6506	1.9733
20.00	1.1990	1.4419	1.7451	2.1348
40.00	1.2102	1.4699	1.7987	2.2289
60.00	1.2142	1.4797	1.8176	2.2626
100.00	1.2173	1.4877	1.8332	2.2905
200.00	1.2198	1.4938	1.8451	2.3120
400.00	1.2210	1.4969	1.8511	2.3230
600.00	1.2214	1.4979	1.8531	2.3266
1000.00	1.2217	1.4988	1.8548	2.3296
2000.00	1.2220	1.4994	1.8560	2.3318
	0.50	0.60	0.65	0.70
0.10	0.4190	0.3404	0.3039	0.2689
0.20	0.4998	0.4279	0.3943	0.3619
0.40	0.6470	0.5907	0.5639	0.5379
0.60	0.7778	0.7391	0.7203	0.7020
1.00	1.0000	1.0000	1.0000	1.0000
2.00	1.4001	1.5002	1.5536	1.6095
4.00	1.8577	2.1272	2.2830	2.4563
6.00	2.1122	2.5047	2.7428	3.0184
10.00	2.3865	2.9376	3.2906	3.7190
20.00	2.6551	3.3901	3.8883	4.5253
40.00	2.8177	3.6790	4.2841	5.0849
60.00	2.8770	3.7875	4.4358	5.3051
100.00	2.9266	3.8795	4.5656	5.4962
200.00	2.9651	3.9516	4.6683	5.6491
400.00	2.9848	3.9888	4.7215	5.7289
600.00	2.9914	4.0013	4.7396	5.7561
1000.00	2.9967	4.0114	4.7541	5.7780
2000.00	3.0007	4.0190	4.7650	5.7945
	0.75	0.80	0.85	0.87
0.10	0.2351	0.2020	0.1690	0.1553
0.20	0.3306	0.3002	0.2702	0.2581
0.40	0.5126	0.4880	0.4638	0.4543
0.60	0.6840	0.6663	0.6490	0.6421
1.00	1.0000	1.0000	1.0000	1.0000
2.00	1.6680	1.7295	1.7943	1.8213
4.00	2.6511	2.8725	3.1289	3.2447
6.00	3.3429	3.7336	4.2208	4.4562
10.00	4.2539	4.9489	5.9122	6.4285
20.00	5.3762	6.5908	8.5382	9.7550
40.00	6.2065	7.9239	11.0310	13.2610
60.00	6.5457	8.5009	12.2320	15.0890
100.00	6.8458	9.0284	13.4040	16.9710
200.00	7.0903	9.4702	14.4450	18.7310
400.00	7.2193	9.7081	15.0310	19.7580
600.00	7.2634	9.7902	15.2370	20.1270
1000.00	7.2991	9.8569	15.4060	20.4320
2000.00	7.3261	9.9075	15.5350	20.6670

### c. Adapting the Rayleigh Equation.

By the Rayleigh equation (II-2), the transverse conductivity is a function of the Rayleigh parameter  $mv_t$ , where  $m \equiv (\bar{k}_t - 1)/(\bar{k}_t + 1)$ . A portion of the Han-Cosner data for the hexagonal array (Table II-4) is displayed in Figure II-8 as a function of the Rayleigh parameter. The trend for the hexagonal array agrees well with the Rayleigh equation (II-2). The Rayleigh parameter serves to correlate the conductivity data. The Rayleigh solution is nearly correct, both qualitatively and quantitatively.

By the same type of reasoning as used for the square array, the Rayleigh equation is modified to more nearly describe the accurate transverse conductivity for the hexagonal array. Thus, let

$$\bar{k} = (1 + Fmv_t)/(1 - Fmv_t) \quad (\text{II-12})$$

where

$$m = (\bar{k}_t - 1)/(\bar{k}_t + 1)$$

and  $F$  is the adjustment factor.

From a study of six semi-empirical equations for the adjustment factor  $F$ , the following two are recommended to best serve in adjusting the Rayleigh solution. The more accurate version is

$$F_i = 1 + 0.079v_t^6 \left[ 1 + 11(4/3)v_t + (19.5)(v_t - 3/4)^2 \right] (\bar{k}_t - a)/(\bar{k}_t + a) \quad (\text{II-13})$$

where

$$a = 2.25 \text{ for } \bar{k}_t > 2, a = 5/3 \text{ for } \bar{k}_t \approx 2 \text{ and } a \approx \bar{k}_t \text{ for } 1 < \bar{k}_t < 2$$

The combination of equations (II-12) and (II-13) replicates the Han-Cosner data for the hexagonal array (Table II-4) to  $\pm 0.1$  per cent for all  $\bar{k}_t$  and  $v_t < 0.8$ . It is accurate to within 0.5 per cent for all values of  $\bar{k}_t$  and  $v_t$  in Table II-4, except when both  $v_t > 0.85$  and  $\bar{k}_t > 100$ .

The second version for the adjustment factor is

$$F_{ii} = 1 + (v_t^7/9)(\bar{k}_t - a)/(\bar{k}_t + a) \quad (\text{II-14})$$

where  $a$  has the same values as for equation (II-13).

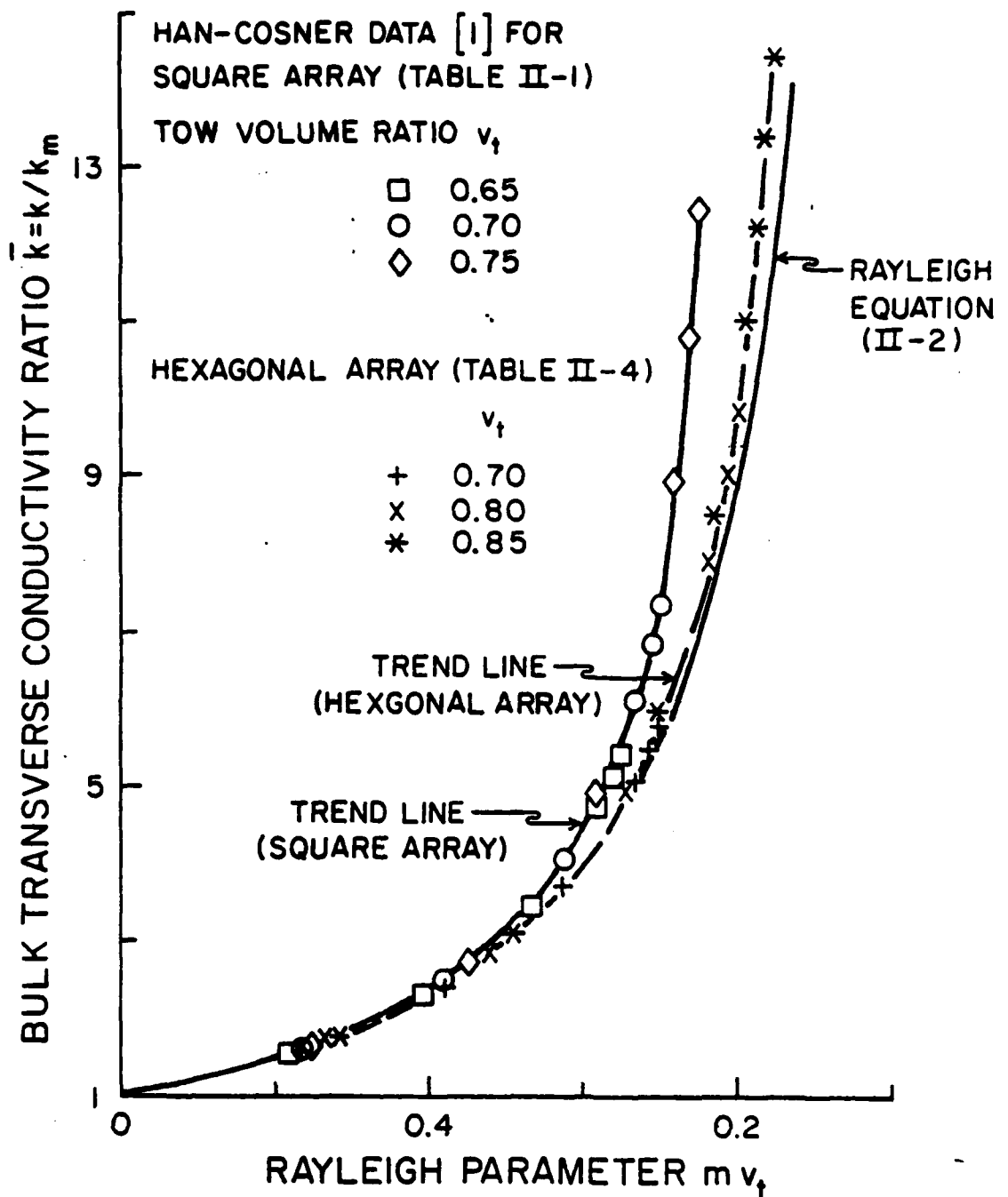


Figure II-8. Comparison of the Trend Line Defined by the Accurate Values of the Transverse Conductivity for An Hexagonal Array (Table II-4) with the Rayleigh Equation (II-2).

This version  $F_{ii}$  when used with equation (II-12) describes the accurate data (Table II-4) to  $\pm 0.1$  per cent through  $v_t = 0.7$ , to within  $3/4$  per cent through  $v_t = 0.8$  and to within roughly 2 per cent at the highest  $v_t = 0.87$ . For the usual ranges  $v_t \lesssim 3/4$  and  $k_t \lesssim 750$ , either version ( $F_i$  or  $F_{ii}$ ) serves to describe the hexagonal data (Table II-4) reasonably well.

Comparative results obtained in predicting the transverse conductivity for the hexagonal array are illustrated in Figure II-9. The basic Rayleigh equation is reasonably accurate for a tow-volume ratio  $v_t$  less than approximately  $2/3$ . At higher packing densities, the unadjusted Rayleigh equation (II-2) can differ appreciably from the accurate data (Figure II-9).

The anisotropy of this array (ratio of  $k$  transverse to  $k$  longitudinal) is essentially the same as for the square array.

### Rectangular Array

#### a. Geometrical Characteristics.

With parallel circular fibers aligned in a rectangular array (Figure II-10), the tow-matrix system is characterized principally by the tow volume ratio  $v_t$ , the tow-to-matrix conductivity ratio  $k_t$  ( $k_t/k_m$ ) and the fiber diagonal angle  $\theta$  (or the array aspect ratio  $R = c/C$ ).

With reference to Figure II-10, neither the depth spacing ratio  $S \equiv D/C$  nor the width spacing ratio  $s \equiv D/c$  can exceed unity. Thus, for a fiber diagonal angle  $\theta \leq 45$  degrees, the maximum possible tow-volume ratio  $v_t$  is defined by ( $S = 1$ )

$$v_{\max} = (\pi/4)(D^2/cC) = (\pi/4)/R = (\pi/4) \tan \theta \quad (\text{II-15})$$

For  $\theta \geq 45^\circ$ ,  $v_{\max}$  occurs when  $s = 1$  and

$$v_{\max} = (\pi/4)(D^2/cC) = (\pi/4) R = (\pi/4)/\tan \theta \quad (\text{II-16})$$

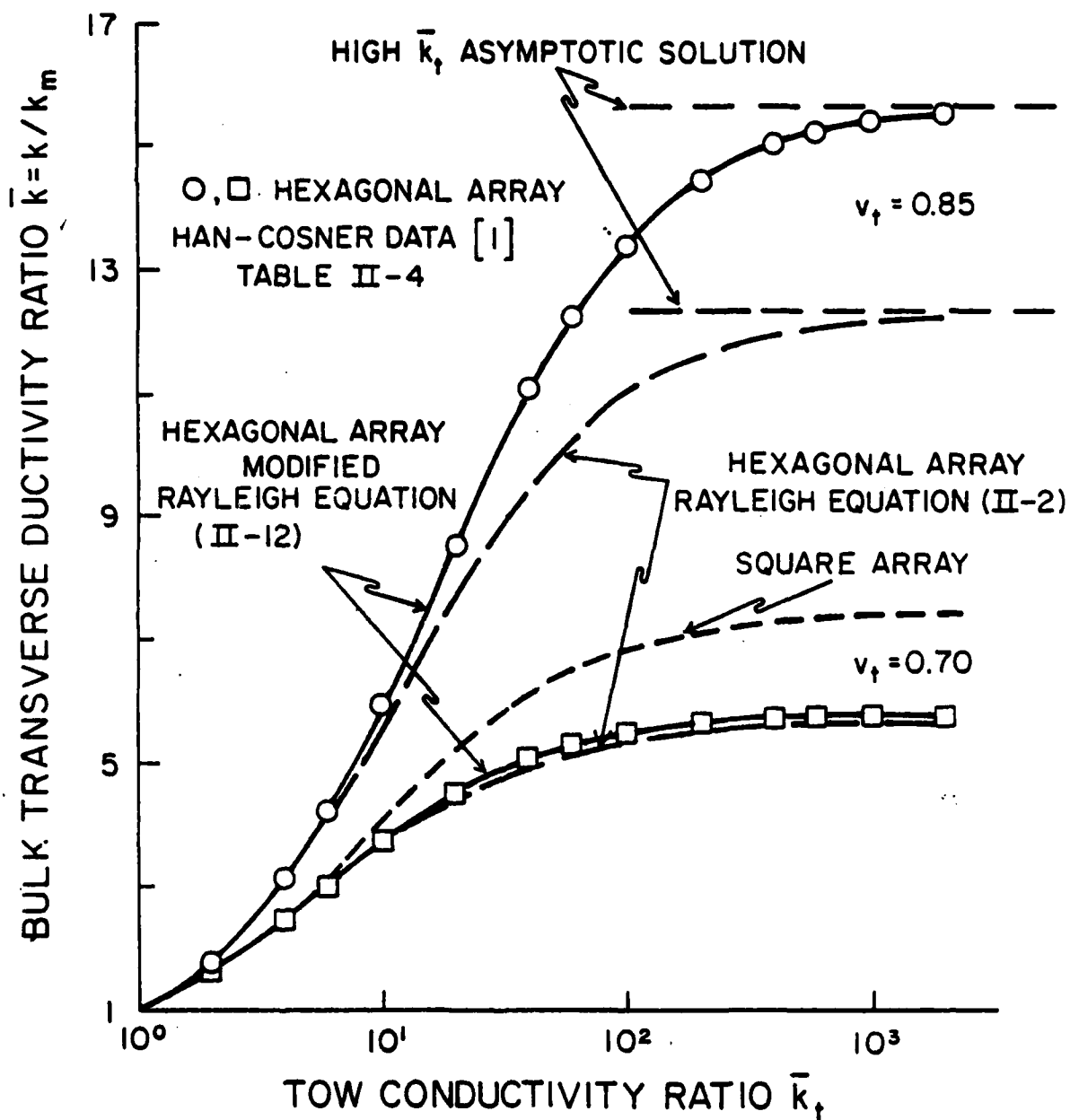


Figure II-9. Illustrating Comparative Results Obtained by Use of the Rayleigh Equations for the Hexagonal Array.

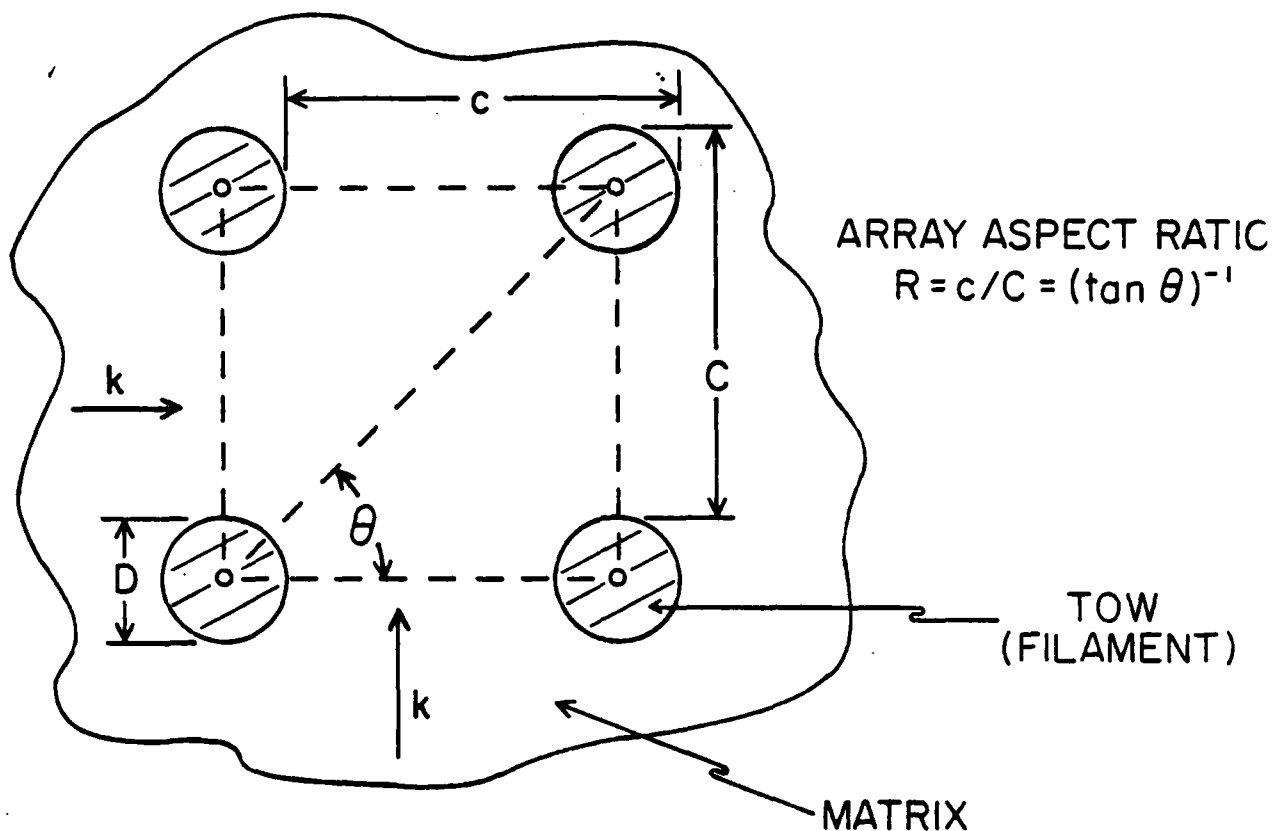


Figure II-10. Unidirectional Tow-Matrix System Having Constant-Diameter Filaments Embedded in a Rectangular Array.

These limitations are summarized in Table II-5 for the range on the fiber diagonal angle  $\theta$  studied by Han and Cosner [1]. Since the tow-volume ratio  $v_t$  for fiber composites commonly exceeds 0.40, it is apparent from examination of the maximum volume ratios in Table II-5 that aligned regular arrays will usually have fiber diagonal angles in the approximate range  $35^\circ - 55^\circ$ .



Table II-5. Geometrical Characteristics of the Rectangular Array Under the Conditions of Maximum Packing (Maximum Tow Volume Ratio  $v_t$ ).  
 $S = D/C$ ,  $s = D/c$ ,  $R = c/C$  (Figure II-10).

	Fiber Diagonal Angle $\theta$ , Degrees			
	<u>30</u>	<u>35</u>	<u>40</u>	<u>45</u>
Depth Spacing Ratio $S$	1	1	1	1
Width Spacing Ratio $s$	0.577	0.700	0.839	1
Tow Volume Ratio $v_{\max}$	0.453	0.550	0.659	0.785
Array Aspect Ratio $R$	1.73	1.43	1.19	1

	Fiber Diagonal Angle $\theta$ , Degrees			
	<u>50</u>	<u>55</u>	<u>60</u>	<u>65</u>
Width Spacing Ratio $s$	1	1	1	1
Depth Spacing Ratio $S$	1.19	1.43	1.73	2.14
Tow Volume Ratio $v_{\max}$	0.659	0.550	0.453	0.336
Array Aspect Ratio $R$	0.839	0.700	0.577	0.466

The data developed by Han and Cosner for fiber angles of 30, 60 and 65 degrees (Table II-6) are therefore, likely to be most useful in the study of conductivity paths for randomly distributed, parallel filaments.

The thickness (depth) of the matrix gap between the fibers plays a key role in transverse conduction. When the depth (thickness) of this gap is small (relative to the fiber spacing), the transverse conductivity can depart appreciably from the conductivity of the matrix. As the tow-volume ratio approaches its limit (maximum possible packing density), the transverse conductivity shifts in major ways toward the tow conductivity. The ratio of the thickness of the matrix material between the fibers to the fiber spacing distance is  $(C-D)/C = 1 - (v_t/v_{\max})^{1/2} = 1 - (\bar{v})^{1/2}$  for  $\theta \leq 45^\circ$ . For  $\theta \geq 45^\circ$ , the minimum matrix gap occurs laterally and  $(c - D)/c = 1 - (\bar{v})^{1/2}$ . Allowable fiber diagonal angles as set by both in-line and lateral gap thicknesses of zero, 10 and 20 per cent of the fiber spacing distance are compared in Figure II-11 with the maximum gap thicknesses used in the development of the accurate transverse conductivity data for the rectangular array. The lateral spacing distance (when evaluating transverse conduction) is not especially critical. The minimum transverse matrix gaps in the Han-Cosner study for fiber diagonal angles less than 45 degrees are seen to be roughly 15 per cent of the fiber spacing distance.

#### b. Transverse Conductivity Data.

The transverse conductivity of a tow-matrix system consisting of parallel, circular filaments embedded in a rectangular array (Figure II-10) was investigated by Han and Cosner [1] for a range on the tow-to-matrix conductivity ratio  $\bar{k}_t$  from 0.1 to 2000, for a range on the fiber diagonal angle  $\theta$  of 30 through 65 degrees and for a range on the tow volume ratio  $v_t$  from 0.1 to a value for each  $\theta$  approaching the limiting  $v_{\max}$ . Their data for this array are presented in Table II-6.

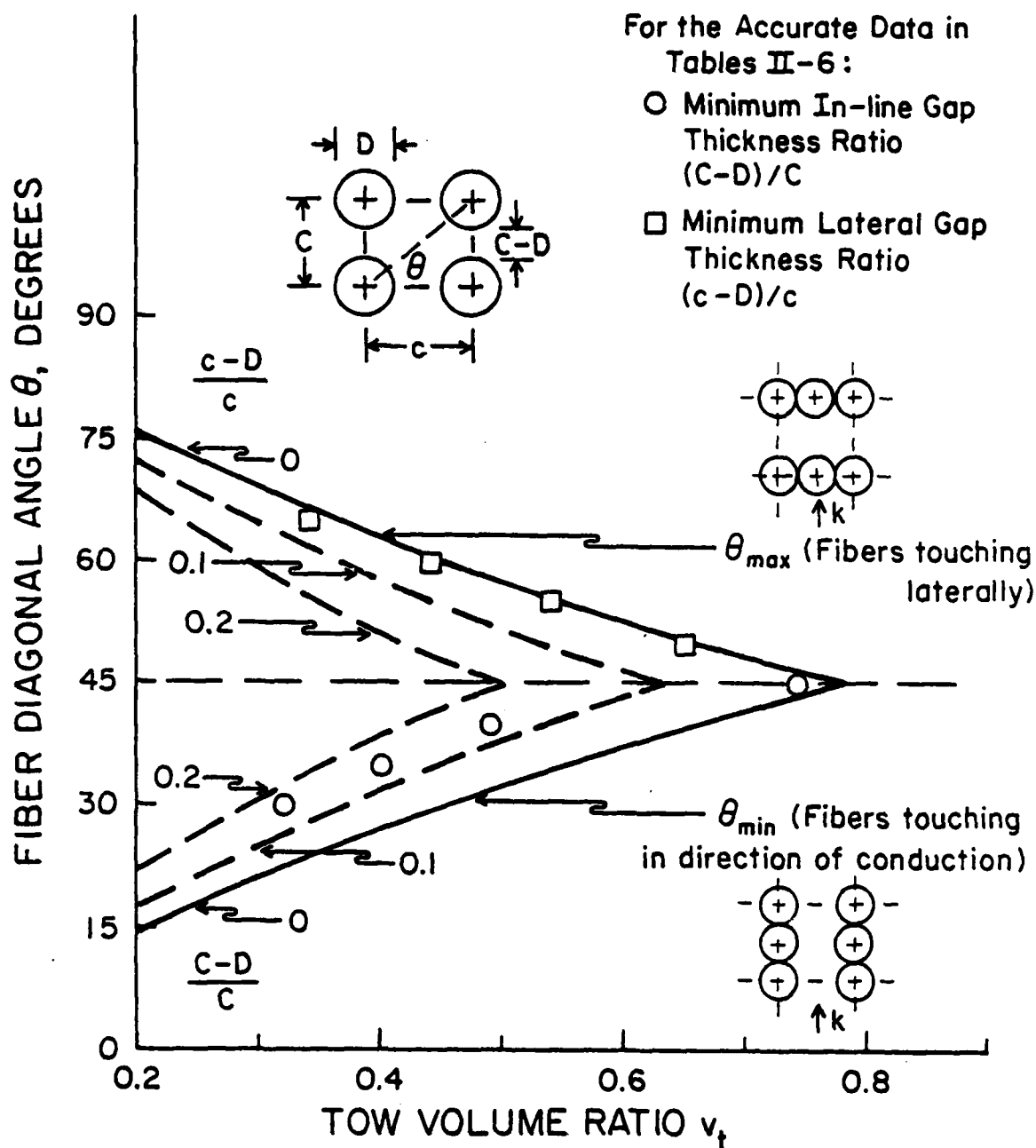


Figure II-11. Illustrating the Interrelationship of Fiber Diagonal Angle and the Minimum Matrix Gap for the Han-Cosner Rectangular Array Data (Table II-6).

Table II-6. Han-Cosner Values of the Bulk Transverse (In-Line) Relative Conductivity ( $\bar{k} = k/k_m$ ) for A Tow-Matrix System Having Circular Filaments (Uniform Diameter) Unidirectionally Embedded in A Rectangular Array. Homogeneous Tow, Transversely Isotropic. Homogeneous Matrix, Isotropic. No Voids. No Interfacial Resistances. [1]. See Footnote to Table II-1.

1)  $\theta = 30^\circ$ ,  $v_{\max} = 0.453$ ,  $R = 1.73$

Tow-to-Matrix Conductivity Ratio $\bar{k}_t$	Tow Volume Ratio $v_t$			
	0.10	0.20	0.30	0.32
0.10	0.8575	0.7474	0.6592	0.6435
0.20	0.8810	0.7851	0.7059	0.6916
0.40	0.9205	0.8516	0.7914	0.7802
0.60	0.9522	0.9083	0.8680	0.8603
1.00	1.0000	1.0000	1.0000	1.0000
2.00	1.0710	1.1517	1.2450	1.2656
4.00	1.1347	1.3071	1.5391	1.5967
6.00	1.1641	1.3863	1.7100	1.7959
10.00	1.1922	1.4664	1.9008	2.0243
20.00	1.2165	1.5402	2.0947	2.2634
40.00	1.2299	1.5828	2.2156	2.4163
60.00	1.2346	1.5980	2.2604	2.4738
100.00	1.2385	1.6105	2.2982	2.5225
200.00	1.2414	1.6201	2.3277	2.5607
400.00	1.2429	1.6250	2.3428	2.5804
600.00	1.2434	1.6266	2.3480	2.5871
1000.00	1.2438	1.6280	2.3521	2.5924
2000.00	1.2441	1.6289	2.3552	2.5964

Table II-6. (Cont.)

ii)  $\theta = 35^\circ$ ,  $v_{\max} = 0.550$ ,  $R = 1.43$

Tow-to-Matrix Conductivity Ratio $\bar{k}_t$	Tow Volume Ratio $v_t$				
	0.10	0.20	0.30	0.37	0.40
0.10	0.8541	0.7368	0.6397	0.5807	0.5571
0.20	0.8787	0.7775	0.6913	0.6380	0.6165
0.40	0.9194	0.8480	0.7840	0.7431	0.7263
0.60	0.9518	0.9069	0.8651	0.8373	0.8258
1.00	1.0000	1.0000	1.0000	1.0000	1.0000
2.00	1.0702	1.1481	1.2352	1.3028	1.3337
4.00	1.1318	1.2924	1.4934	1.6685	1.7554
6.00	1.1599	1.3633	1.6324	1.8823	2.0126
10.00	1.1864	1.4333	1.7788	2.1222	2.3113
20.00	1.2092	1.4962	1.9189	2.3674	2.6285
40.00	1.2217	1.5319	2.0022	2.5211	2.8339
60.00	1.2261	1.5445	2.0323	2.5782	2.9116
100.00	1.2296	1.5548	2.0574	2.6264	2.9778
200.00	1.2323	1.5627	2.0768	2.6641	3.0298
400.00	1.2337	1.5668	2.0867	2.6835	3.0567
600.00	1.2341	1.5681	2.0900	2.6900	3.0658
1000.00	1.2345	1.5692	2.0926	2.6953	3.0731
2000.00	1.2348	1.5700	2.0947	2.6992	3.0786

Table II-6. (Cont.)

iii)  $\theta = 40^\circ$ ,  $v_{\max} = 0.659$ ,  $R = 1.19$ .

Tow-to-Matrix Conductivity Ratio $\bar{k}_t$	Tow Volume Ratio $v_t$			
	0.10	0.20	0.30	0.40
0.10	0.8513	0.7275	0.6224	0.5314
0.20	0.8768	0.7709	0.6787	0.5972
0.40	0.9186	0.8449	0.7779	0.7165
0.60	0.9515	0.9058	0.8627	0.8218
1.00	1.0000	1.0000	1.0000	1.0000
2.00	1.0695	1.1453	1.2282	1.3195
4.00	1.1296	1.2817	1.4632	1.6849
6.00	1.1566	1.3468	1.5834	1.8887
10.00	1.1820	1.4101	1.7056	2.1090
20.00	1.2036	1.4659	1.8185	2.3257
40.00	1.2155	1.4972	1.8837	2.4573
60.00	1.2196	1.5082	1.9070	2.5055
100.00	1.2230	1.5172	1.9263	2.5457
200.00	1.2255	1.5241	1.9411	2.5770
400.00	1.2268	1.5276	1.9486	2.5930
600.00	1.2272	1.5288	1.9511	2.5984
1000.00	1.2276	1.5297	1.9531	2.6027
2000.00	1.2278	1.5304	1.9546	2.6059
	0.50	0.59		
0.10	0.4505	0.3840		
0.20	0.5240	0.4633		
0.40	0.6598	0.6120		
0.60	0.7831	0.7498		
1.00	1.0000	1.0000		
2.00	1.4209	1.5231		
4.00	1.9659	2.3024		
6.00	2.3065	2.8691		
10.00	2.7109	3.6478		
20.00	3.1511	4.6692		
40.00	3.4425	5.4764		
60.00	3.5541	5.8202		
100.00	3.6496	6.1318		
200.00	3.7252	6.3907		
400.00	3.7643	6.5294		
600.00	3.7776	6.5771		
1000.00	3.7883	6.6158		
2000.00	3.7963	6.6452		

Table II-6. (Cont.)

iv)  $\theta = 45^\circ$ ,  $v_{\max} = 0.785$ ,  $R = 1$  (See Table II-1)v)  $\theta = 50^\circ$ ,  $v_{\max} = 0.659$ ,  $R = 0.84$ 

Tow-to-Matrix Conductivity Ratio $\bar{k}$	Tow Volume Ratio $v_t$			
	0.10	0.20	0.30	0.40
0.10	0.8460	0.7092	0.5863	0.4742
0.20	0.8732	0.7581	0.6529	0.5557
0.40	0.9170	0.8392	0.7659	0.6966
0.60	0.9509	0.9037	0.8582	0.8142
1.00	1.0000	1.0000	1.0000	1.0000
2.00	1.0684	1.1405	1.2167	1.2975
4.00	1.1258	1.2645	1.4183	1.5911
6.00	1.1512	1.3211	1.5140	1.7368
10.00	1.1746	1.3745	1.6066	1.8819
20.00	1.1945	1.4206	1.6881	2.0135
40.00	1.2053	1.4460	1.7337	2.0885
60.00	1.2090	1.4548	1.7497	2.1150
100.00	1.2120	1.4620	1.7627	2.1369
200.00	1.2143	1.4675	1.7727	2.1537
400.00	1.2155	1.4702	1.7778	2.1622
600.00	1.2159	1.4712	1.7795	2.1651
1000.00	1.2162	1.4719	1.7809	2.1674
2000.00	1.2164	1.4725	1.7819	2.1691
	0.50	0.60	0.65	
0.10	0.3689	0.2636	0.2018	
0.20	0.4643	0.3750	0.3276	
0.40	0.6306	0.5668	0.5351	
0.60	0.7716	0.7302	0.7098	
1.00	1.0000	1.0000	1.0000	
2.00	1.3834	1.4756	1.5244	
4.00	1.7881	2.0180	2.1497	
6.00	2.0002	2.3221	2.5138	
10.00	2.2196	2.6530	2.9333	
20.00	2.4260	2.9808	3.3400	
40.00	2.5471	3.1812	3.5000	
60.00	2.5906	3.2548	3.7051	
100.00	2.6267	3.3164	3.7881	
200.00	2.6545	3.3643	3.8530	
400.00	2.6687	3.3889	3.8863	
600.00	2.6735	3.3971	3.8976	
1000.00	2.6773	3.4038	3.9066	
2000.00	2.6802	3.4088	3.9134	

Table II-6. (Cont.)

vi)  $\theta = 55^\circ$ ,  $v_{\max} = 0.550$ ,  $R = 0.70$

Tow-to-Matrix Conductivity Ratio $k_t$	Tow Volume Ratio $v_t$			
	0.10	0.20	0.30	0.40
0.10	0.8429	0.6977	0.5622	0.4327
0.20	0.8710	0.7502	0.6362	0.5269
0.40	0.9161	0.8357	0.7584	0.6837
0.60	0.9506	0.9025	0.8555	0.8095
1.00	1.0000	1.0000	1.0000	1.0000
2.00	1.0678	1.1380	1.2109	1.2866
4.00	1.1238	1.2557	1.3971	1.5503
6.00	1.1483	1.3083	1.4824	1.6749
10.00	1.1708	1.3573	1.5632	1.7951
20.00	1.1897	1.3990	1.6329	1.9009
40.00	1.1999	1.4217	1.6713	1.9600
60.00	1.2035	1.4296	1.6847	1.9807
100.00	1.2063	1.4360	1.6956	1.9976
200.00	1.2085	1.4409	1.7039	2.0106
400.00	1.2096	1.4434	1.7081	2.0171
600.00	1.2100	1.4442	1.7095	2.0193
1000.00	1.2103	1.4448	1.7106	2.0211
2000.00	1.2105	1.4453	1.7115	2.0224
	0.50	0.54		
0.10	0.2999	0.2354		
0.20	0.4179	0.3703		
0.40	0.6104	0.5807		
0.60	0.7643	0.7463		
1.00	1.0000	1.0000		
2.00	1.3660	1.3988		
4.00	1.7192	1.7923		
6.00	1.8926	1.9890		
10.00	2.0644	2.1861		
20.00	2.2193	2.3660		
40.00	2.3073	2.4692		
60.00	2.3385	2.5059		
100.00	2.3642	2.5362		
200.00	2.3838	2.5594		
400.00	2.3938	2.5712		
600.00	2.3971	2.5751		
1000.00	2.3998	2.5783		
2000.00	2.4018	2.5807		



Table II-6. (Cont.)

vii)  $\theta = 60^\circ$ ,  $v_{\max} = 0.453$ ,  $R = 0.577$ 

Tow-to-Matrix Conductivity Ratio $\bar{k}_t$	Tow Volume Ratio $v_t$				
	0.10	0.20	0.30	0.40	0.44
0.10	0.8388	0.6820	0.5270	0.3643	0.2866
0.20	0.8683	0.7396	0.6125	0.4824	0.4258
0.40	0.9150	0.8312	0.7484	0.6654	0.6317
0.60	0.9502	0.9009	0.8520	0.8032	0.7837
1.00	1.0000	1.0000	1.0000	1.0000	1.0000
2.00	1.0671	1.1350	1.2041	1.2746	1.3033
4.00	1.1214	1.2457	1.3740	1.5086	1.5647
6.00	1.1448	1.2939	1.4489	1.6137	1.6833
10.00	1.1662	1.3381	1.5183	1.7122	1.7950
20.00	1.1841	1.3752	1.5770	1.7966	1.8913
40.00	1.1937	1.3953	1.6088	1.8428	1.9442
60.00	1.1970	1.4022	1.6198	1.8588	1.9626
100.00	1.1997	1.4078	1.6288	1.8719	1.9777
200.00	1.2018	1.4121	1.6356	1.8819	1.9891
400.00	1.2028	1.4143	1.6391	1.8869	1.9949
600.00	1.2031	1.4150	1.6402	1.8886	1.9969
1000.00	1.2034	1.4156	1.6411	1.8900	1.9984
2000.00	1.2036	1.4160	1.6418	1.8910	1.9996

Table II-6. (Concluded).

viii)  $\theta = 65^\circ$ ,  $v_{\max} = 0.366$ ,  $R = 0.466$ .

Tow-to-Matrix Conductivity Ratio $\bar{k}_t$	Tow Volume Ratio $v_t$			
	0.10	0.20	0.30	0.34
0.10	0.8330	0.6578	0.4652	0.3726
0.20	0.8644	0.7236	0.5732	0.5058
0.40	0.9134	0.8247	0.7330	0.6947
0.60	0.9497	0.8987	0.8469	0.8259
1.00	1.0000	1.0000	1.0000	1.0000
2.00	1.0661	1.1313	1.1958	1.2215
4.00	1.1183	1.2335	1.3476	1.3937
6.00	1.1404	1.2767	1.4118	1.4667
10.00	1.1604	1.3156	1.4698	1.5327
20.00	1.1771	1.3478	1.5179	1.5877
40.00	1.1859	1.3650	1.5436	1.6171
60.00	1.1890	1.3709	1.5525	1.6272
100.00	1.1915	1.3757	1.5597	1.6354
200.00	1.1934	1.3794	1.5651	1.6417
400.00	1.1943	1.3812	1.5678	1.6448
600.00	1.1946	1.3818	1.5688	1.6458
1000.00	1.1949	1.3823	1.5695	1.6467
2000.00	1.1951	1.3827	1.5700	1.6473

The error-spread studies conducted by Han and Cosner show that, for this model and its idealizations, the results are very accurate for  $\theta \lesssim 45^\circ$  if tow volume ratio  $v_t$  does not exceed roughly two-thirds of the maximum possible tow volume ratio  $v_{\max}$ . For  $\theta < 45^\circ$  and  $v_t$  at the maximum levels included in Table II-6, the error spread is approximately one per cent. With  $\theta > 45^\circ$  and the tow volume ratio at the maximum levels included in Table II-6, the error spread does not exceed roughly one fourth of one per cent.

The values of the transverse conductivity for this rectangular array for  $\bar{k}_t < 1$  are again available only to  $\bar{k}_t = 0.1$ . Since  $\bar{k}_t$  for composites can be nearly one decade lower, in these instances, the transverse conductivity can be estimated through use of the reciprocity procedure. This procedure here, however, differs somewhat from the direct reciprocal procedure applicable to the square and hexagonal arrays --- both of which are symmetrical with respect to the in-line fiber directions. The reciprocity procedure for the rectangular array requires the use both of the reciprocal of the tow conductivity ratio  $\bar{k}_t$  and the complementary fiber angle. For example, if it is desired to estimate the transverse conductivity for the conditions  $v_t = 0.4$ ,  $\theta = 35^\circ$  and  $\bar{k}_t = 10^{-2}$ , then one uses the data in Table II-6 to determine that  $\bar{k} = 1.998$  for  $v_t = 0.4$ ,  $\bar{k}_t = 100$  and  $\theta = 55^\circ$ . Therefore,  $\bar{k}$  for  $\theta = 35^\circ$ ,  $\bar{k}_t = 10^{-2}$  and  $v_t = 0.4$  is about  $1.998^{-1} = 0.501$ .

### c. Modified Rayleigh Equation.

The diagonal angle at which the fibers are organized in this rectangular array can have a significant influence on the transverse conductivity, especially if the diagonal angle is less than 45 degrees and the tow conductivity departs appreciably from that of the matrix (see Table II-6). The pattern of the effect of the fiber angle is illustrated in Figure II-12.

The first-order effect of the fiber diagonal angle on the transverse conductivity is felt through the change in the in-line gap

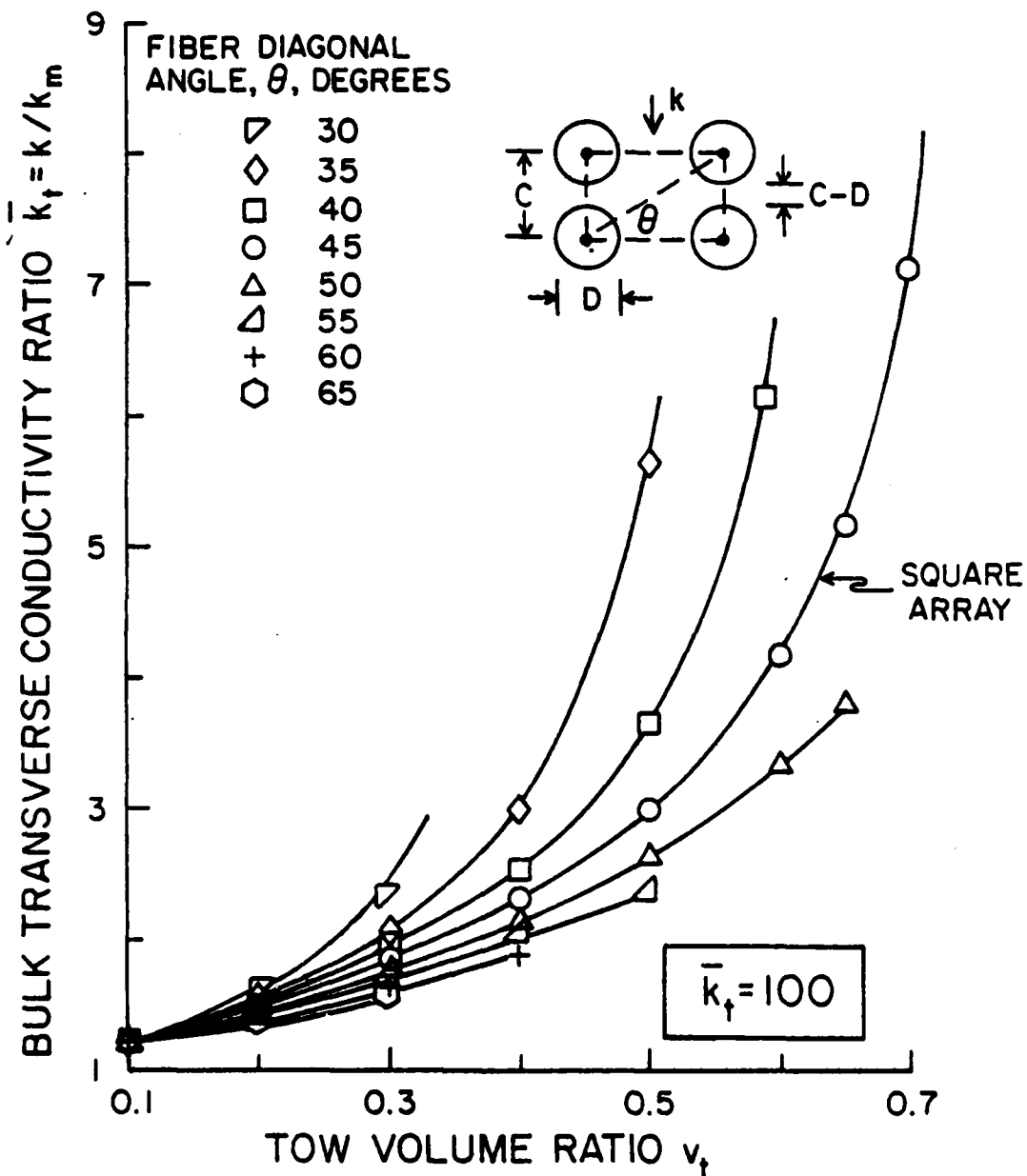


Figure II-12. Illustrating the Influence of Fiber Diagonal Angle on the Transverse Conductivity of A Rectangular Array. Han-Cosner Data, Table II-6 [1].

thickness. Hence, the Rayleigh parameter  $mv_t$  should be influenced in some manner by the way the change in the fiber angle alters the maximum density to which the fibers can be packed. The ratio  $\bar{v} = v_t/v_{\max}$  should, therefore, become an important parameter, especially when the fiber angle is less than 45 degrees.

Starting, therefore, from the Rayleigh equation (II-2), and expecting the primary angular effect to relate to the relative packing density  $\bar{v} = v_t/v_{\max}$ , we will assume the Rayleigh equation should be modified as

$$\bar{k}_\theta = (1 + mv_t/C_\theta)/(1 - mv_t/C_\theta)$$

where  $C_\theta$  is an angle adjustment factor. To ensure this expression yields the transverse conductivities for a square array, the adjustment factor  $F$  (for the square array) is introduced and, accordingly,  $C_{45^\circ} \equiv 1$ . Thus, modification of the Rayleigh equation assumes the form

$$\bar{k}_\theta = (C_\theta + F_{sq}mv_t)/(C_\theta - F_{sq}mv_t) \quad (II-17)$$

Further, since

$$\bar{k}_{sq} = (1 + F_{sq}mv_t)/(1 - F_{sq}mv_t)$$

therefore,

$$F_{sq}mv_t = (\bar{k}_{sq} - 1)/(\bar{k}_{sq} + 1)$$

and it follows that, for the rectangular array

$$C_\theta = [(\bar{k}_\theta + 1)/(\bar{k}_\theta - 1)]/[(\bar{k}_{sq} + 1)/(\bar{k}_{sq} - 1)] \quad (II-18)$$

Thus, the angle adjustment factor  $C_\theta$  can be evaluated directly from the accurate Han-Cosner data (Table II-6) using equation (II-18).

It is found that  $C_\theta$  is described approximately by the following equations (for use in equation II-17).

$$C_\theta = 1 - 1.25 \sin(1 - \tan\theta)(v_t/v_{\max})^{3/2}, \quad \theta \leq 45^\circ \quad (II-19)$$

$$C_{\theta} = 1 + 1.05 m v_t (\tan \theta - 1), \theta \geq 45^{\circ} \quad (\text{II-20})$$

The extent to which they describe the actual values of  $C_{\theta}$  is illustrated in Figure II-13 for  $\bar{k}_t = 10$ .

The ability of this method, equations (II-17), (II-19) and (II-20), to replicate the accurate Han-Cosner data for rectangular arrays (Table II-6) is similar to that for the square array with  $\bar{v} \leq 2/3$ . For higher values of the relative volume  $\bar{v}$  (as  $v_t$  approaches  $v_{\max}$ ) and for  $\theta < 45^{\circ}$ , typically, the deviations from the accurate data are 2 to 4 per cent. For  $\theta > 45^{\circ}$ , the deviation is within one per cent. Overall, with the exceptions of values of the tow volume ratio at the higher levels when the angle is at the lowest level included in Table II-6, the method replicates the Han-Cosner data to within one per cent.

In summary, for given bulk characteristics of a tow-matrix system (given levels of  $v_t$  and  $\bar{k}_t$  --- volume of tow relative to the volume of the system and conductivity of tow relative to that for the matrix), the accurate Han-Cosner data (in-line) for a rectangular array show that the fiber packing geometry can alter the transverse conductivity in major ways. This influence is illustrated in Figure II-14, where for  $\bar{k}_t = 100$  the effects of the geometrical factors (fiber volume fraction and packing angle) on transverse conductivity are shown. In this illustration, for  $v_t = 0.5$ , an angular change from  $55^{\circ}$  to  $35^{\circ}$  is seen to alter the transverse conductivity by a ratio of roughly two to one.

#### Staggered Regular Array

The staggered regular array (Figure II-15) takes on the special cases of the square array ( $\theta = 45^{\circ}$ ) and the hexagonal array ( $\theta = 30^{\circ}$  and  $60^{\circ}$ ). As the fiber diagonal angle  $\theta$  is varied, this particular array shows a transverse conductivity pattern typically as illustrated in Figure II-16. At low array angles, the proximity of the in-line fibers (even to the point of touching) produces large departure of the bulk transverse conductivity from that of the matrix.

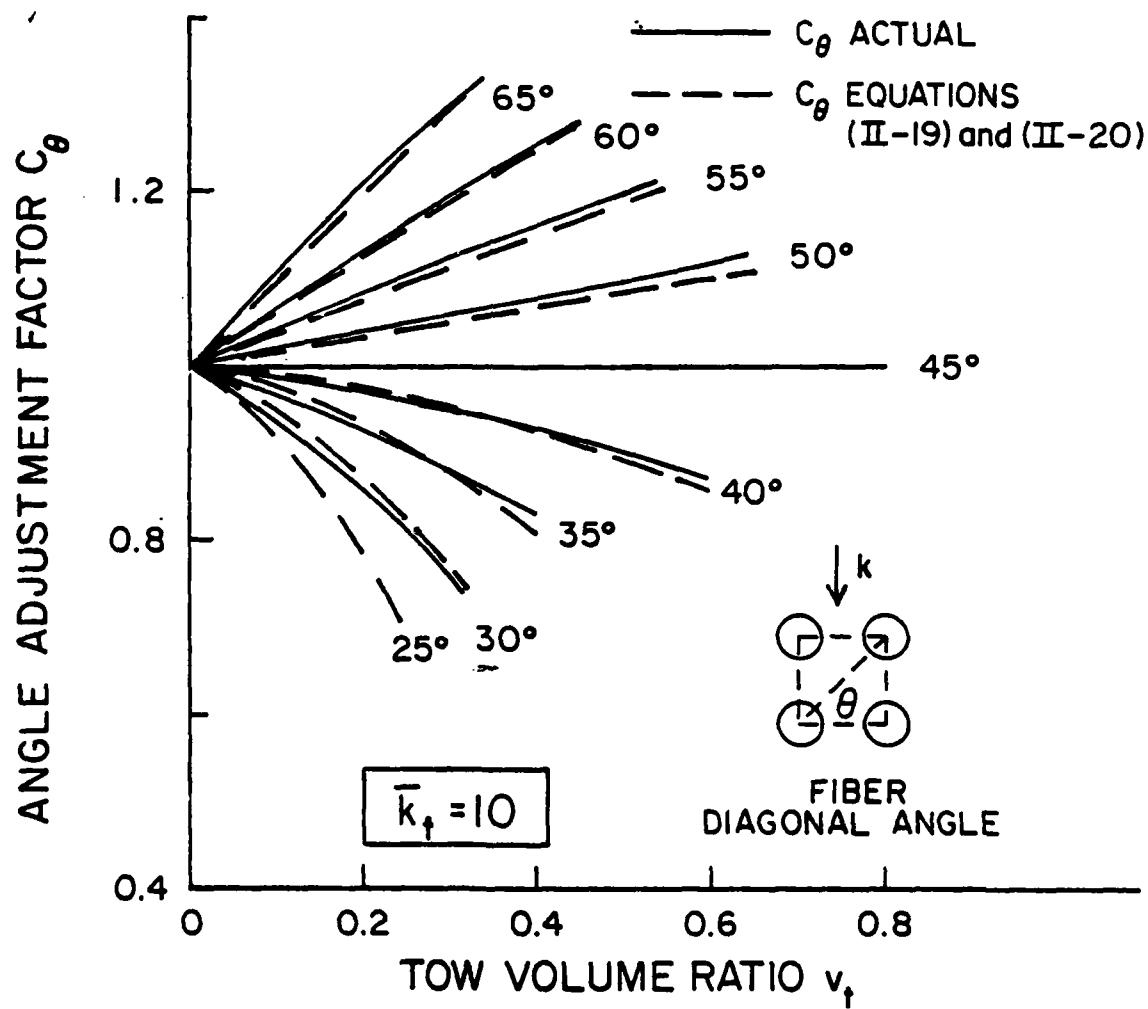


Figure II-13. Illustrating the Validity of the Semi-Empirical  $C_\theta$  Equations (II-19) and (II-20) for the Rectangular Array.

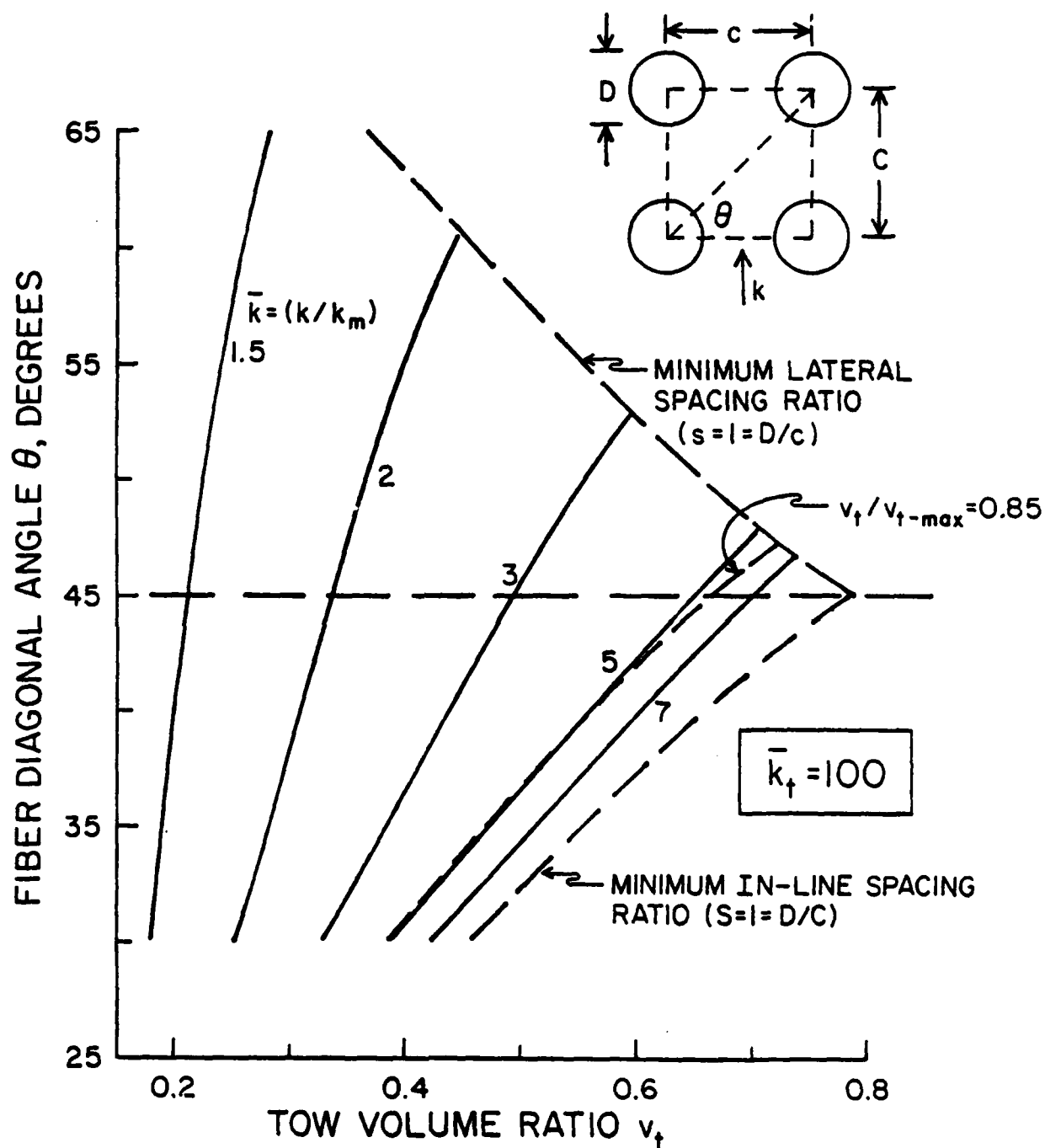


Figure II-14. Illustrating the Influence of Tow Volume Ratio and Packing Angle on the Transverse Conductivity of A Tow-Matrix System Consisting of Unidirectional Fibers Embedded in An In-Line Rectangular Array. Based on Data in Table II-6 [1].



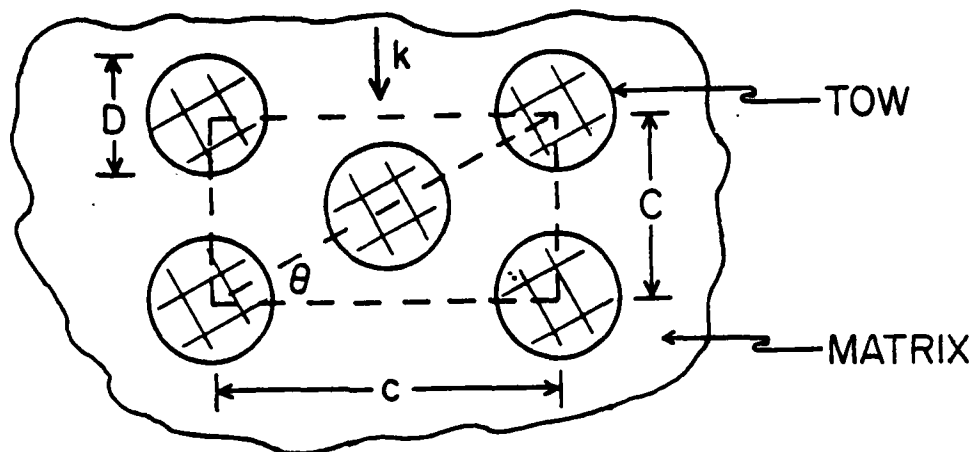


Figure II-15. Staggered Regular Array.

When the in-line fibers touch (minimum fiber angle), the row of in-line fibers establishes a direct conduction path. As this angle is increased from its minimum, the matrix gap between the in-line fibers thickens monotonically while the matrix gap between the fiber along a diagonal line passes through a minimum. The separation of the in-line fibers increases, but the fibers in adjacent rows move closer to each other along the diagonal (for the same tow volume fraction), and both paths (the diagonal and in-line) are then contributing to the overall bulk conduction. At still larger fiber angles, both matrix gaps thicken and the influence of the fibers on the bulk conductivity lessens.

a. Geometrical Factors

The in-line spacing ratio  $S \equiv D/C$  (Figure II-15) for this array is related to the fiber volume ratio  $v_t$  and the angle  $\theta$  by

$$\begin{aligned} v_t &= 2 (\pi/4) D^2/cC = (\pi/2) s S \\ \tan \theta &= C/c = s/S \\ S/(v_t)^{1/2} &= (2/\pi \tan \theta)^{1/2} \end{aligned} \quad (\text{II-21})$$

where  $s \equiv D/c$  (Figure II-15). The corresponding diagonal spacing

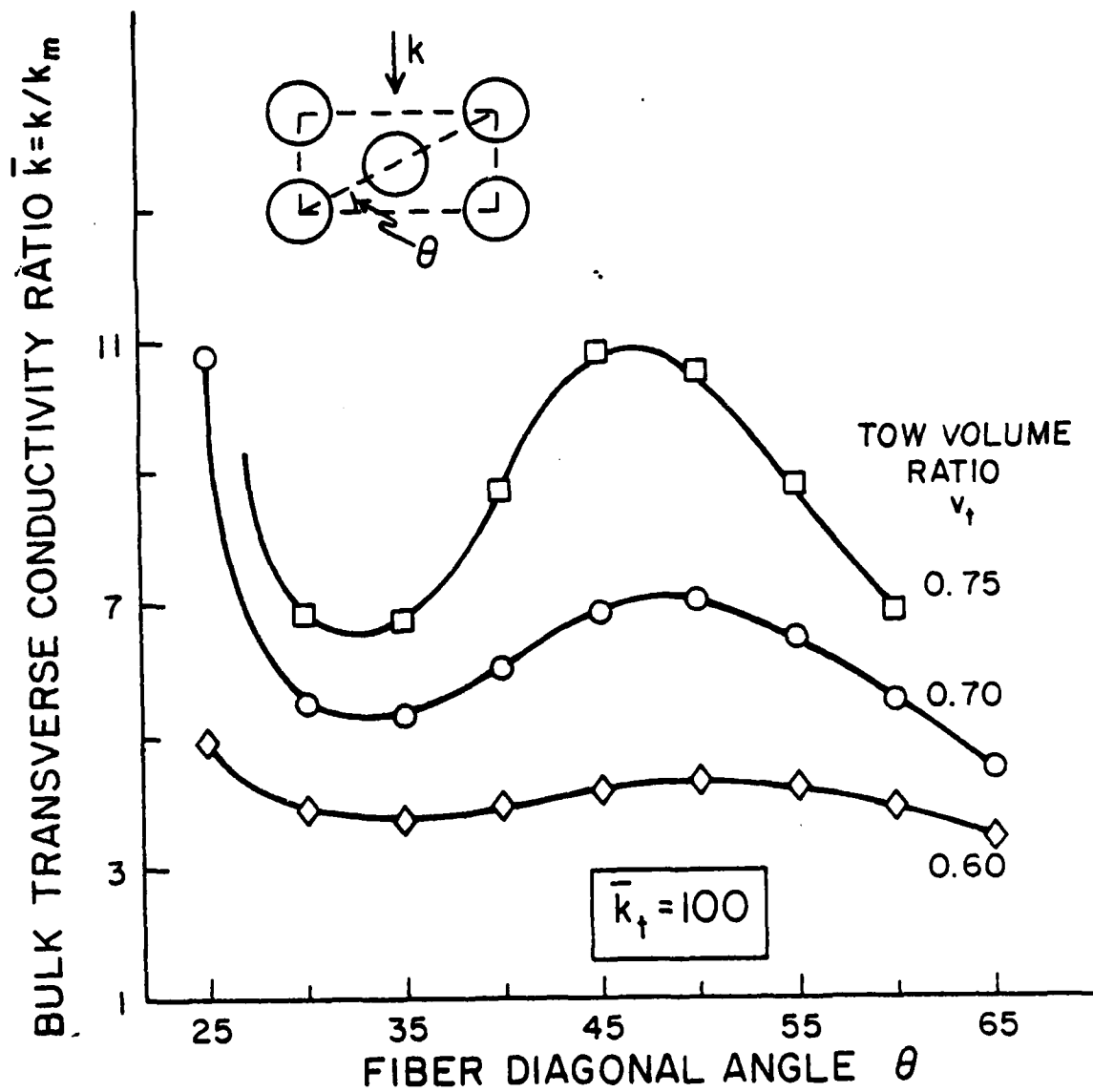


Figure II-16. Illustrating the Influence of Fiber Diagonal Angle on the Transverse Conductivity of A Staggered Array. Data from Table II-7 [1].

ratio  $\ell \equiv D/L$ , where  $2L = C/\sin \theta$ , is given by

$$\ell = 2D \sin \theta / C = 2 S \sin \theta$$

Or, using equation (II-21)

$$\ell / (v_t)^{1/2} = (8/\pi)^{1/2} (\sin \theta \cos \theta)^{1/2} \quad (\text{II-22})$$

The ratio of the tow volume fraction to its maximum possible level ( $\bar{v} = v_t/v_{\max}$ ) is an index to the relative packing density of the fibers. For  $\theta \leq 30^\circ$ ,  $v_{\max} = (\pi/2) \tan \theta$  and, therefore (from equation II-21)

$$\begin{aligned} S/(\bar{v})^{1/2} &= 1 \\ \ell/(\bar{v})^{1/2} &= 2 \sin \theta \end{aligned} \quad (\text{II-23})$$

For  $30^\circ \leq \theta \leq 60^\circ$ ,  $v_{\max} = (\pi/8)/(\sin \theta \cos \theta)$  and

$$\begin{aligned} S/(\bar{v})^{1/2} &= (2 \sin \theta)^{-1} \\ \ell/(\bar{v})^{1/2} &= 1 \end{aligned} \quad (\text{II-24})$$

With  $\theta \geq 60^\circ$ ,  $v_{\max} = (\pi/2)/\tan \theta$  and

$$\begin{aligned} S/(\bar{v})^{1/2} &= (\tan \theta)^{-1} \\ \ell/(\bar{v})^{1/2} &= 2 \cos \theta \end{aligned} \quad (\text{II-25})$$

The general patterns on the in-line and the diagonal spacing ratios,  $S$  and  $\ell$ , as influenced by the fiber diagonal angle are shown in Figure II-17. The diagonal spacing ratio  $\ell$  ( $D/L$ , Figure II-17) for equal relative packing density (constant relative volume  $\bar{v}$ ) is seen to dominate throughout the angle range 30-60 degrees. The in-line spacing ratio  $S$  decreases appreciably between 30 and 60 degrees. Below 30 degrees, the in-line spacing ratio is larger, though both are seen to be important. Above 60 degrees, the diagonal spacing ratio prevails. Thus, from the patterns on these geometrical factors, it is evident that both the diagonal and the in-line series conduction paths in addition to the continuous matrix path, can be important, and that

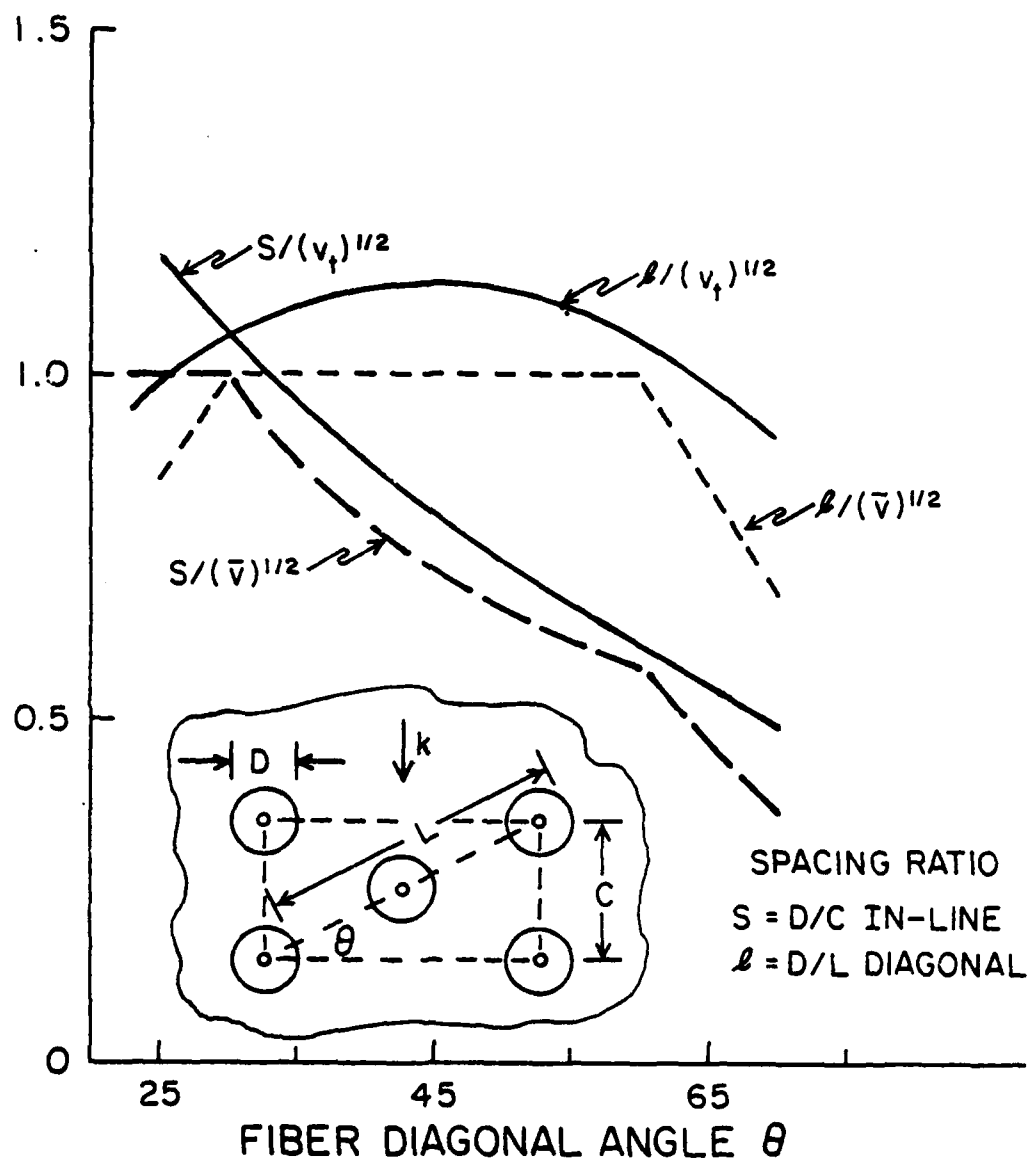


Figure II-17. Illustrating the Patterns on the Variation in the Fiber Spacing Ratios with the Fiber Diagonal Angle for the Staggered Regular Array.

these factors when combined with the transverse temperature gradient are capable of producing the general pattern shown in Figure II-16 for the variation in the transverse conductivity with the fiber packing angle.

b. Transverse Conductivity Data for the Staggered Array.

The transverse conductivity of a tow-matrix system consisting of parallel, circular fibers embedded in a staggered regular array (Figure II-15) was also studied by Han and Cosner [1] for a range on the tow-to-matrix conductivity ratio  $\bar{k}_t$  from 0.1 to 2000, for a range on the fiber diagonal angle from 25 to 65 degrees and for a range on the tow volume ratio  $v_t$  from 0.1 to values approaching the maximum possible packing level for each fiber diagonal angle. Their comprehensive data for the staggered array are summarized in Table II-7.

The error-spread studies for this array were used to limit the maximum values of the tow-volume ratio  $v_t$  included in Table II-7; the maximum values of  $v_t$  correspond to an expected error spread of one per cent. For the second highest level of the tow volume ratio  $v_t$  shown in Table II-7, the average error spread is only one-fourth to one-third of one per cent.

The use of the reciprocity method to define values of the transverse conductivity at  $\bar{k}_t < 0.10$  appears to be applicable also to these data, providing both the reciprocal of  $\bar{k}_t$  and the complement of the fiber diagonal angle  $\theta$  are used. For example, if the tow-to-matrix conductivity ratio  $\bar{k}_t$  is  $10^{-2}$ ,  $v_t = 0.70$  and  $\theta = 35^\circ$ , then  $\bar{k} = k/k_m$   $6.457^{-1} = 0.1549$ , since (from Table II-7)  $\bar{k} = 6.457$  at  $\bar{k}_t = 100$ ,  $v_t = 0.70$  and  $\theta = 55^\circ$ .

Table II-7. Han-Cosner Values of the Bulk Transverse (In-Line) Relative Conductivity ( $\bar{k} = k/k_m$ ) for A Tow-Matrix System Consisting of Circular Filaments (Uniform Diameter) Unidirectionally Embedded in A Staggered Regular Array. Homogeneous Tow, Transversely Isotropic. Homogeneous Matrix, Isotropic. No Voids. No Interfacial Resistances. [1]. See Footnote to Table II-1.

1)  $\theta = 25^\circ$ ,  $v_{\max} = 0.7324$

Tow-to-Matrix Conductivity Ratio $\bar{k}_t$	Tow Volume Ratio $v_t$			
	0.10	0.20	0.30	0.40
0.10	0.8505	0.7247	0.6173	0.5243
0.20	0.8762	0.7689	0.6750	0.5918
0.40	0.9183	0.8440	0.7761	0.7137
0.60	0.9514	0.9055	0.8619	0.8207
1.00	1.0000	1.0000	1.0000	1.0000
2.00	1.0693	1.1445	1.2261	1.3153
4.00	1.1289	1.2786	1.4546	1.6650
6.00	1.1557	1.3422	1.5698	1.8547
10.00	1.1807	1.4036	1.6856	2.0556
20.00	1.2021	1.4576	1.7915	2.2488
40.00	1.2137	1.4877	1.8522	2.3641
60.00	1.2178	1.4983	1.8738	2.4059
100.00	1.2211	1.5069	1.8916	2.4407
200.00	1.2236	1.5135	1.9053	2.4676
400.00	1.2248	1.5169	1.9122	2.4814
600.00	1.2253	1.5180	1.9146	2.4860
1000.00	1.2256	1.5189	1.9164	2.4897
2000.00	1.2259	1.5196	1.9179	2.4925
	0.50	0.60	0.65	0.69
0.10	0.4427	0.3698	0.3360	0.3101
0.20	0.5176	0.4504	0.4191	0.3949
0.40	0.6561	0.6026	0.5773	0.5575
0.60	0.7814	0.7441	0.7260	0.7119
1.00	1.0000	1.0000	1.0000	1.0000
2.00	1.4132	1.5215	1.5803	1.6297
4.00	1.9222	2.2477	2.4487	2.6341
6.00	2.2245	2.7337	3.0772	3.4202
10.00	2.5677	3.3458	3.9341	4.5928
20.00	2.9229	4.0609	5.0441	6.3307
40.00	3.1479	4.5650	5.9099	7.9064
60.00	3.2320	4.7651	6.2756	8.6429
100.00	3.3031	4.9396	6.6054	9.3488
200.00	3.3588	5.0799	6.8784	9.9658
400.00	3.3875	5.1533	7.0241	10.3080
600.00	3.3971	5.1783	7.0742	10.4280
1000.00	3.4049	5.1985	7.1148	10.5260
2000.00	3.4108	5.2138	7.1456	10.6010

Table II-7. (Cont.)

ii)  $\theta = 30^\circ$ ,  $v_{\max} = 0.9069$ 

(See Table II-4)

iii)  $\theta = 35^\circ$ ,  $v_{\max} = 0.8358$ 

Tow-to-Matrix Conductivity Ratio $\bar{k}_t$	Tow Volume Ratio $v_t$				
	0.10	0.20	0.30	0.40	0.50
0.10	0.8481	0.7165	0.6012	0.4993	0.4081
0.20	0.8745	0.7631	0.6634	0.5735	0.4918
0.40	0.9176	0.8414	0.7706	0.7048	0.6432
0.60	0.9512	0.9045	0.8599	0.8172	0.7763
1.00	1.0000	1.0000	1.0000	1.0000	1.0000
2.00	1.0688	1.1423	1.2208	1.3051	1.3958
4.00	1.1272	1.2706	1.4337	1.6211	1.8394
6.00	1.1532	1.3302	1.5374	1.7835	2.0823
10.00	1.1773	1.3870	1.6392	1.9489	2.3415
20.00	1.1978	1.4364	1.7302	2.1021	2.5927
40.00	1.2090	1.4637	1.7816	2.1909	2.7435
60.00	1.2129	1.4733	1.7997	2.2226	2.7984
100.00	1.2160	1.4811	1.8146	2.2488	2.8441
200.00	1.2184	1.4870	1.8260	2.2689	2.8796
400.00	1.2196	1.4900	1.8317	2.2792	2.8977
600.00	1.2200	1.4910	1.8337	2.2826	2.9037
1000.00	1.2203	1.4919	1.8352	2.2854	2.9086
2000.00	1.2206	1.4925	1.8364	2.2875	2.9123
	0.60	0.65	0.70	0.75	0.80
0.10	0.3252	0.2862	0.2483	0.2109	0.1725
0.20	0.4169	0.3814	0.3470	0.3133	0.2796
0.40	0.5853	0.5576	0.5307	0.5043	0.4783
0.60	0.7370	0.7179	0.6992	0.6808	0.6626
1.00	1.0000	1.0000	1.0000	1.0000	1.0000
2.00	1.4939	1.5461	1.6007	1.6580	1.7182
4.00	2.0987	2.2488	2.4166	2.6069	2.8281
6.00	2.4570	2.6851	2.9518	3.2725	3.6773
10.00	2.8632	3.2000	3.6160	4.1561	4.9284
20.00	3.2834	3.7572	4.3796	5.2668	6.7758
40.00	3.5495	4.1240	4.9108	6.1103	8.4648
60.00	3.6490	4.2642	5.1203	6.4611	9.2628
100.00	3.7332	4.3840	5.3022	6.7749	10.0340
200.00	3.7991	4.4787	5.4480	7.0327	10.7130
400.00	3.8330	4.5278	5.5242	7.1698	11.0930
600.00	3.8445	4.5444	5.5501	7.2168	11.2260
1000.00	3.8537	4.5577	5.5710	7.2549	11.3360
2000.00	3.8606	4.5678	5.5868	7.2837	11.4190

Table II-7. (Cont.)

iv)  $\theta = 40^\circ$ ,  $v_{\max} = 0.7975$ .

Tow-to-Matrix Conductivity Ratio $\bar{k}_t$	Tow Volume Ratio $v_t$				
	0.10	0.20	0.30	0.40	0.50
0.10	0.8482	0.7169	0.6018	0.4997	0.4075
0.20	0.8746	0.7634	0.6639	0.5739	0.4918
0.40	0.9176	0.8415	0.7709	0.7051	0.6434
0.60	0.9512	0.9046	0.8600	0.8174	0.7764
1.00	1.0000	1.0000	1.0000	1.0000	1.0000
2.00	1.0689	1.1424	1.2211	1.3058	1.3971
4.00	1.1273	1.2711	1.4350	1.6243	1.8471
6.00	1.1533	1.3309	1.5393	1.7889	2.0966
10.00	1.1775	1.3879	1.6421	1.9574	2.3654
20.00	1.1980	1.4376	1.7341	2.1141	2.6287
40.00	1.2092	1.4650	1.7861	2.2052	2.7882
60.00	1.2131	1.4746	1.8044	2.2378	2.8466
100.00	1.2163	1.4825	1.8195	2.2648	2.8953
200.00	1.2187	1.4885	1.8311	2.2855	2.9331
400.00	1.2199	1.4915	1.8369	2.2961	2.9524
600.00	1.2203	1.4925	1.8389	2.2996	2.9589
1000.00	1.2206	1.4933	1.8404	2.3025	2.9642
2000.00	1.2209	1.4939	1.8416	2.3046	2.9681
	0.60	0.65	0.70	0.75	0.77
0.10	0.3223	0.2814	0.2408	0.1993	0.1814
0.20	0.4154	0.3788	0.3429	0.3069	0.2922
0.40	0.5852	0.5572	0.5297	0.5027	0.4920
0.60	0.7371	0.7180	0.6992	0.6806	0.6733
1.00	1.0000	1.0000	1.0000	1.0000	1.0000
2.00	1.4965	1.5497	1.6056	1.6647	1.6893
4.00	2.1171	2.2768	2.4595	2.6737	2.7722
6.00	2.4937	2.7442	3.0485	3.4365	3.6310
10.00	2.9305	3.3149	3.8191	4.5427	4.9563
20.00	3.3942	3.9586	4.7685	6.1251	7.0599
40.00	3.6945	4.3986	5.4744	7.5080	9.1511
60.00	3.8083	4.5704	5.7641	8.1388	10.2000
100.00	3.9051	4.7188	6.0213	8.7344	11.2530
200.00	3.9813	4.8372	6.2312	9.2480	12.2140
400.00	7.0207	4.8989	6.3423	9.5304	12.7660
600.00	4.0340	4.9199	6.3803	9.6288	12.9620
1000.00	4.0447	4.9368	6.4110	9.7091	13.1240
2000.00	4.0528	4.9495	6.4343	0.7702	13.2480



Table II-7. (Cont.)

v)  $\theta = 45^\circ$ ,  $v_{\max} = 0.7854$ .

Tow-to-Matrix Conductivity Ratio $k_t$	Tow Volume Ratio $v_t$					
	0.10	0.20	0.30	0.40	0.50	
0.10	0.8487	0.7187	0.6053	0.5049	0.4140	
0.20	0.8750	0.7647	0.6664	0.5778	0.4968	
0.40	0.9178	0.8421	0.7721	0.7070	0.6460	
0.60	0.9512	0.9048	0.8604	0.8181	0.7775	
1.00	1.0000	1.0000	1.0000	1.0000	1.0000	
2.00	1.0690	1.1429	1.2223	1.3080	1.4010	
4.00	1.1277	1.2728	1.4395	1.6339	1.8657	
6.00	1.1538	1.3334	1.5463	1.8045	2.1283	
10.00	1.1782	1.3915	1.6520	1.9806	2.4155	
20.00	1.1990	1.4421	1.7472	2.1459	2.7011	
40.00	1.2102	1.4701	1.8011	2.2426	2.8763	
60.00	1.2142	1.4799	1.8202	2.2773	2.9408	
100.00	1.2174	1.4880	1.8359	2.3061	2.9948	
200.00	1.2198	1.4941	1.8479	2.3283	3.0368	
400.00	1.2210	1.4972	1.8540	2.3396	3.0583	
600.00	1.2214	1.4982	1.8561	2.3434	3.0656	
1000.00	1.2217	1.4991	1.8577	2.3464	3.0714	
2000.00	1.2220	1.4997	1.8590	2.3487	3.0758	
	0.60	0.65	0.70	0.72	0.74	0.75
0.10	0.3293	0.2880	0.2465	0.2282	0.2095	0.2051
0.20	0.4212	0.3846	0.3485	0.3333	0.3181	0.3127
0.40	0.5885	0.5608	0.5335	0.5226	0.5117	0.5068
0.60	0.7386	0.7196	0.7010	0.6935	0.6862	0.6826
1.00	1.0000	1.0000	1.0000	1.0000	1.0000	1.0000
2.00	1.5028	1.5576	1.6154	1.6395	1.6643	1.6765
4.00	2.1510	2.3224	2.5206	2.6107	2.7076	2.7550
6.00	2.5561	2.8318	3.1725	3.3374	3.5225	3.6140
10.00	3.0372	3.4731	4.0005	4.3692	4.7392	4.9301
20.00	3.5617	4.2229	5.2114	5.7877	6.5450	6.9714
40.00	3.9093	4.7523	6.1104	6.9669	8.1821	8.9284
60.00	4.0426	4.9627	6.4905	7.4858	8.9468	9.8812
100.00	4.1566	5.1463	6.8334	7.9652	9.6792	10.8190
200.00	4.2470	5.2940	7.1175	8.3703	10.3190	11.6580
400.00	4.2938	5.3713	7.2692	8.5899	10.6740	12.1330
600.00	4.3096	5.3977	7.3213	8.6659	10.7980	12.3000
1000.00	4.3224	5.4189	7.3636	8.7277	10.8990	12.4380
2000.00	4.3320	5.4350	7.3957	8.7747	10.9770	12.5430

Table II-7 (Cont.)

vi)  $\theta = 50^\circ$ ,  $v_{\max} = 0.7975$ .

Tow-to-Matrix Conductivity Ratio $k_t$	Tow Volume Ratio $v_t$				
	0.10	0.20	0.30	0.40	0.50
0.10	0.8493	0.7205	0.6090	0.5109	0.4228
0.20	0.8754	0.7659	0.6690	0.5821	0.5031
0.40	0.9180	0.8427	0.7733	0.7090	0.6491
0.60	0.9513	0.9050	0.8609	0.8189	0.7787
1.00	1.0000	1.0000	1.0000	1.0000	1.0000
2.00	1.0691	1.1433	1.2234	1.3101	1.4045
4.00	1.1280	1.2745	1.4439	1.6427	1.8810
6.00	1.1544	1.3360	1.5531	1.8185	2.1536
10.00	1.1790	1.3950	1.6616	2.0012	2.4541
20.00	1.1999	1.4466	1.7597	2.1737	2.7556
40.00	1.2113	1.4752	1.8155	2.2752	2.9418
60.00	1.2152	1.4852	1.8353	2.3117	3.0105
100.00	1.2184	1.4934	1.8516	2.3420	3.0681
200.00	1.2209	1.4997	1.8641	2.3654	3.1130
400.00	1.2221	1.5029	1.8704	2.3773	3.1361
600.00	1.2225	1.5039	1.8725	2.3813	3.1438
1000.00	1.2229	1.5048	1.8742	2.3845	3.1501
2000.00	1.2231	1.5054	1.8755	2.3869	3.1548
	0.60	0.65	0.70	0.74	
0.10	0.3412	0.3016	0.2617	0.2294	
0.20	0.4299	0.3947	0.3599	0.3321	
0.40	0.5928	0.5657	0.5392	0.5184	
0.60	0.7402	0.7215	0.7032	0.6888	
1.00	1.0000	1.0000	1.0000	1.0000	
2.00	1.5080	1.5637	1.6224	1.6725	
4.00	2.1749	2.3509	2.5532	2.7457	
6.00	2.5968	2.8810	3.2281	3.5854	
10.00	3.1023	3.5528	4.1487	4.8291	
20.00	3.6581	4.3432	5.3400	6.6376	
40.00	4.0289	4.9036	6.2672	8.2314	
60.00	4.1716	5.1270	6.6581	8.9603	
100.00	4.2939	5.3220	7.0101	9.6489	
200.00	4.3909	5.4791	7.3012	10.2430	
400.00	4.4412	5.5613	7.4565	10.5690	
600.00	4.4583	5.5894	7.5099	10.6830	
1000.00	4.4720	5.6120	7.5531	10.7760	
2000.00	4.4824	5.6291	7.5859	10.8470	

Table II-7. (Cont.)

vii)  $\theta = 55^\circ$ ,  $v_{\max} = 0.8358$ .

Tow-to-Matrix Conductivity Ratio $\bar{k}_t$	Tow Volume Ratio $v_t$				
	0.10	0.20	0.30	0.40	0.50
0.10	0.8494	0.7210	0.6101	0.5131	0.4271
0.20	0.8754	0.7663	0.6697	0.5836	0.5060
0.40	0.9180	0.8428	0.7736	0.7096	0.6503
0.60	0.9513	0.9050	0.8610	0.8191	0.7791
1.00	1.0000	1.0000	1.0000	1.0000	1.0000
2.00	1.0691	1.1434	1.2237	1.3105	1.4049
4.00	1.1281	1.2749	1.4447	1.6438	1.8811
6.00	1.1545	1.3366	1.5543	1.8199	2.1526
10.00	1.1791	1.3958	1.6633	2.0029	2.4507
20.00	1.2001	1.4475	1.7618	2.1755	2.7485
40.00	1.2115	1.4763	1.8179	2.2769	2.9316
60.00	1.2155	1.4864	1.8378	2.3135	2.9990
100.00	1.2187	1.4946	1.8541	2.3437	3.0555
200.00	1.2212	1.5009	1.8666	2.3671	3.0995
400.00	1.2224	1.5041	1.8730	2.3790	3.1221
600.00	1.2228	1.5052	1.8751	2.3830	3.1297
1000.00	1.2231	1.5060	1.8768	2.3862	3.1358
2000.00	1.2234	1.5067	1.8781	2.3886	3.1404
	0.60	0.65	0.70	0.75	0.77
0.10	0.3493	0.3125	0.2765	0.2404	0.2258
0.20	0.4351	0.4017	0.3691	0.3371	0.3243
0.40	0.5948	0.5683	0.5426	0.5175	0.5076
0.60	0.7409	0.7224	0.7042	0.6864	0.6794
1.00	1.0000	1.0000	1.0000	1.0000	1.0000
2.00	1.5081	1.5635	1.6217	1.6831	1.7084
4.00	2.1705	2.3412	2.5348	2.7576	2.8547
6.00	2.5846	2.8552	3.1781	3.5743	3.7558
10.00	3.0749	3.4939	4.0270	4.7399	5.0921
20.00	3.6062	4.2264	5.0761	6.3424	7.0368
40.00	3.9560	4.7335	5.8552	7.6686	8.7517
60.00	4.0896	4.9327	6.1742	8.2500	9.5363
100.00	4.2038	5.1054	6.4568	8.7855	10.2780
200.00	4.2940	5.2436	6.6873	9.2369	10.9180
400.00	4.3407	5.3157	6.8090	9.4812	11.2690
600.00	4.3565	5.3402	6.8506	9.5656	11.3920
1000.00	4.3692	5.3599	6.8843	9.6343	11.4920
2000.00	4.3788	5.3749	6.9098	9.6864	11.5680

Table II-7. (Cont.)

viii)  $\theta = 60^\circ$ ,  $v_{\max} = 0.9069$ 

Tow-to-Matrix Conductivity Ratio $\bar{k}_t$		Tow Volume Ratio $v_t$				
		0.10	0.20	0.30	0.40	0.50
0.10		0.8487	0.7188	0.6058	0.5068	0.4190
0.20		0.8750	0.7647	0.6667	0.5789	0.4998
0.40		0.9178	0.8421	0.7721	0.7073	0.6470
0.60		0.9512	0.9048	0.8605	0.8182	0.7778
1.00		1.0000	1.0000	1.0000	1.0000	1.0000
2.00		1.0690	1.1429	1.2222	1.3077	1.4001
4.00		1.1277	1.2727	1.4390	1.6317	1.8577
6.00		1.1538	1.3333	1.5455	1.8002	2.1122
10.00		1.1782	1.3913	1.6506	1.9733	2.3865
20.00		1.1990	1.4419	1.7451	2.1348	2.6551
40.00		1.2102	1.4699	1.7987	2.2289	2.8177
60.00		1.2142	1.4797	1.8176	2.2626	2.8770
100.00		1.2173	1.4877	1.8332	2.2905	2.9266
200.00		1.2198	1.4938	1.8451	2.3120	2.9651
400.00		1.2210	1.4969	1.8511	2.3230	2.9848
600.00		1.2214	1.4979	1.8531	2.3266	2.9914
1000.00		1.2217	1.4988	1.8548	2.3296	2.9967
2000.00		1.2220	1.4994	1.8560	2.3318	3.0007
		0.60	0.65	0.70	0.75	0.80
0.10	0.3404	0.3039	0.2689	0.2351	0.2020	0.1690
0.20	0.4279	0.3943	0.3619	0.3306	0.3002	0.2702
0.40	0.5907	0.5639	0.5379	0.5126	0.4880	0.4638
0.60	0.7391	0.7203	0.7020	0.6840	0.6663	0.6490
1.00	1.0000	1.0000	1.0000	1.0000	1.0000	1.0000
2.00	1.5002	1.5536	1.6095	1.6680	1.7295	1.7943
4.00	2.1272	2.2830	2.4564	2.6511	2.8726	3.1295
6.00	2.5047	2.7428	3.0184	3.3429	3.7339	4.2221
10.00	2.9376	3.2906	3.7191	4.2541	4.9494	5.9152
20.00	3.3901	3.8883	4.5253	5.3764	6.5917	8.5447
40.00	3.6790	4.2842	5.0850	6.2068	7.9252	11.0420
60.00	3.7875	4.4359	5.3052	6.5459	8.5023	12.2440
100.00	3.8795	4.5656	5.4962	6.8461	9.0300	13.4190
200.00	3.9516	4.6684	5.6492	7.0906	9.4720	14.4620
400.00	3.9888	4.7216	5.7290	7.2197	9.7100	15.0480
600.00	4.0013	4.7396	5.7561	7.2638	9.7921	15.2550
1000.00	4.0114	4.7541	5.7780	7.2995	9.8588	15.4240
2000.00	4.0191	4.7651	5.7946	7.3265	9.9094	15.5540

Table II-7. (Concluded).

ix)  $\theta = 65^\circ$ ,  $v_{\max} = 0.7324$ .

Tow-to-Matrix Conductivity Ratio $\bar{k}_t$	Tow Volume Ratio $v_t$				
	0.10	0.20	0.30	0.40	0.50
0.10	0.8469	0.7125	0.5932	0.4865	0.3895
0.20	0.8738	0.7603	0.6577	0.5643	0.4784
0.40	0.9173	0.8401	0.7680	0.7004	0.6367
0.60	0.9510	0.9040	0.8589	0.8156	0.7738
1.00	1.0000	1.0000	1.0000	1.0000	1.0000
2.00	1.0686	1.1413	1.2185	1.3006	1.3884
4.00	1.1264	1.2671	1.4248	1.6029	1.8065
6.00	1.1520	1.3250	1.5236	1.7548	2.0282
10.00	1.1758	1.3799	1.6199	1.9071	2.2592
20.00	1.1959	1.4273	1.7051	2.0461	2.4777
40.00	1.2069	1.4535	1.7529	2.1258	2.6065
60.00	1.2107	1.4626	1.7697	2.1540	2.6529
100.00	1.2138	1.4700	1.7835	2.1774	2.6914
200.00	1.2161	1.4757	1.7940	2.1953	2.7211
400.00	1.2173	1.4786	1.7994	2.2043	2.7362
600.00	1.2177	1.4795	1.8011	2.2074	2.7413
1000.00	1.2180	1.4803	1.8026	2.2098	2.7454
2000.00	1.2182	1.4809	1.8037	2.2117	2.7485
	0.60	0.65	0.70	0.72	
0.10	0.2990	0.2546	0.2083	0.1820	
0.20	0.3981	0.3592	0.3203	0.3012	
0.40	0.5764	0.5472	0.5186	0.5063	
0.60	0.7335	0.7139	0.6945	0.6866	
1.00	1.0000	1.0000	1.0000	1.0000	
2.00	1.4824	1.5320	1.5837	1.6049	
4.00	2.0426	2.1760	2.3216	2.3839	
6.00	2.3591	2.5531	2.7712	2.8669	
10.00	2.7046	2.9764	3.2924	3.4348	
20.00	3.0475	3.4092	3.8441	4.0455	
40.00	3.2573	3.6805	4.2001	4.4450	
60.00	3.3343	3.7814	4.3347	4.5971	
100.00	3.3989	3.8665	4.4489	4.7268	
200.00	3.4491	3.9329	4.5398	4.8291	
400.00	3.4748	3.9671	4.5852	4.8820	
600.00	3.4834	3.9786	4.6009	4.8999	
1000.00	3.4904	3.9879	4.6135	4.9143	
2000.00	3.4956	3.9949	4.6231	4.9252	

c. Modified Rayleigh Equation.

The Rayleigh parameter  $mv_t$  once again serves as a first-order correlation parameter for the staggered regular array (Figure II-18). However, the secondary effect of the fiber diagonal angle is seen to be appreciable, so that modification of the Rayleigh equation is necessary to produce a working equation having reasonable levels of accuracy.

Of the various modification procedures explored, the following method based on the relative packing density (which in one way is similar to the Neilson modification [16] of the Halpin-Tsai equation [12] and in another way similar to one of the two Donea bound equations [9] --- though the numerical results are quite different) is estimated to be the most useful. Here, a relative Rayleigh parameter is used, along with an adjustment factor for the fiber angle. The extent to which the transverse conductivity of the staggered array is correlated by the Rayleigh parameter modified to the relative volume ( $m\bar{v} = mv_t/v_m$ ) is shown in Figure II-19 to be within approximately  $\pm 15$  per cent. However, the hexagonal array ( $30^\circ$ ) and the square array ( $45^\circ$ ) are covered by equations (II-3) and (II-12), respectively. Thus, with reference to Figure II-19, and after extensive exploration, the best method is judged to be as follows. Let

$$\bar{k} = k/k_m = (\bar{C} + \bar{F}m\bar{v})/\bar{C} - \bar{F}m\bar{v} \quad (\text{II-26})$$

where

$$\bar{F} = 1 + [(\bar{v})^6/9](\bar{k}_t - a)/(\bar{k}_t + a)$$

$$m = (\bar{k}_t - 1)/(\bar{k}_t + 1)$$

$$\bar{v} = v_t/v_{\max}$$

$$a = 2.25 \text{ for } \bar{k}_t > 2, a = 5/3 \text{ for } \bar{k}_t \approx 2 \text{ and } a = \bar{k}_t \text{ for } 1 < \bar{k}_t < 2$$

and where

$$\bar{C} = 1.242 \text{ for } \theta \text{ of } 25, 35 \text{ and } 40 \text{ degrees}$$

$$\bar{C} = 1.183 \text{ for } \theta \text{ of } 50 \text{ and } 55 \text{ degrees}$$

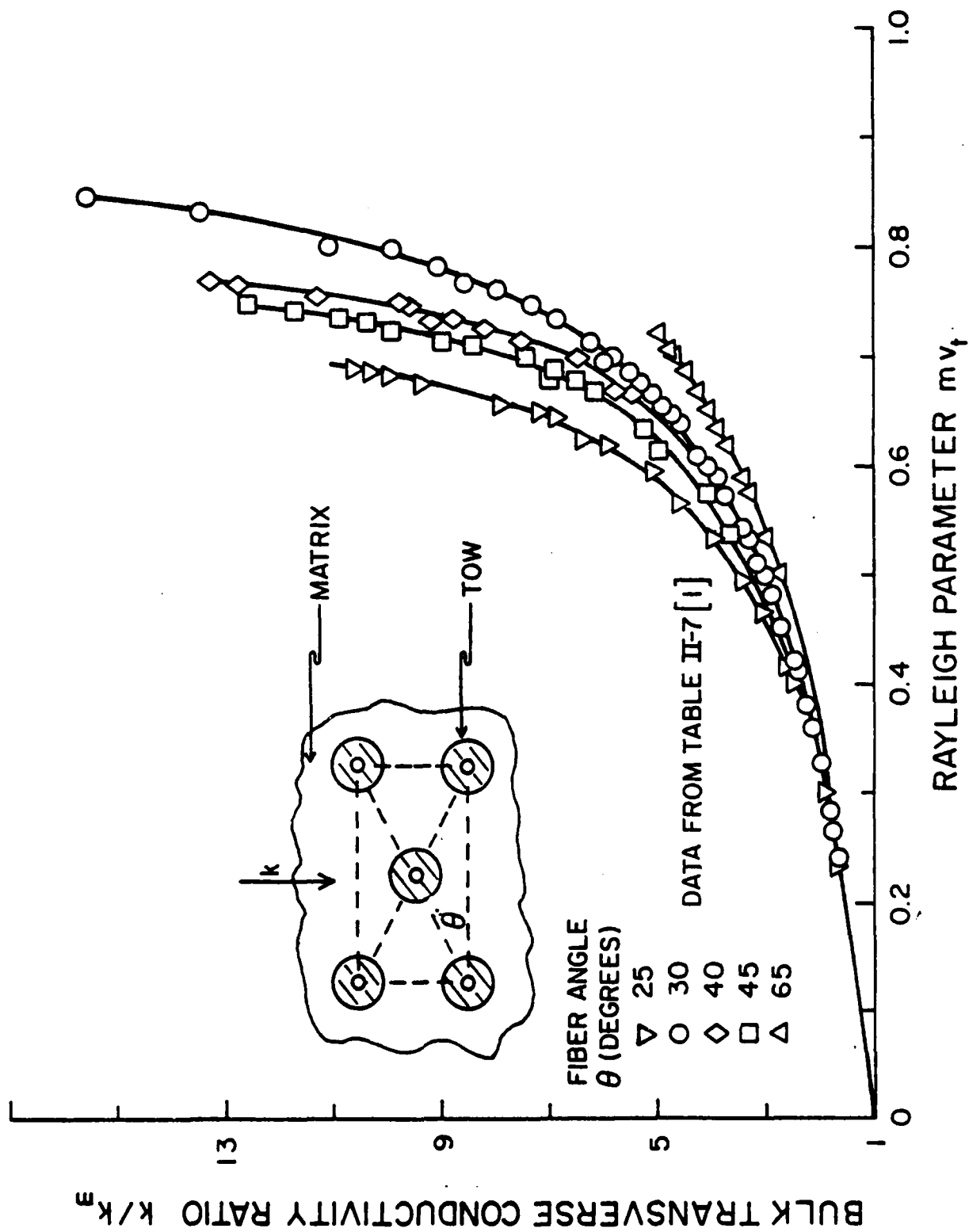


Figure II-18. Illustrating the extent to which the Rayleigh Parameter  $mv_t$  Correlates the Staggered Array Conductivity.

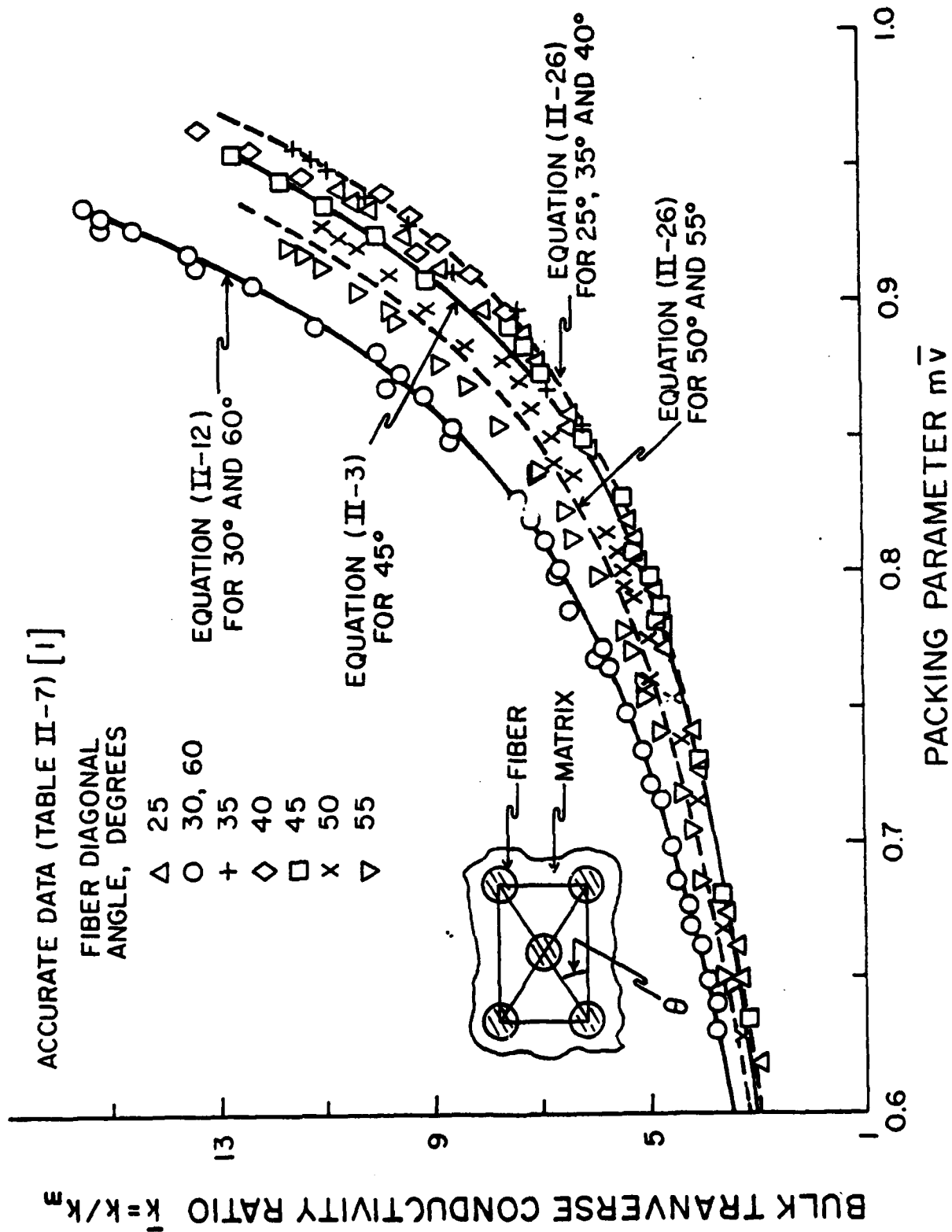


Figure II-19. Correlation of Transverse Conductivity for the Staggered Array by Use of a Packing Parameter (the Rayleigh Parameter Based on Relative Volume).



This method produces results within approximately  $\pm 5$  per cent of the accurate data (Table II-7). For mid-range levels of both the tow volume ratio  $v_t$  and the tow conductivity ratios  $\bar{k}_t$ , its accuracy is essentially  $\pm 2$  per cent.

For a fiber diagonal angle of  $65^\circ$ , the following method describes the accurate data (Table II-7) to within one per cent.

$$\bar{k} = k/k_m = (C + Fmv_t)/(C - Fmv_t) \quad (\text{II-27})$$

where

$$F = 1 + (v_t^7/9)(\bar{k}_t - a)/(\bar{k}_t + a)$$

$$C = 1.26 + 0.14 mv_t$$

$$m = (\bar{k}_t - 1)/(\bar{k}_t + 1)$$

and with  $a$  having values as for Equation (II-26).

The Rayleigh equation modified to use a Rayleigh parameter based on the relative tow packing density ( $m\bar{v}$  rather than  $mv_t$ ) and of the simple form

$$\bar{k} = (1 + 0.9 m\bar{v})/(1 - 0.9 m\bar{v}) \quad (\text{II-28})$$

defines, for a wide range of fiber diagonal angles in a staggered array, the transverse conductivity to within  $\pm 20$  per cent. For greater accuracy (to within 5 per cent), equations (II-26) and (II-27) would be used, except for the hexagonal and square arrays. For the latter two arrays, equations (II-3) and (II-12) define the conductivities more precisely.

### SECTION III

#### Use of One-Dimensional Conduction Models to Estimate the Transverse Conductivity of Unidirectional, Filamentary Composite Materials

Simplifying the rather complex transverse conduction patterns in multi-phase materials by assuming the bulk transverse conductivity in a particular direction can be estimated from a one-dimensional conduction analysis of a multi-phase series path is a procedure which has produced useful results in a number of studies, e.g. [18], [23], [24]. The most prominent example of the application of one-dimensional conduction analysis to a conventional composite material is the paper by Springer and Tsai [18] --- a widely referenced study which demonstrates that the method produces qualitatively correct results at reasonably good levels of accuracy.

In this Section III, one-dimensional conduction analysis is used to define the conductivity of various tow-matrix series paths. These results are then applied in parallel with matrix paths to define approximate models for the transverse conductivities. Typically, these unadjusted models are accurate to  $\pm 25$ -35 per cent. They are then adjusted and modified to replicate the accurate Han-Cosner data [1] to within several per cent..... usually within one per cent. Again, the use of relative fiber packing density (the ratio of the actual fiber volume to the maximum level possible) is found to be helpful in adapting the models to the various packing configurations.

#### Square Array

##### a. Approximate Model for Transverse Conductivity Based on Fibers of Equivalent Uniform Thickness.

The bulk transverse conductivity of a tow-matrix system consisting of circular fibers embedded unidirectionally in a square array (Figure III-1) can be estimated from a simple, one-dimensional

**F/O 12/1**

AFOSR-78-3440

AFWAL-TR-80-3155

2

2012

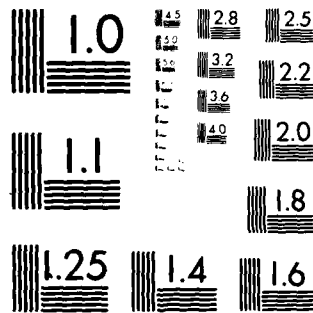
2000

END

DATE \_\_\_\_\_

FILMED

3-8



MICROCOPY RESOLUTION TEST CHART  
NATIONAL BUREAU OF STANDARDS-1963-A

conduction analysis. With reference to the approximate analysis of this tow-matrix system in Section B, the conduction is assumed to occur in two parallel paths --- the matrix path of approximate width  $(c-D)$  (Figure III-1) having a conductivity  $k_m$  and the tow-matrix series path of approximate width  $D$  having a conductivity  $k_{m-t}$ . Thus, assuming unidirectional conduction parallel to the in-line fibers, the bulk transverse conductivity in the direction  $S$  (parallel to  $C$ ) is defined roughly by

$$k_S c \doteq k_m (c-D) + k_{m-t-S} D$$

or, since for this square array  $c = C$

$$\bar{k}_S = k_S / k_m \doteq 1 + s (\bar{k}_{m-t-S} - 1) \quad (\text{III-1})$$

where  $s$  is the width spacing ratio  $D/c$ , equal for the square array to the depth spacing ratio  $S = D/C$ . The volume fraction occupied by the fibers is  $v_t = (\pi/4)(D^2/cC)$ . Using the simplifying condition that the fibers are square in section having an equivalent thickness  $D(\pi/4)^{1/2}$ , then  $v_t = s_e S_e$ , where  $s_e$  and  $S_e$  are the effective spacing ratios. For a square array,  $S_e = (v_t)^{1/2}$ .

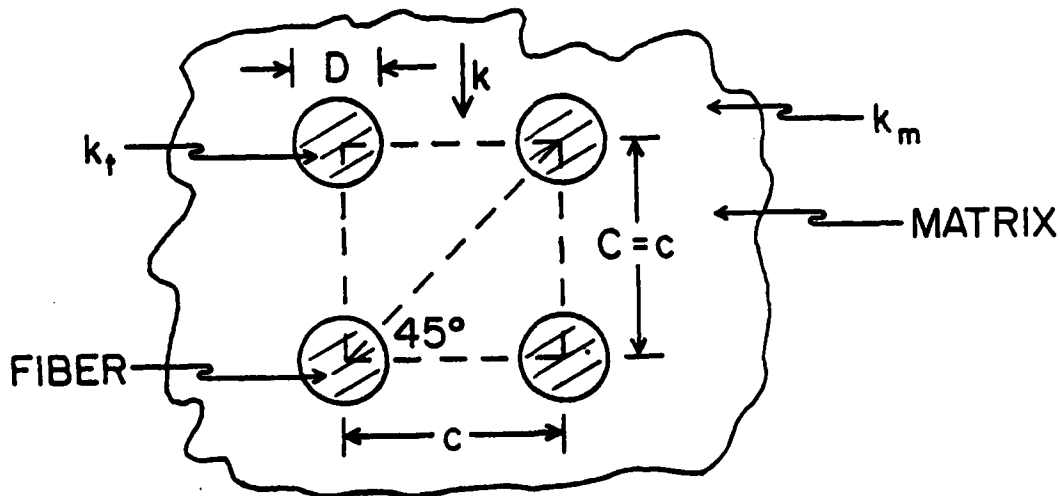


Figure III-1. Tow-Matrix System having Unidirectional Fibers Embedded in A Square Array.

The unidirectional conduction analysis of this tow-matrix series path (Section B) shows that for in-line tow elements of uniform thickness,  $\bar{k}_{m-t-S} = (1 - N_S)^{-1}$ , where  $N_S = M_S S$ , with  $M = 1 - \bar{k}_{t-S}^{-1}$ . Thus, to a first approximation, for this in-line array, equation (III-1) becomes

$$\bar{k}_S - 1 = s N_S (1 - N_S)^{-1} = M_S v_t (1 - N_S)^{-1}$$

or

$$Y_S = (1 - N_S)^{-1} = \bar{k}_{m-t-S} \quad (\text{III-2})$$

where

$$Y_S = (\bar{k}_S - 1) / M_S v_t$$

and

$$N_S = M_S S = M_S (v_t)^{1/2}$$

Equation (III-2), if rearranged, is the same as the Springer-Tsai equation for square fibers embedded in a square array [18].

The validity of this approximate analysis is indicated to a limited extent by the Zinsmeister-Purohit data [19], but comprehensively by the Han-Cosner data [1].

Zinsmeister and Purohit tested the accuracy of the Springer-Tsai equation for square fibers in a square array (based on one-dimensional conduction analysis) against results obtained for an identical tow-matrix system by finite-difference calculations. Their results agree (Table III-I) to within roughly 10 per cent, except at the highest volume fraction where excellent agreement exists. Overall, this particular model, equation (III-2), is seen to do quite well, in that the primary variables are functionally related in a comparably simple manner and the quantitative results are reasonably good.

Table III-1. Comparison of Zinsmeister-Purohit Transverse Conductivity Data for Square Fibers in A Square Array [19] with The Approximate Equation (III-2) Based on One-Dimensional Analysis.

Fiber Volume Fraction $v_t$		Fiber-to-Matrix Conductivity Ratio $\bar{k}_t$			
		$10^{-2}$	$10^{-1}$	10	$10^2$
0.1975	$k_{eq}$	0.5655	0.6445	1.296	1.349
	$k_{fi-diff}$	0.6493	0.7059	1.399	1.508
	(Ratio)	(0.871)	(0.913)	(0.927)	(0.895)
0.445		0.3429	0.4282	2.002	2.297
		0.3709	0.4525	2.160	2.588
		0.924	0.946	0.927	0.888
0.79		0.1212	0.2099	4.554	7.514
		0.1212	0.2107	4.627	7.771
		(1.000)	(0.996)	(0.984)	(0.967)

The Han-Cosner data for circular fibers embedded in a square array provide a much better basis for assessing this simplified model, in that their data cover greater ranges on the principal variables (tow-to-matrix conductivity ratio  $\bar{k}_t$  and tow volume ratio  $v_t$ ) and the tow in their study is a filament of circular section. The validity of this approximate model,  $Y_S = (1 - N_S)^{-1}$ , equation (III-2) when applied to circular fibers in a square array is illustrated in Figure III-2 for  $\bar{k}_t > 1$ . The model is qualitatively correct. Further, it is seen that the quantitative validity can be rendered reasonably good (within roughly 10 per cent, except low at tow volume ratios) by the simple introduction of a constant adjustment factor.

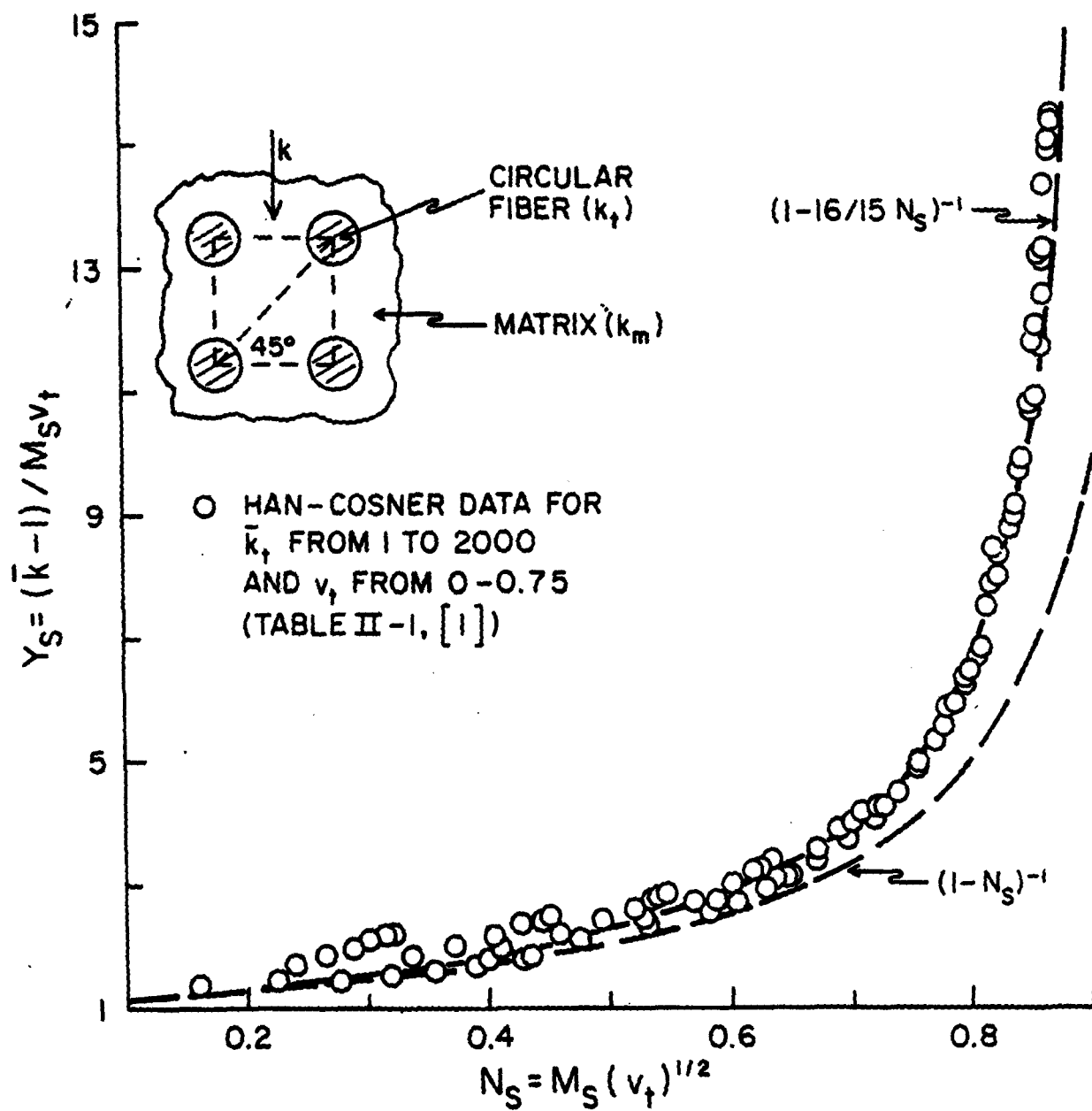


Figure III-2. Illustrating the Conceptual Validity of the One-Dimensional Model for Parallel, Circular Fibers Embedded in A Square Array.  $\bar{k}_f > 1$ .



In short, the simplest form of one-dimensional conduction analysis using fibers of equivalent uniform thickness produces qualitatively valid results for parallel circular fibers embedded in a square array.

b. One-Dimensional Analysis of the Square Array Based on A Circular Fiber.

Springer and Tsai [18] also applied one-dimensional conduction analysis to the circular fiber and showed the results to be superior to the equivalent square fiber model. The series conductivity  $k_{m-t}$  for a circular fiber (Section B) is shown to be a function of

$N_S = M_S S$ , where  $M_S = 1 - \bar{k}_{t-S}^{-1}$ ,  $\bar{k}_{t-S} = k_{t-S}/k_m$  and  $S = D/C$  (Figure III-1). For a square array,  $v_t = (\pi/4)S^2$ .

Since, for the two parallel conduction paths

$$\bar{k}_S = 1 + s (\bar{k}_{m-t-S}^{-1})$$

and for a square array,  $s = S = (4v_t/\pi)^{1/2}$ , therefore

$$(\bar{k}_S - 1)/(v_t)^{1/2} = (4/\pi)^{1/2} (\bar{k}_{m-t-S}^{-1}) \quad (\text{III-3})$$

and

$$(\bar{k}_S - 1)/(v_t)^{1/2} = f(N_S) = f(\bar{k}_{t-S}, v_t) \quad (\text{III-4})$$

where  $k_{m-t-S}$  is defined by equation (B-21) and (B-22) in Section B.

The quantitative validity of this model is shown in Figure III-3, where the accurate Han-Cosner data [1] for circular fibers in a square array (Table II-1) are used to evaluate the proportionality factor in equation (III-3). The model is reasonably good. For example, since values of the bulk conductivity for  $\bar{k}_t < 1$  can be predicted from the values for  $\bar{k}_t > 1$ , then, as a first approximation, one can simply use a single value of the proportionality factor. On this basis, the ability of the model to predict the transverse conductivity is essentially  $\pm 10$  per cent overall and about  $\pm 5$  per cent for the more usual range on  $v_t$  of 0.3-0.7.

An alternative to the model described by equation (III-3) is

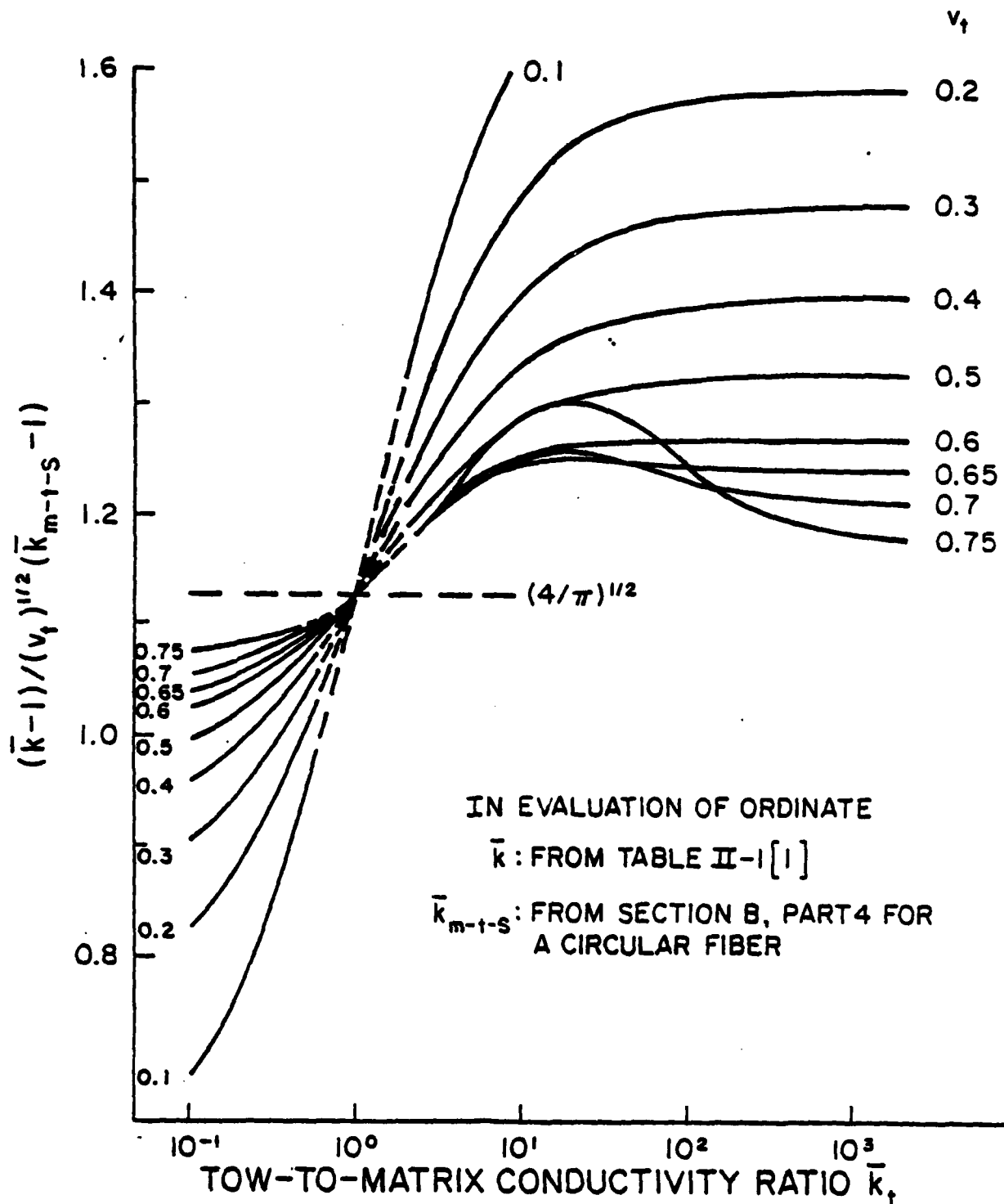


Figure III-3. Validity of One-Dimensional Conduction Analysis for the Tow-Matrix System Consisting of Parallel, Circular Fibers Embedded in A Square Array.

obtained as follows. Since, to a first approximation,  $\bar{k}_{m-t} = (1 - N)^{-1}$ , therefore, equation (III-3) can be revised to  $\bar{k} - 1 \doteq s [(1 - N)^{-1} - 1] \doteq sN/(1 - N) \doteq s S M \bar{k}_{m-t}$ , or, therefore

$$Y_S = F \bar{k}_{m-t-S} \quad (\text{III-5})$$

In this model, the functional form of the generalized transverse conductivity for tow having uniform thickness has been adapted to the tow-matrix series conductivity of a circular fiber. Note that in this model

$$Y_S = (\bar{k}_S - 1) / M_S v_t = f(N_S) = f(\bar{k}_{t-S}, v_t) \text{ circular fiber} \quad (\text{III-6})$$

The equations describing the series conductivity  $\bar{k}_{m-t}$  for a fiber, equations (B-21) and (B-22) in Section B, are somewhat cumbersome to use. Various simplified forms of these expressions were examined. And, taking into account both their accuracy and functional compatibility with the models, the following expressions are judged to be good substitutes for equations (B-21) and (B-22).

$$\bar{k}_{m-t-cir} = 1 + (\pi/4)(N)(1 - bN)^w \quad (\text{III-7})$$

$$\bar{k}_t > 1 : b = 0.99, w = -0.80$$

$$\bar{k}_t < 1 : b = 5/6, w = -0.98$$

Using this substitute, the model equation (III-1) now becomes

$$(\bar{k}_S - 1) = s (\bar{k}_{m-t-S} - 1) = (\pi/4)(sN)(1 - bN)^w$$

or, since  $N = MS$  and  $v_t = (\pi/4)(sS)$ ,

$$(\bar{k}_S - 1) / M_S v_t = Y_S \propto (1 - bN_S)^w \quad (\text{III-8})$$

This, then, is an alternate model for the circular fiber having the generalized conductivity in a functional form consistent with the previous models, but more accessible in the interpretation of the influence of primary variables on the transverse conductivity.

The agreement between this model, equation (III-8), and the Han-Cosner data is shown in Figure III-4. By striking an average value of  $F$  for  $\bar{k}_t > 1$ , the accuracy of the model is again essentially  $\pm 10$  per cent overall and  $\pm 5$  per cent within the more usual range tow-volume ratio  $v_t$  of 0.3-0.7.

Variable adjustments can be introduced in these models to improve their accuracy. For the model  $Y_S = F \bar{k}_{m-t-s}$ , equation (III-5), where  $\bar{k}_{m-t-s}$  is defined by equations (B-21) and (B-22) in Section B, the use of the following empirical relationship to describe the proportionality factor  $F$  for a square array (circular fibers)

$$F = 1 + 0.21M^2/(v_t)^{1/2}, \bar{k}_t > 1 \quad (\text{III-9})$$

results in the Han-Cosner conductivity data (Table II-1) being replicated to within one per cent for  $v_t < 2/3$  and to within from 2 to 7 per cent for  $v_t$  in the range 0.7-0.75.

For the model described by equation (III-8), the following set of empirical equations for the proportionality constant  $F$  reproduces the Han-Cosner data for the square array (circular fiber) to within one per cent for  $v_t \leq 0.7$  and to within 2 per cent at  $v_t$  of 0.75. For  $v_t \leq 0.6$ :

$$F = 1 + 0.3(1 - v_t)^{5/3} [2 - (3/\bar{k}_t)] \text{ for } \bar{k}_t \geq 3/2 \quad (\text{III-10})$$

$$F = 1 \text{ for } 1 < \bar{k}_t < 3/2$$

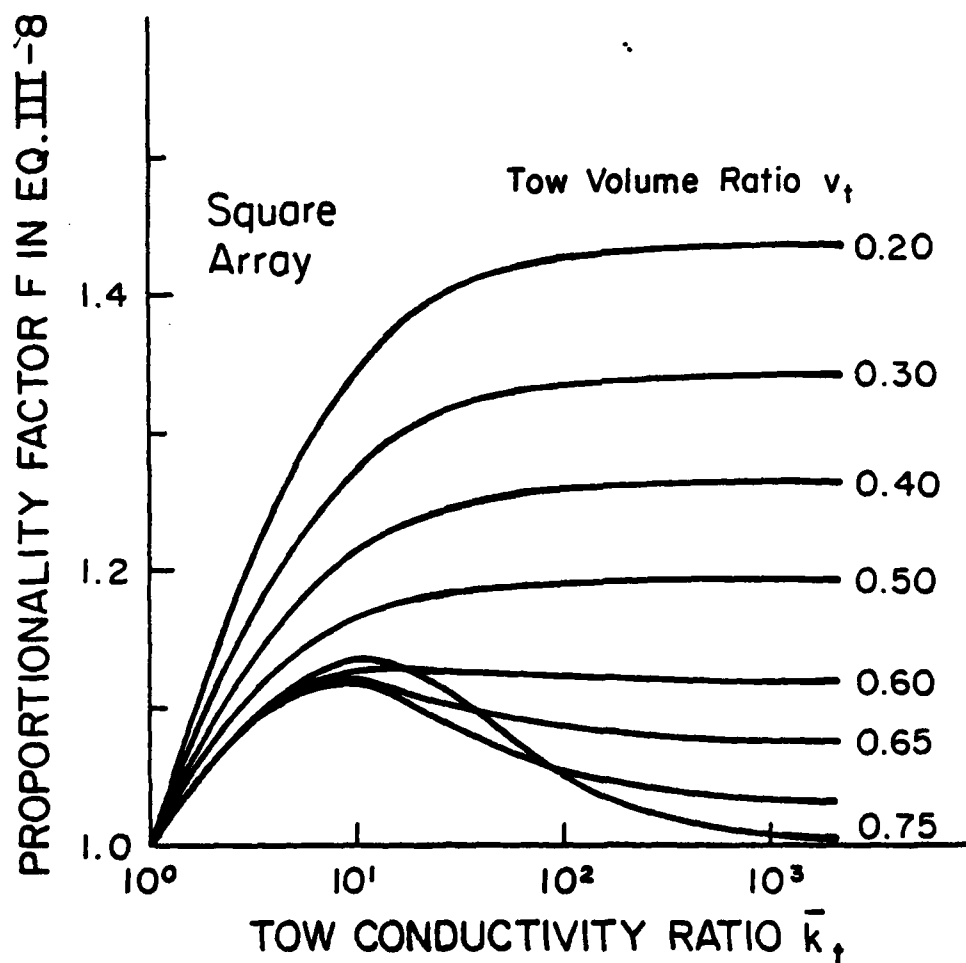


Figure III-4. Agreement of Revised One-Dimensional Model for a Circular Fiber, Equation III-8, with the Han-Cosner Data (Table II-1). Square Array.

For  $0.6 < v_t \leq 0.75$ :

$$F = [F_{v_t=0.6, \bar{k}_t}] - (3/4)(v_t - 0.6)(1 - 10 \bar{k}_t^{-1}) \text{ for } \bar{k}_t > 10 \quad (\text{III-11})$$

$$F = [F_{v_t=0.6, \bar{k}_t}] \text{ for } 3/2 \leq \bar{k}_t \leq 10$$

$$F = 1 \text{ for } 1 < \bar{k}_t < 3/2$$

#### c. Choice of Series Tow-Matrix Model.

Various series-path models in Section B were applied to one-dimensional models to determine which fiber configurations produce reasonably accurate results for the transverse conductivity of circular fibers embedded in a square array. Series-path models studied were for the fiber cross-sectional configurations of a square, circle, rectangle, octagon, various wedge shapes, and the circle and square having adjusted thickness and width dimensions. It was concluded that, for tow-matrix systems using circular fibers, models of the greatest usefulness are those based on circular and square shapes, where, for the latter, the cross-section area of the fiber should be the same as for the circular section. For non-circular fibers, the actual shape (or an approximation thereof) should be used. Specifically, for a circular fiber, the equivalent spacing ratios become (with reference to Figure III-1)  $S_e = D_e/C$  and  $s_e = D_e/c$ , and  $v_t = s_e S_e$ , since  $D_e = D (\pi/4)^{1/2}$ . For a square array,  $S_e = (v_t)^{1/2}$  and  $N_e = M S_e = M(v_t)^{1/2}$ . The results also showed that unidirectional analysis based on the simplification  $\bar{k}_{m-t} \approx (1 - N)^{-1}$ , so that  $Y \propto \bar{k}_{m-t}$ , is a generally useful procedure.

#### d. Results for Circular Fibers in A Square Array Based on Tow Elements of Equivalent Uniform Thickness.

Starting from the conclusion that simplification without excessive compromise is obtained by replacing the circular fiber in the tow-matrix series path with a fiber of uniform thickness, it is then assumed

that an important form for the generalized transverse conductivity of a square array is an adaptation of the basic model, equation (III-2), in the arrangement

$$Y_S = F_1 [1 - F_2 M_S v_t^{1/2}]^{-1} \quad (\text{III-12})$$

where  $F_1$  and  $F_2$  are factors to adjust the effective fiber dimensions and where  $N_S$  is represented by  $M_S v_t^{1/2}$ .

If  $F_1 = F_2 = 1$ , then equation (III-12) becomes an approximate relationship for a circular fiber in a square array.

$$Y_S = [1 - M_S v_t^{1/2}]^{-1} \quad (\text{III-13})$$

Its accuracy is summarized in Table III-2.

Table III-2. Ratio  $k_{eq}/k_{H-C}$  for Model Equation (III-13). Circular Fiber in Square Array.  $k$  Values from Table II-1 [1].

Tow-Volume Ratio $v_t$	Tow-to-Matrix Conductivity Ratio $k_t$			
	<u>2</u>	<u>10</u>	<u>100</u>	<u>1000</u>
0.1	0.991	0.956	0.940	0.938
0.3	0.998	0.935	0.911	0.908
0.5	0.998	0.927	0.893	0.888
0.7	0.991	0.874	0.737	0.714
0.75	0.991	0.822	0.572	0.526

By the introduction of a constant thickness adjustment factor  $F_2 = 1.06$ , with  $F_1 = 1$ ,

$$Y_S = [1 - 1.06 M_S v_t^{1/2}]^{-1} \quad (\text{III-14})$$

Its accuracy is quite good at mid-range values of  $v_t$  (Table III-3), and much improved over equation (III-13).

Table III-3. Ratio  $k_{eq}/k_{H-C}$  for Model Equation (III-14).  
Circular Fiber in Square Array.  $\bar{k}$ -Values from Table II-1 [1].

Tow-Volume Ratio $v_t$	Tow-to-Matrix Conductivity Ratio $k_t$			
	<u>2</u>	<u>10</u>	<u>100</u>	<u>1000</u>
0.3	0.991	0.948	0.925	0.922
0.5	0.999	0.986	0.975	0.973
0.7	1.008	1.015	0.977	0.968
0.75	1.010	0.989	0.843	0.806

If the model equation (III-12) is used with  $F_2 = 1.06$  and with  $F_1$  defined by

$$F_1 = 1 + [1 - (3/2 \bar{k}_t)] |v - 0.6|^{4/3} \quad (III-15)$$

then the accuracy pattern (Table III-4) shows excellent results for  $v_t \leq 2/3$ .

Table III-4. Ratio  $k_{eq}/k_{H-C}$  for Model Equation (III-12) with  $F_1$  by Equation (III-15) and  $F_2 = 1.06$ .  $\bar{k}$ -Values from Table II-1 [1].

Tow-Volume Ratio $v_t$	Tow-to-Matrix Conductivity Ratio $\bar{k}_t$		
	<u>2</u>	<u>10</u>	<u>1000</u>
0.1	0.997	0.995	0.990
0.3	1.0	1.006	0.999
0.5	1.002	1.009	1.003
0.7	1.013	1.035	1.007
0.75	1.018	1.042	0.860



Using  $F_1 = F_2^2$  (which implies that the fiber depth and width are both adjusted by equal amounts) and  $N_S = (4/\pi)^{1/2} M v_t^{1/2}$ , then

$$Y_S = F^2 (1 - F N_S)^{-1} \quad (\text{III-16})$$

With

$$F = 1 + 0.48 M_S (1 - v_t) (0.38 - v_t) \quad (\text{III-17})$$

the accuracy pattern is quite good (Table III-5), except for  $v_t \approx 0.75$  with  $k_t \geq 20$ .

---

Table III-5. Ratio  $k_{eq}/k_{H-C}$  for Model Equations (III-16) and (III-17). Accurate k-Values from Table II-1 [1].

Tow-Volume Ratio $v_t$	Tow-to-Matrix Conductivity Ratio $k_t$		
	<u>2</u>	<u>10</u>	<u>1000</u>
0.1	1.0	0.995	0.990
0.3	1.002	1.004	1.003
0.5	0.999	1.002	1.005
0.7	1.003	1.014	0.997
0.75	1.006	1.012	0.900

---

A model for this square array which, though somewhat more cumbersome, forms a useful basis for the rectangular arrays (taken up next) is

$$Y_S = F_1 [1 - F_2 M_S v_t^{1/2}]^{-1} \quad (\text{III-18})$$

where

$$F_1 = 1 + M_S (0.6 - v_t)^{4/3} I[1.6 - v_t] \quad (\text{III-19})$$

$$F_2 = 1 + [1 - (4/3 \bar{k}_t)] \left\{ 0.0592 + 2 (v_t - 0.65)^2 I[v_t/0.65] \right\} \quad (\text{III-20})$$

The square array accuracy pattern for this combination is essentially  $\pm$  one half of one per cent for the entire range of  $\bar{k}_t$  values if  $v_t \leq 0.7$ . It reproduces the accurate data to within two per cent at the highest  $v_t$  of 0.75.

#### Rectangular Array

The approximate analysis for in-line tow elements (Section A) indicates that the transverse conductivity for a rectangular array (Figure II-10) should be correlated to a first approximation by use of the relative packing density ( $\bar{v} = v_t/v_{\max}$ ) and the functional relationships

$$Y_S = F[1 - M_S(\bar{v})^{1/2}]^{-1} \text{ for } \theta \leq 45^\circ \quad (\text{III-21})$$

$$Y_S = F[1 - M_{S \max}(\bar{v})^{1/2}]^{-1} \text{ for } \theta > 45^\circ \quad (\text{III-22})$$

The Han-Cosner data for the rectangular array (Table II-6) are used in Figures III-5 and III-6 to test the ability of these parameters to unify the conductivity data. For  $\theta \leq 45^\circ$ , the proportionality factor in equation (III-21) is seen to be very nearly correlated by the relative volume  $\bar{v}$  and the tow-to-matrix conductivity ratio  $\bar{k}_t$  --- as suggested by the approximate analysis. For  $\theta > 45^\circ$ , again the correlation is reasonably good, as the conductivity parameter  $Y$  is primarily a function of the relative volume  $\bar{v}$  and secondarily of  $Mv_m$ .

If the proportionality factor  $F$  in questions (III-21) and (III-22)

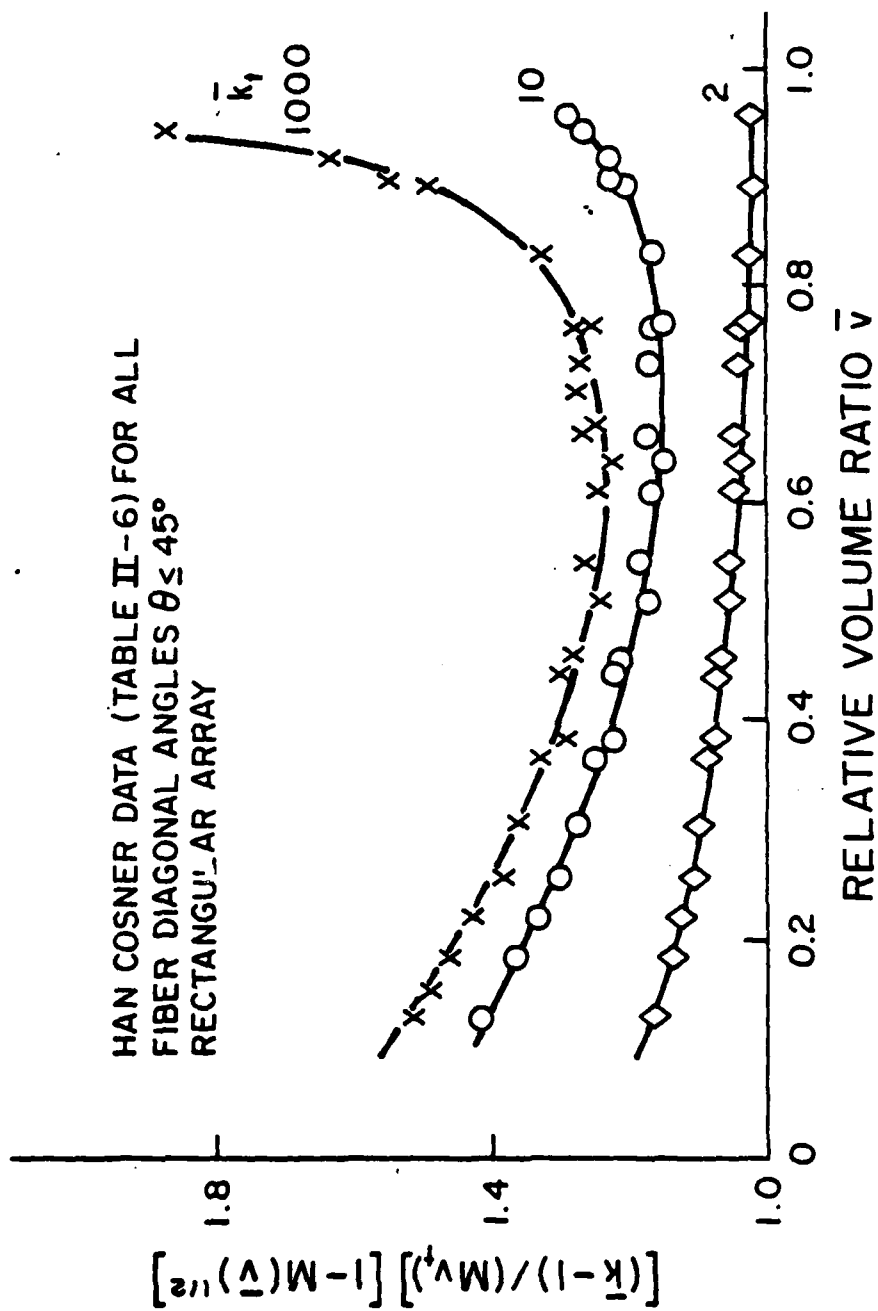


Figure III-5. Test of the Approximate Model Equation III-21.

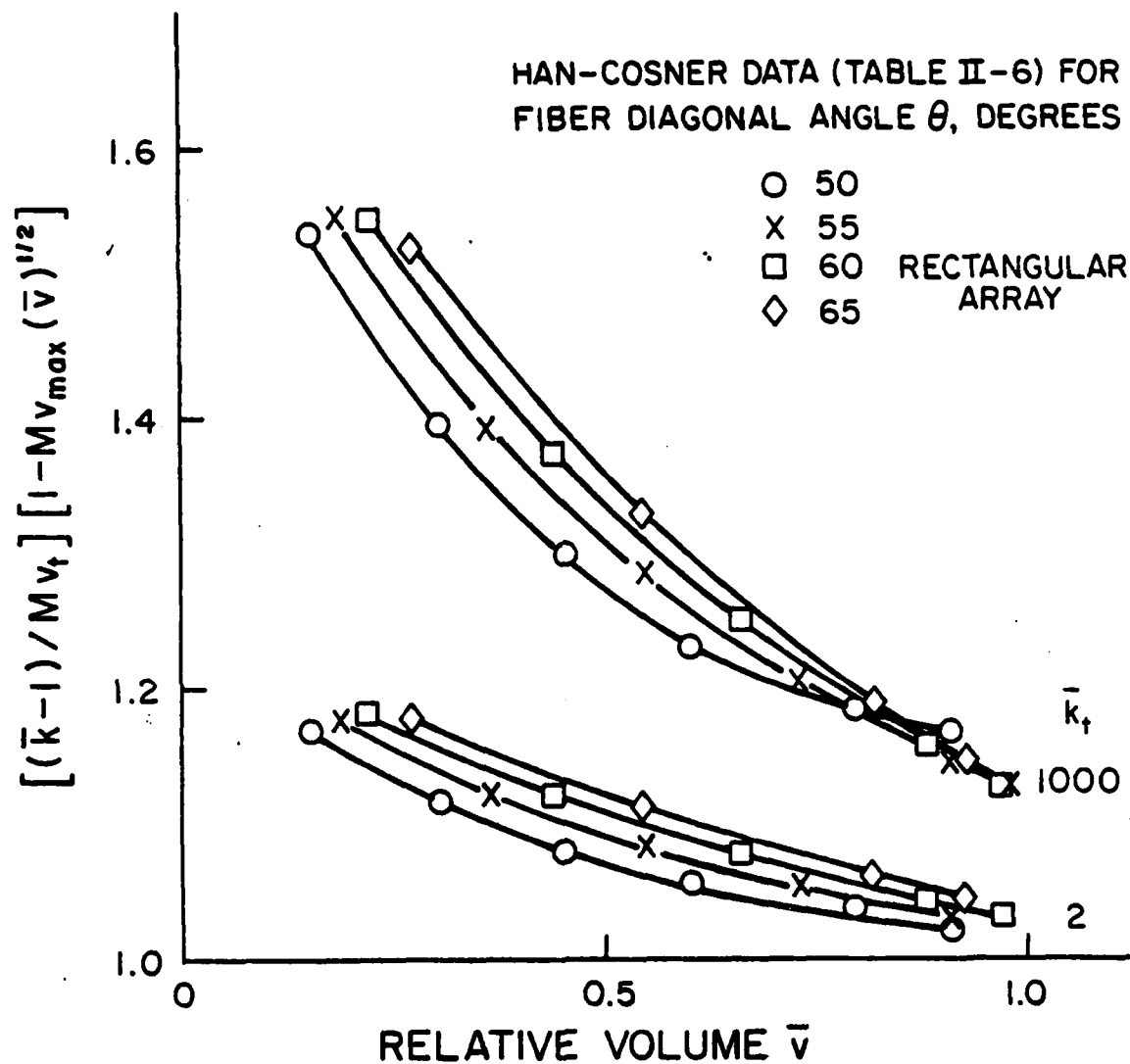


Figure III-6. Test of the Approximate Model Equation III-22.

is described empirically by (for  $\bar{k}_t > 1$ )

$$F - 1 = 0.041 M^2 / (\bar{v})^{1.5} (1 - M \bar{v}) \text{ for } \theta \leq 45^\circ \quad (\text{III-23})$$

$$F - 1 = 0.55 (1 - 0.8 \bar{v}) [1 - (3/2) \bar{k}_t^{-1}] \text{ for } \theta > 45^\circ \quad (\text{III-24})$$

then the accurate data for this array (Table II-6) are replicated to within  $\pm 3$  per cent for all fiber angles  $30^\circ \leq \theta \leq 65^\circ$ ,  $v_t \leq 0.7$  and for all values of the tow-to-matrix conductivity ratio  $\bar{k}_t$ . With  $v_t > 0.7$ , the departure is up to 3-6 per cent. The reciprocity procedures are to be used for  $\bar{k}_t < 1$ .

The following alternate model for the rectangular array replicates the accurate conductivity data to within two per cent for the entire range of all variables in Table II-6. However, excluding the regions of both very high and very low packing density, the method agrees with the Han-Cosner data (Table II-6) to within one half of one per cent. For  $\bar{k}_t > 1$ :

$$Y_S = F_1 [1 - F_2 M_S (v_t / \tan \theta)^{1/2}]^{-1} \quad (\text{III-25})$$

$$F_1 = 1 + (M) I [1.6 - v_t] (0.6 - v_t)^{\exp} \quad (\text{III-26})$$

$$\exp = 4 / (3 \tan \theta) \text{ for } \theta \leq 45^\circ \text{ and } 4/3 \text{ for } \theta > 45^\circ \quad (\text{III-27})$$

$$F_2 = 1 + [1 - (4) / (3 \bar{k}_t)] [0.0592 + 2 I [v_t / 0.65] (v_t - 0.65)^2]$$

For  $\bar{k}_t < 1$ , the reciprocity procedures are to be used, with both the reciprocal of  $\bar{k}_t$  and the complementary angle being used to define the reciprocal of the desired transverse conductivity. To illustrate, suppose it is desired to predict the transverse conductivity of this rectangular array for a tow volume ratio  $v_t = 0.40$ , a fiber diagonal angle of  $35^\circ$  and a tow-to-matrix conductivity ratio of 0.10. Therefore, using  $\bar{k}_t = 10$ ,  $\theta = 55^\circ$  and  $v_t = 0.4$ , equation (III-26) defines  $F_1 = 1.1053$ , equation (III-27) defines  $F_2 = 1.0513$  and equation (III-25)

gives  $Y_S = 2.2139$ . Thus,  $\bar{K} = 1 + Mv_t Y = 1 + (1 - 10^{-1})(0.4)(2.2139 = 1.7970$  --- which is the predicted transverse conductivity at  $\bar{K}_t = 10$ ,  $\theta = 55^\circ$  and  $v_t = 0.4$ . (The accurate value for this condition is shown in Table II-6 to be 1.7951). Finally, then, the predicted value for  $\bar{K}_t = 0.1$ ,  $\theta = 35^\circ$  and  $v_t = 0.40$  is  $1.7970^{-1} = 0.5565$ . Table II-6 shows the accurate value to be 0.5571.

In summary, one-dimensional conduction analysis yields reasonably good "first order" values of the transverse conductivity for the rectangular array. Its modification through the use of adjustment factors yields results usually within two per cent of the accurate conductivity values. Also, the generalizing parameters indicated by the approximate conduction analysis in Section A are found to correlate the accurate data quite well.

#### Staggered Regular Array

The geometrical characteristics of the staggered regular array (Figure II-15) were reviewed in Section II. Here the objective is to adapt an approximate model for the tow-matrix series path to this staggered array. The basis of the adaptation is to link the model to the key conduction paths --- to the key depth spacing ratios --- of the array.

Since, the in-line and diagonal depth spacing ratios ( $S$  and  $\ell$ ) have been shown to be a function of the relative packing density (the relative volume  $\bar{v} = v_t/v_{max}$ ) and the fiber angle  $\theta$  (Figure II-17), it is to be expected, therefore, that transverse conductivities for this array can be correlated most generally through consideration of relative volume  $\bar{v}$ , rather than the volume fraction  $v_t$ .

The basis form of the model used for the rectangular array is

$$Y_S = F_1 [1 - F_2 M_S (v_t / \tan \theta)^{1/2}]^{-1}$$

When shifted to the relative volume  $\bar{v}$  (for  $\theta \leq 45^\circ$ ,  $v_{\max}$  for this array is  $(\pi/4)\tan \theta$ )

$$Y_S = F_1 [1 - F_{2S} (\pi/4)^{1/2} (\bar{v})^{1/2}]^{-1} \quad (\text{III-28})$$

Equation (III-28) is next adapted to the various fiber angles. The relative volume for the staggered array (Section II) is

$$\bar{v} = v_t / (\pi/2) \tan \theta \text{ for } \theta \leq 30^\circ$$

$$\bar{v} = v_t (8/\pi) \cos \theta \sin \theta \text{ for } 30^\circ \leq \theta \leq 60^\circ$$

so that the expected correlation equations for the staggered array are

$$Y_S = F_1 [1 - F_{2S} (2)^{-1/2} (v_t / \tan \theta)^{1/2}]^{-1} \text{ for } \theta \leq 30^\circ \quad (\text{III-29})$$

$$Y_S = F_1 [1 - F_{2S} (2^{1/2} \sin \theta) (v_t / \tan \theta)^{1/2}]^{-1} \text{ for } 30^\circ \leq \theta \leq 60^\circ \quad (\text{III-30})$$

For  $\theta > 60^\circ$ , it is expected that equation (III-30), rather than equation (III-29), will best serve as the model since the lateral proximity of the fibers (as  $\bar{v} \rightarrow 1$ ), unlike transverse proximity, does not have much influence on the transverse conductivity.

#### a. Hexagonal Array.

For fiber diagonal angles of 30 and 60 degrees, the staggered array is hexagonal and the conductivities for these two angles are equal. The one-dimensional model indicates this also since the diagonal spacing ratio  $\ell$  and the depth (in-line) spacing ratio  $S$  (Figure II-17) are equal for the hexagonal array. Thus, the key series-path conductivities are equal.

Equation (III-30) for  $\theta = 30^\circ = 60^\circ$  is

$$Y_S = F_1 [1 - F_2 M_S (3/4)^{1/4} (v_t)^{1/2}]^{-1} \quad (\theta = 30^\circ = 60^\circ) \quad (\text{III-31})$$

This equation when used for  $\bar{k}_t > 1$  with

$$F_2 = 1 + [1 - (5\bar{k}_t)^{-1}] \left\{ 0.094 + 0.45 \left[ \frac{6\bar{v}}{5} \right] [\bar{v} - (5/6)]^2 \right\} \quad (\text{III-32})$$

and with

$$F_1 = 0.99 + (2/3)[1 - (4/3\bar{k}_t)](1 - \bar{v})^{2.2} \quad (\text{III-33})$$

where  $\bar{v} = v_t/0.907$  for the hexagonal array, reproduces the accurate Han-Cosner data (Table II-7) to within one per cent (Table III-6), except at the highest values of both  $\bar{k}_t$  and  $v_t$ . The reciprocal procedure is to be used for  $\bar{k}_t < 1$ .

Table III-6. Accuracy of Equation (III-31) for the Hexagonal Array  
(Relative to the Transverse Conductivity Data in Table II-7 [1].)

Tow-Volume Ratio $v_t$	Tow-to-Matrix Conductivity Ratio $\bar{k}_t$		
	<u>2</u>	<u>10</u>	<u>1000</u>
0.2	1.001	1.009	1.003
0.4	1.001	1.005	0.994
0.6	0.998	0.998	0.990
0.80	0.996	0.998	0.996
0.85	0.996	0.998	0.942



b. Other Fiber Angles.

Equations (III-31), (III-32) and (III-33) may be adapted to other fiber angles (for  $\bar{k}_t > 1$ ) by letting

$$Y_S = F_1 [1 - F_2 M_S (\pi/4)^{1/2} (\bar{v})^{1/2}]^{-1} \quad (\text{III-34})$$

$$\bar{v} = v_t / v_{\max} \quad (\text{III-35})$$

$$F_2 = 1 + [1 - (5\bar{k}_t)^{-1}] \left\{ a + b I [6\bar{v}/5][\bar{v} - (5/6)]^2 \right\} \quad (\text{III-36})$$

$$F_1 = 0.99 + (2/3)[1 - (4/3\bar{k}_t)](1 - \bar{v})^{2.2} \quad (\text{III-37})$$

where:

Fiber Angle $\theta$	$a$	$b$	$v_{\max}$
25°	0.07	1	0.7324
30° (60°)	0.094	0.45	0.9069
35°	0.045	2	0.8358
40°	0.04	2	0.7975
45°	0.059	2	0.7854
50°	0.075	1	0.7975
55°	0.09	0	0.8358
65°	0.1	0	1.05

The reciprocity procedure is to be used for  $\bar{k}_t < 1$ .

The staggered array with a fiber angle of 45 degrees is square and identical to the rectangular array for 45 degrees. Thus, the transverse conductivities as defined by these equations should be identical to those defined by equations (III-18), (III-19) and (III-20). The latter set of equations is a bit more accurate, since here the 45 degree case is fitted to a single set of equations selected for the entire range of fiber angles.

Equations (III-34) through (III-37) have the following accuracy patterns for  $0.001 \leq \bar{k}_t \leq 2000$ .

<u>Fiber Angle <math>\theta</math></u>	<u>Accuracy Pattern</u>
25°	Within one per cent for $v_t \leq 0.65$ Within five per cent at $v_t \approx 0.7$
30°(60°)	Within one per cent for $v_t \leq 0.8$ Within five per cent at $v_t \approx 0.85$
35°	Within one per cent for $v_t \leq 0.7$ Within three per cent at $v_t \approx 0.75$
40°	Within one per cent for $v_t \leq 0.65$ Within five per cent at $v_t \approx 0.7$
45°	Within one per cent for $v_t \leq 0.65$ Within five per cent at $v_t \approx 0.7$
50°	Within one per cent for $v_t \leq 0.65$ Within two per cent at $v_t \approx 0.70$
55°	Within one per cent for $v_t \leq 0.65$ Within two per cent at $v_t \approx 0.7$
65°	Within one per cent for $v_t \leq 0.7$

c. Unified Model for Staggered Array.

In principle, there are three primary conduction paths within the staggered array: (i) The continuous matrix path, (ii) an in-line tow-matrix series path having an approximate series resistance of  $(1 - N_S)$  relative to that of the matrix, and (iii) a tow-matrix series path along the fiber diagonal having an approximate resistance of  $(1 - N_\ell)$  relative to that of the matrix. If, to a first approximation, we assume each of these paths feels the same transverse temperature gradient, then (with  $s$  again representing the lateral spacing ratio  $D/c$ , Figure II- 15)

$$k = (1 - s) k_m + s (k_{m-t-S} + k_{m-t-\ell})$$

or

$$\bar{k} - 1 = s(\bar{k}_{m-t-S} + \bar{k}_{m-t-\ell} - 1)$$

Further, since to a first approximation

$$\bar{k}_{m-t-S} \doteq (1 - N_S)^{-1}$$

and

$$\bar{k}_{m-t-\ell} \doteq (1 - N_\ell)^{-1}$$

where  $N_S = MS$  and  $N_\ell = M\ell$ . Equations (II-21) and (II-22) define the in-line and diagonal depth spacing ratios ( $S$  and  $\ell$ ), so that (including the factor of  $(\pi/4)^{1/2}$  to adjust from the fiber diameter to a fiber of uniform thickness having the same  $v_t$ ) it follows

$$N_S = (2/\pi)^{1/2}(\pi/4)^{1/2}(M)(v_t/\tan \theta)^{1/2} = X/(2)^{1/2}$$

$$N_\ell = (8/\pi)^{1/2}(\pi/4)^{1/2}(M)(v_t \sin \theta \cos \theta)^{1/2} = (2)^{1/2}(\sin \theta)X$$

where

$$X \equiv M (v_t / \tan \theta)^{1/2}$$

Next, since

$$v_t = 2 s S = 2 s^2 / \tan \theta$$

therefore

$$(\bar{k} - 1)(2)^{1/2} / (v_t \tan \theta)^{1/2} \doteq (1 - N_S)^{-1} + (1 - N_\ell)^{-1} - 1$$

And, if the depth and width adjustment factors are introduced (as in previous models), then

$$(\bar{k} - 1)(2)^{1/2} / (v_t \tan \theta)^{1/2} = F_1' [(1 - F_S N_S)^{-1} + (1 - F_\ell N_\ell)^{-1} - 1]$$

It was found that  $F_1'$  varies approximately in proportion to the tow conductivity parameter  $M$  and that the spacing correction factors  $F_S$  and  $F_\ell$  can be represented approximately by  $(1 + 0.12 N^2)$ .

The resulting unified model for the transverse conducting  $\bar{k}$  of a staggered array is

$$(\bar{k} - 1)(2)^{1/2} / (X \tan \theta) = F_1 [(1 - F_S N_S)^{-1} + (1 - F_\ell N_\ell)^{-1} - 1] \quad (\text{III-38})$$

For this model, the companion equations are

$$X = M(v_t / \tan \theta)^{1/2} \quad (\text{III-39})$$

$$M = 1 - \bar{k}_t^{-1} \quad (\text{III-40})$$

$$N_S = X/(2)^{1/2} \quad (\text{III-41})$$

$$N_{\ell} = (2)^{1/2} (\sin \theta)(X) \quad (\text{III-42})$$

$$F_S = 1 + 0.12 N_S^2 \quad (\text{III-43})$$

$$F_{\ell} = 1 + 0.12 N_{\ell}^2 \quad (\text{III-44})$$

$$1 - F_L = 0.1(0.1 \theta^{\circ} - 1)(1 - v_t) \quad (\text{III-45})$$

These equations are for the tow conductivity ratio  $\bar{k}_t > 1$ . The reciprocity procedure is to be used for  $\bar{k}_t < 1$ .

This unified model reproduces the accurate data (Table II-7) to within  $\pm 8$  per cent for  $v_t \leq 0.75$ , except for the lowest fiber angle of 25 degrees. The model underestimates the transverse conductivity by 15 per cent at 25 degrees and  $v_t = 0.6$ ,  $\bar{k}_t = 1000$ . The use of an effective fiber angle of about 23 degrees (for  $\theta = 25^{\circ}$ ) brings the results within several per cent for  $v_t \leq 0.65$ .

For midrange values of the tow volume ratio  $v_t$  and the fiber diagonal angle  $\theta$ , the unified model predicts transverse conductivities within  $\pm 5$  per cent of the accurate data for the entire range of tow conductivity ratios.

## SECTION IV

### Adaptation of the Conduction Models for Unidirectional Fibers to A Bidirectional Packing Geometry

In this Section IV, certain of the approximate models for unidirectional fiber packing (Sections II and III) are used to develop conductivity models for a bidirectional fiber packing geometry (Figure IV-1). The geometrical packing pattern is alternating orthogonal rows of circular filaments in a rectangular array.

The validity of these models can be assessed since Han and Cosner [1] determined accurate conductivities for alternating orthogonal laminae, with each layer containing a single row of identical isotropic, circular filaments embedded in an isotropic matrix. Though the tow and matrix materials in these studies are the same in each layer, the resulting models could be adapted to both intra- and interhybrid layers by introducing the constituent properties for each layer.

#### a. Accurate Data.

Han and Cosner [1] studied this type of packing geometry for the special case of an equal transverse (in-line) spacing ratio within each layer, i.e. (with reference to Figure IV-1)  $x = z$ , with uniform  $D$ . They considered two values of the lateral fiber spacing ratio ( $D/y$ ) in their evaluation of the conductivities: (i) equal to the in-layer (transverse) spacing, i.e.  $y = x = z$ , a cubical array and (ii) twice the in-layer spacing,  $y = 2x = 2z$ , a rectangular solid array having a lateral aspect ratio of 2. The effective overall (bulk) conductivities  $k_x = k_z$  and  $k_y$  (Figure IV-1) were evaluated by methods of numerical analysis [1]. Their results are summarized in Tables IV-1 and IV-2.

The bulk conduction in the direction  $x$ (or  $z$ ) is the aggregate of the conduction through essentially three parallel paths: (a) longitudinally through one half of the fibers, (b) open matrix space and (c) the tow-matrix series path, i.e. transversely through one half of

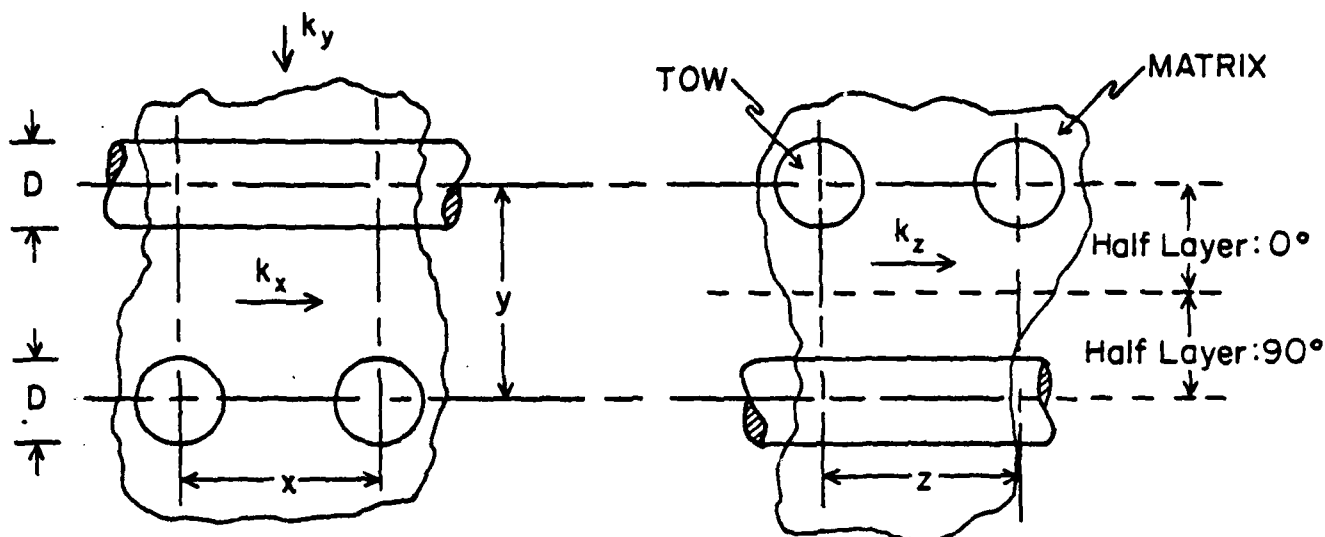


Figure IV-1. A Bidirectional Packing Pattern Consisting of Alternating Orthogonal Rows of Filamentary Tow Embedded in A Matrix.

the fibers. In contrast, conduction in the direction  $y$  has only two primary paths: (i) the tow-matrix series path and (ii) the open matrix space. Therefore, the conductivities  $k_x = k_z$  always will depart from the matrix conductivity to a greater extent than the conductivity  $k_y$ , since the magnitude of the series-path conductivity  $k_{m-t}$  always lies between the parallel-path conductivity and the matrix conductivity. For example, with a tow volume ratio  $v_t = 0.50$ , a tow-to-matrix conductivity ratio  $\bar{k}_t = 40$  and  $x = y = z$  (cubical array), the data in Table IV-1 show that  $\bar{k}_x = \bar{k}_{yz} = \bar{k}_y = 2.77$ .

b. Adaptation of Modified Rayleigh Equation (as Developed for Unidirectional Fibers).

With reference to Figure IV-1 and directions  $x$  and  $z$ , one half of each layer involves the continuous parallel paths of fiber and matrix having bulk longitudinal conductivity  $k = k_t v_t + k_m v_m$ , and the other half has transverse fibers embedded in a matrix having a bulk transverse conductivity defined approximately by the modified Rayleigh equation. Thus, the overall bulk conductivity  $k_x$  (and  $k_z$ ) (of the entire fiber system) would be the average of these two conductivities. Allowing for some interaction between these two subsystems by including an adjustment factor  $F_x$ , then the basic model

Tow-to-Matrix Conductivity Ratio, $k_t/k_m$	Tow Volume Ratio $v_t$									
	0.4		0.5		0.6		0.65		0.70	
	$\bar{k}_x = \bar{k}_z$	$\bar{k}_y$	$\bar{k}_x = \bar{k}_z$	$\bar{k}_y$	$\bar{k}_x = \bar{k}_z$	$\bar{k}_y$	$\bar{k}_x = \bar{k}_z$	$\bar{k}_y$	$\bar{k}_x = \bar{k}_z$	$\bar{k}_y$
0.2	0.631	0.570	0.554	0.489	0.475	0.413	0.438	0.376	0.403	0.299
0.5	0.783	0.761	0.734	0.710	0.684	0.662	0.660	0.639	0.638	0.589
2	1.355	1.306	1.449	1.397	1.555	1.495	1.607	1.548	1.659	1.599
4	1.920	1.624	2.18	1.845	2.49	2.11	2.65	2.26	2.82	2.44
7	2.64	1.841	3.11	2.18	3.68	2.61	3.99	2.89	4.34	3.23
10	3.30	1.953	3.96	2.36	4.76	2.91	5.20	3.27	5.71	3.74
20	5.39	2.11	6.59	2.62	8.06	3.35	8.85	3.88	9.82	4.64
40	9.45	2.20	11.6	2.77	14.3	3.64	15.6	4.29	17.3	5.23
70	15.5	2.24	19.1	2.85	23.4	3.78	25.6	4.50	28.0	5.56
100	21.5	2.26	26.6	2.88	32.5	3.84	35.4	4.95	38.6	5.71

105

Table IV-1 Calculated Bulk Conductivities ( $\bar{k} = k/k_m$ ) of A Filamentary Composite Having Alternating Orthogonal Layers of equally Spaced Circular, Isotropic Fibers. Data Source [1].  
These Data for  $x = y = z$ . (Figure IV-1).



Tow Volume Ratio  $v_t$ 

Tow-to-Matrix Conductivity Ratio, $k_t/k_m$	0.2		0.25		0.30		0.325		0.35	
	$\bar{k}_x = \bar{k}_z$	$\bar{k}_y$	$\bar{k}_x = \bar{k}_z$	$\bar{k}_y$	$\bar{k}_x = \bar{k}_z$	$\bar{k}_y$	$\bar{k}_x = \bar{k}_z$	$\bar{k}_y$	$\bar{k}_x = \bar{k}_z$	$\bar{k}_y$
0.2	0.815	0.725	0.777	0.650	0.738	0.585	0.720	0.545	0.702	0.720
0.5	0.891	0.855	0.867	0.825	0.842	0.805	0.830	0.780	0.819	0.855
2	1.178	1.125	1.225	1.170	1.278	1.195	1.303	1.215	1.329	1.235
4	1.460	1.235	1.592	1.295	1.745	1.350	1.824	1.385	1.908	1.410
7	1.820	1.295	2.06	1.670	2.34	1.440	2.49	1.480	2.67	1.515
10	2.15	1.315	2.48	1.400	2.88	1.480	3.10	1.520	3.35	1.565
20	3.20	1.350	3.79	1.440	4.52	1.525	4.90	1.580	5.39	1.625
40	5.22	1.370	6.32	1.466	7.63	1.550	8.31	1.600	9.13	1.650
70	8.24	1.381	10.1	1.477	12.2	1.573	13.3	1.624	14.5	1.674
100	11.3	1.384	13.8	1.480	16.8	1.578	18.2	1.629	19.8	1.680

Table IV-2. Same Tow-Matrix System as for Table IV-1, except  $y = 2x = 2z$  (Figure IV-1). Data Source [1].

for the x-z bulk conductivity is

$$\bar{k}_x = \bar{k}_z = (1/2)(\bar{k}_{lg} + F_x \bar{k}_{tr}) \quad (IV-1)$$

with the weave being half longitudinal and half transverse.

For a cubical array ( $x = y = z$ , Table IV-1), the equivalent transverse fiber spacing is 45 degrees and from Section II, the transverse bulk conductivity by the modified Rayleigh equation is defined by equations (II-3) and (II-5). The longitudinal bulk conductivity is defined by  $\bar{k}_{lg} = 1 + (\bar{k}_t - 1)v_t$ . Hence, these relationships and the accurate data (Table IV-1) allow test of this model equation (IV-1).

For a cubical array, the value of the adjustment factor  $F_x$  ranges from 1.0 to 1.11 (for the range of data in Table IV-1). However, by use of the model with  $F_x = 1$ , equation (IV-1) replicates the Han-Cosner data for  $k_x$  and  $k_z$  to within  $\pm 0.5$  per cent.

When the same model is applied to the bidirectional packing geometry having a lateral aspect ratio of 2 (Table IV-2), the adjustment factor  $F_x$  in equation (IV-1) ranges from 1.0 to nearly 2. However, if the modified Rayleigh equation (II-17) for a rectangular array having a lateral aspect ratio of 2 is used (equation II-19 for  $\tan \theta = 1/2$ ), then values of  $k_x = k_z$  (using  $F_x = 1$ ) are predicted to within  $\pm 5$  per cent of the accurate data (for the range of conditions in Table IV-2).

By retaining the use of the square array for the modified Rayleigh equation (II-3) (just as for the cubical array) and by applying the following empirical adjustment factor

$$F_{x,AR=2} = 1 + 1.1 v_t (10v_t - 1) [f(\bar{k}_t)]^2 \quad (IV-2)$$

where

$$f(\bar{k}_t) = (\bar{k}_t - a) / (\bar{k}_t + a)$$

$$a = 2.25 \text{ for } \bar{k}_t > 2.25$$

$$a = 5/3 \text{ for } \bar{k}_t \approx 2$$

$$a = \bar{k}_t \text{ for } 1 < \bar{k}_t < 2$$

then this adjusted model agrees with the accurate data in Table IV-2 to within  $\pm 0.5$  per cent.

For  $\bar{k}_t < 1$ , the value of  $k_{trans}$  in equation (IV-1) should be evaluated using the reciprocity procedure.

For the conductivity in the direction transverse to all fibers, i.e.  $k_y$ , and for the cubical array, the effective fiber diagonal angle is 45 degrees. Thus, the angle adjustment factor  $C_\theta$  for the rectangular array equation (II-19) is unity. Further, letting the adjustment factor  $F$  in equation (II-17) also be unity, then the relationship reduces to the Rayleigh solution, and it defines values of the transverse conductivity  $\bar{k}_y$  (cubical array) to within one per cent of the accurate data, except for the highest tow-volume ratio  $v_t = 0.7$  (where the difference reaches 6 per cent at  $k_t = 100$ ).

For  $y = 2x = 2z$ , i.e. an array having an aspect ratio of 2, the effective fiber diagonal angle for the rectangular array (in the direction  $y$ ) is  $\tan^{-1}2$ , and by equation (II-20)

$$C_\theta = 1 + 1.05 mv_t (\tan \theta - 1)$$

or

$$C_{\theta-AR=2} = 1 + 1.05 mv_t \quad (IV-3)$$

Thus, using the modified Rayleigh equation (II-17) for a rectangular array with  $F = 1$ , the transverse conductivity  $k_y$  is

$$\bar{k}_y = (C_\theta + mv_t)/(C_\theta - mv_t) \quad (IV-4)$$

where  $C_\theta$  is defined by equation (IV-3). This relationship reproduces the accurate values of the conductivity  $\bar{k}_y$  (Table IV-2) to  $\pm 0.5$  per cent.

It can be reduced to the simple relationship  $\bar{k}_y = 1 + 2mv_t$  (for  $\tan \theta = 2$ ) and still provide an accuracy of one per cent.

In summary, the modified Rayleigh equation for fibers packed unidirectionally can be used to predict conductivities for bi-directional packing geometries to an accuracy level of several per cent. The models organize the principal variables to indicate, quite directly, their influences on the conductivities of this orthotropic tow-matrix system.

c. Adaptation of A One-Dimensional Model to the Bidirectional Weave.

Again with reference to Figure IV-1, the bulk conductivity  $k_x$  (and  $k_z$ ) for this half longitudinal - half transverse weave is defined by

$$\bar{k}_x = \bar{k}_y = (1/2) (\bar{k}_{lg} + F_x \bar{k}_{tr}) \quad (IV-1)$$

where  $\bar{k}_{lg} = 1 + (\bar{k}_t - 1)v_t$ . For cubical array ( $x = y = z$ ) (Table IV-1), the in-line array for the lower-half of the layer has an effective fiber diagonal angle of 45 degrees. Thus, the transverse conductivity  $\bar{k}_{tr}$  in the model equation (IV-1) can be approximated by use of equations (III-18), (III-19) and (III-20) --- a model for the square array based on one-dimensional conduction analysis. Using this procedure and the accurate data (Table IV-1), the adjustment factor  $F_x$  in equation (IV-1) ranges from 0.98 - 1.05. However, by letting  $F_x = 1$ , equation (IV-1) and equation (III-18) (for the square array) provide a method which predicts bulk transverse conductivities  $k_x = k_z$  within 0.5 per cent of the accurate data (Table IV-1).

For the bidirectional weave having a lateral aspect ratio of 2 ( $y = 2x = 2z$ ) (Table IV-2), the apparent fiber diagonal angle is  $\tan^{-1} 0.5$  and the transverse conductivity for the lower-half of the layer (based on one-dimensional conduction analysis) is defined by equations (III-25), (III-26) and (III-27). With these relationships (for  $\tan \theta = 0.5$ ) and letting  $F_x = 1$ , the model, equation (IV-1), reproduces the accurate values of  $\bar{k}_x = \bar{k}_z$  to within several tenth of one per cent, except at the highest values of tow-to-matrix conductivity ratio  $\bar{k}_t$  where the predicted values of  $k_x$  (at  $\bar{k}_t = 100$ ) differ from the accurate values (Table IV-2) by one per cent at  $v_t = 0.3$  and by

two per cent at  $v_t = 0.35$ .

A model for the conductivity  $k_y$  (transversely to all fibers) is defined by the application of the one-dimensional analysis from Section B. With reference to Figure IV-1, let the following spacing ratios be defined

$$s \equiv D/x \quad S \equiv D/y \quad \mathcal{S} \equiv D/z \quad (\text{IV-5})$$

The tow-volume ratio  $v_t$  is related to these spacing ratios by (again with reference to Figure IV-1)

$$v_t = (\pi/4)(D^2/2)(x + y)/xyz = (\pi/8)(S)(\mathcal{S} + s)$$

The Han-Cosner data (Tables IV-1 and IV-2) are for the special case of  $x = z$ ,  $\mathcal{S} = s$ , so that

$$v_t = (\pi/4) s S \quad (\text{IV-6})$$

Letting

$$\tan \theta = y/x = s/S \quad (\text{IV-7})$$

then

$$v_t = (\pi/4)(S^2 \tan \theta) \quad (\text{IV-8})$$

or

$$N_S = N_y = MS = F_2^M (v_t/\tan \theta)^{1/2} \quad (\text{IV-9})$$

by the procedure adopted in Section III for rectangular arrays.

There are three parallel conduction paths in the transverse ( $y$ ) direction within the volume  $xyz$ : (i) the open matrix path, (ii) the series path involving matrix and half a fiber thickness and (iii) the series path involving matrix and one fiber thickness. The relative conduction area of path (i) is  $(1 - s)^2$ , of path (ii)  $2s(1 - s)$  and of path (iii)  $s^2$ , where  $s$  is the lateral spacing ratio  $D/x = D/z$ . Thus, the bulk relative conductivity in the direction  $y$  by

this type of approximate analysis is

$$\bar{k}_y = (1 - s)^2(1) + 2s(1 - s) \bar{k}_{ii} + s^2 \bar{k}_{iii} \quad (\text{IV-10})$$

From the one-dimensional model in Section III

$$\bar{k}_{iii} \doteq (1 - N_S)^{-1} \quad (\text{IV-11})$$

Since

$$N_{ii} = N_{iii}/2$$

therefore

$$\bar{k}_{ii} \doteq [1 - (N_S/2)]^{-1} = 2/(2 - N_S) \quad (\text{IV-12})$$

The combination of equations (IV-9), (IV-10), (IV-11) and (IV-12) yields as the approximate relationship for bulk conductivity across all fibers (direction y)

$$(\bar{k}_y - 1)/Mv_t = [F/(2 - N_S)] (1 + k_N) \quad (\text{IV-13})$$

Here,  $k_N$  is the transverse conductivity for unidirectional filaments, i.e. as developed in Section III

$$(k_N - 1)/Mv_t = F_1(1 - N_S)^{-1} \quad (\text{IV-14})$$

where  $N_S$  is defined by equation (IV-9).

For the cubical array ( $x = y = z$ ), the model described by equation (IV-13) when combined with the accurate data for this array (Table IV-1) yields values of the adjustment factor  $F$  in equation (IV-13) ranging from 0.97 - 1.28. Thus, as it stands, i.e. without adjustment ( $F = 1$ ), the one dimensional methods adapted from Section III to this bidirectional weave produces  $k_y$  conductivities accurate to  $\pm 6$  per cent.

However, letting the adjustment factor  $F$  in equation (IV-13) be defined by

$$F = 1 + m (0.7 - v_t) I [1.7 - v_t] \quad (IV-15)$$

$$m = (\bar{k}_t - 1) / (\bar{k}_t + 1)$$

then the model predicts  $\bar{k}_y$  to within 2 per cent.

This same model when applied to the second array (Table IV-2), for which  $y = 2x$ ,  $\tan \theta = 2$ , results in values of the adjustment factor  $F$ , equation (IV-13), in the range 1.05 - 1.40. Use of the empirical equation

$$F = 1 + (5m/4) (0.5 - v_t) I [1.5 - v_t] \quad (IV-16)$$

$$m = (\bar{k}_t - 1) / (\bar{k}_t + 1)$$

in equation (IV-13) produces results accurate to within ± one per cent.

## SECTION V

### Conclusions

For both unidirectional and bidirectional filamentary composite materials not having voids and other major imperfections, numerical values of the transverse bulk conductivity can be predicted with good accuracy using simplified analytical models. Further, these simplified, approximate models organize the principal variables in comparatively uncomplicated ways; usually, they allow relatively straight forward examination of the influences of a variety of design variables on the magnitudes of the directional conductivities.

When the fiber packing configuration is essentially hexagonal or square or in other near-regular patterns and when the fiber relative packing density is less than approximately nine tenths, both the unadjusted Rayleigh equation and the unadjusted one-dimensional conduction model are capable of predicting bulk transverse conductivity of fiber composites to an accuracy within 15 to 20 per cent over a very wide range of values for the tow-to-matrix conductivity ratio (roughly  $2000^{-1}$  to 2000).

Once the Rayleigh and one-dimensional conduction equations are modified to include adjustment factors, the transverse bulk conductivity is predictable to within several percent of the accurate values developed by Han and Cosner [1]. For normal ranges on the principal variables (fiber shape, fiber packing configuration, fiber volume content, tow-to-matrix conductivity ratio), the models have been adjusted to agree with the accurate Han-Cosner data [1] to within one per cent.

The Han-Cosner data and the models have been found to contain reciprocity features with respect to the tow-to-matrix conductivity ratio. Complementary methods permit use of the transverse bulk conductivity data for tow conductivities greater than the matrix conductivity to predict bulk conductivities of fiber-matrix systems having tow conductivities less than the matrix conductivity.



Simplified models for bidirectional fiber systems are found to predict directional bulk conductivities to within one per cent for the usual ranges on design variables and to within several per cent over a wide range of design conditions.

Simplified, approximate methods can be useful also when attempting to organize generalizing variables for study and correlation of the conductivity data for unconventional composite materials.

The Rayleigh and one-dimensional conduction equations are found to be excellent analytical tools to model the principal conduction paths within a wide variety of types of composite materials.

## A P P E N D I C E S

### Supporting Studies

## SECTION A

### Use of Approximate Analysis of A Two-Phase Composite Material to Identify the Major Factors Influencing Its Transverse Conductivity

The analysis of conduction in a two-phase system based on a simplified, approximate model is useful to identify the major variables involved, their appropriate groupings and their expected effects on the conductivity. The approximate analysis which follows is based on the assumption of one-dimensional conduction in a two-phase composite material, where the tow (the reinforcing material) consists of orthotropic, homogeneous chunks or ribbons or sheets (rectangular solids) both uniformly aligned and dispersed throughout an isotropic, homogeneous matrix (Figure A-1). For the three-dimensional case, the matrix is continuous in three directions and the tow (rectangular solid chunks) is assumed to be embedded in rectangular arrays. For the tow as long, uniform ribbons (filaments), the tow is assumed continuous in one direction and embedded transversely in a rectangular array. For the one-dimensional case, the tow is embedded as parallel sheets of uniform thickness in a matrix continuous in one direction only. Voids, interfacial resistances and material heterogeneities are ignored in all models.

For conduction in a direction parallel to the spacing distance  $C$  (Figure A-1), if the tow thickness  $A$  equals the spacing distance  $C$ , then the tow is continuous in that direction and the conduction is classified "longitudinal", as (in that direction) conduction occurs through two parallel, continuous paths (one tow and one matrix). If the tow in a particular direction is not continuous, e.g.  $A < C$ , the conduction is classified "transverse" as it now involves a tow-matrix series path in parallel with a matrix only path. When  $a' = c'$  (Figure A-1), the tow is continuous in that direction and the model is representative of ribbon-filament composite materials, with the conduction being classified "longitudinal" in the continuous tow

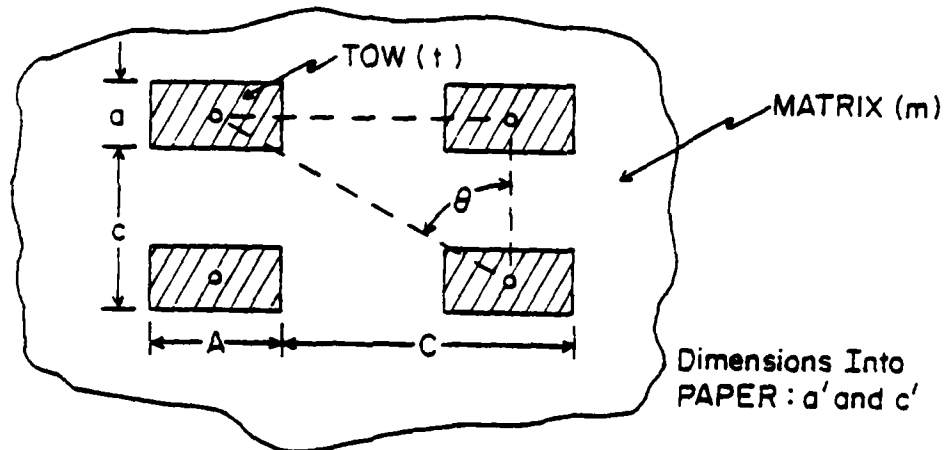


Figure A-1. Illustrating the Model in This Approximate Analysis to Indicate Principal Variables. Tow Embedded in Rectangular Array.

direction and "transverse" in both the directions  $c$  and  $C$ . With both  $a' = c'$  and  $a = c$ , the model represents a laminated composite material (alternating parallel layers of tow and matrix), with conduction being classified longitudinal in two directions (through parallel paths of continuous tow and continuous matrix) and transverse in the third direction  $C$  (a series tow-matrix path).

#### a. Model Analysis.

Let the tow depth-spacing ratio  $S$  (in the direction of the transverse conduction), the tow width-spacing ratio  $s$  (laterally to the transverse conduction) and the length-spacing ratio  $L$  (normal to the  $s$ - $S$  plane) be defined as in Figure A-1

$$S \equiv A/C \quad (A-1)$$

$$s \equiv a/c \quad (A-2)$$

$$L \equiv a'/c' \quad (A-3)$$

Further, let the array aspect ratios  $R$  and  $R'$ , and the tow aspect ratios  $r$  and  $r'$  be defined as

$$R \equiv c/C = (\tan \theta)^{-1} \quad (A-4)$$

$$R' \equiv c'/C \quad (A-5)$$

$$r \equiv a/A \quad (A-6)$$

$$r' \equiv a'/A \quad (A-7)$$

They establish the relative dimensions of the tow and the arrays.

The volume fraction of the system occupied by tow  $v_t$  is

$$v_t \equiv V_t / (V_t + V_m) = Aaa' / Ccc'$$

which by use of the three spacing ratios (A-1, A-2, A-3) becomes

$$v_t = SsL \quad (A-8)$$

i.e. the tow-volume ratio  $v_t$  is the product of the three spacing ratios (depth, width and length).

For chunks of tow dispersed throughout the matrix, each spacing ratio is less than unity --- there is no "longitudinal" conduction (no direction having continuous tow). Thus, without a continuous direction (say along  $c'$ ), the tow spacing ratio  $S$  or  $s$  (or both) will be larger than otherwise, and for a given volume of tow, the transverse conductivity will have the greatest departure from the matrix conductivity. In contrast, for filaments (ribbons), the length spacing ratio  $L = 1$ ,  $v_t = sS$ , and the spacing ratio  $S$  (or  $s$  or both) for a given tow volume ratio  $v_t$  is now less, since a portion of the tow volume is used to provide continuous tow along  $c'$ . Consequently, the matrix gap along  $C$  (or  $c$  or both) is larger, and the transverse conductivity (ies) for this two-dimensional tow-matrix system will be closer to that of the matrix than for the tow dispersed as chunks (having the same  $v_t$ ). If in a two-dimensional tow-matrix system the transverse array is square, then  $S = s = (v_t)^{1/2}$ , whereas for a cubical array  $S = s = L = (v_t)^{1/3}$ . For example, with  $v_t = 2/3$ ,  $S_{2-dim} = 0.82$  and  $S_{3-dim} = 0.87$ ; the in-line matrix thickness between pieces of tow is nearly half again as much for the two-dimensional system having the same  $v_t = 2/3$ . The transverse conductivity of the two-dimensional system (versus a three-dimensional system) is shifted toward the matrix level, but its longitudinal conductivity (in the continuous-tow direction) is shifted away from that of the matrix, thereby making the system anisotropic. For a conventional laminate (tow in sheets),  $s = L = 1$  and  $v_t = S$ . For this system (relative to both the ribbon and chunk systems for a given  $v_t$ ), the difference between the transverse conductivity and the matrix conductivity is

rendered minimal, while the conductivity in either of the two continuous directions shows maximum departure. Thus, this latter system exhibits maximal anisotropy.

In summary, for both isotropic tow and matrix components and for a given tow value fraction  $v_t$ , a three-dimensional distribution of the tow can yield maximum (or minimum) levels of the transverse conductivity, with the two-dimensional and one-dimensional distributions of tow shifting the transverse conductivities more and more toward the matrix conductivity while creating comparatively high (or low) conductivities in the continuous direction(s) of the tow.

Considering the direction C, for example, the transverse conduction is defined approximately by the sum of the conduction through a matrix path of width  $(c - a)$  (Figure A-1) and that through a parallel path of width  $(a)$  --- the latter being a tow-matrix series path (m-t). Thus, for this approximate analysis

$$q_S = q_{m-S} + q_{m-t-S} \quad (A-9)$$

where

$$q_S \equiv k_S c c' \Delta T / C$$

$$q_{m-S} \doteq k_m (c c' - a a') (\Delta T / C)$$

$$q_{m-t-S} \doteq k_{m-t-S} a a' \Delta T / C$$

Hence, from these relationships, the effective transverse conductivity  $k_S$  (C direction) is defined by

$$(k_S - k_m) / (k_{m-t-S} - k_m) \doteq sL = v_t / S \quad (A-10)$$

For the tow-matrix series path, since

$$q_{m-t-S} \doteq q_{m-S} \doteq q_{t-S}$$

and

$$\Delta T \doteq \Delta T_m + \Delta T_t$$

it follows that

$$(k_{m-t-S})^{-1} = S / k_{t-S} + (1 - S) / k_m \quad (A-11)$$

or

$$\bar{k}_{m-t-S} \equiv k_{m-t-S}/k_m = (1 - M_S S)^{-1} = (1 - N_S)^{-1} \quad (A-12)$$

where

$$M_S \equiv 1 - (k_m/k_{t-S}) = 1 - \bar{k}_{t-S}^{-1} \quad (A-13)$$

$$N_S \equiv M_S S \quad (A-14)$$

$$\bar{k}_{t-S} \equiv k_{t-S}/k_m \quad (A-15)$$

From equation (A-10), it follows that the bulk (effective) transverse conductivity of the composite material is

$$(k_S/k_m) - 1 = (v_t/S) \left[ (1 - N_S)^{-1} - 1 \right] = M_S v_t (1 - N_S)^{-1}$$

Or, with the transverse relative conductivity defined by

$$\bar{k}_S \equiv k_S/k_m \quad (A-16)$$

it follows that for this model

$$(\bar{k}_S - 1)/M_S v_t \equiv Y_S = (1 - N_S)^{-1} \quad (A-17)$$

Thus, this approximate analysis indicates that a generalized relationship for the bulk transverse conductivity in the direction (i) of a two-phase composite material is of the form

$$Y_i \equiv (1 - N_i)^{-1} \quad (A-18)$$

with

$$Y_i \equiv (\bar{k}_i - 1)/M_i v_t \quad (A-19)$$

The term  $(1 - N_i)$  defines the thermal resistance of the tow-matrix series path (relative to the resistance of the same length of path having matrix material only).  $N_i$  defines the fractional extent to which the addition of tow alters the resistance of the path from that of the matrix alone.

For example, with cubes of tow (for which their conductivity is 10 times that of the matrix, i.e.  $\bar{k}_t = k_t/k_m = 10$  --- say glass or a ceramic material embedded in a resinous matrix) uniformly dispersed at a volume ratio  $v_t = 0.6$ ,  $S = s = L$ ,  $S = (0.6)^{1/3} = 0.843$  and  $N_S = N_s =$

$N_L = M_S S = (1-0.1) (0.843) = 0.759$ ,  $1-N_S = 0.241$ . Thus, the resistance of the tow-matrix series path is roughly one fourth of that for the matrix alone. The bulk transverse conductivity of this two-phase material is (by equation A-17)  $Y_S = \bar{K}_{m-t-S} = (0.241)^{-1} = 4.15 = [k_S/k_m - 1]/M_S v_t$ , or  $k_S/k_m = 1 + 4.15 \times 0.9 \times 0.6 = 3.24$ .

For long filaments square in cross-section (with  $\bar{K}_t = 10$ ) and uniformly dispersed transversely with  $v_t = 0.6$ , with  $L = 1$ , then  $S = s = (0.6)^{1/2} = 0.775$ , therefore  $N_S = M_S S = 0.9 \times 0.775 = 0.697$  and  $1 - N_S = 0.303$ . The resistance of this tow-matrix series path is 30 percent of the matrix alone and the bulk transverse conductivity  $k_S/k_m = 1 + 0.9 \times 0.6(0.303)^{-1} = 2.78$ . If the same amount and type of tow is distributed in the same matrix as sheets to form a laminate, then  $L = s = 1$ ,  $S = v_t = 0.6$ ,  $M_S S = 0.54$  and  $1 - N_S = 0.46$ . The relative resistance of the tow matrix series path ( $v_t = 0.6$ ,  $\bar{K}_t = 10$ ) for this layered composite is 0.46 --- nearly twice that for the same tow uniformly distributed as cubical chunks. The transverse conductivity of this layered material is  $k_S/k_m = 1 + 0.9 \times 0.6(0.46)^{-1} = 2.17$ .

Parallel aramid fibers (square in cross-section) distributed uniformly with  $v_t = 0.6$  in a resinous matrix would have, again,  $S = s = (0.6)^{1/2} = 0.775$ . However, the conductivity of the aramid tow likely would be about one fifth of that for a resinous matrix, so that  $M_S = 1 - (1/0.2) = -4$  and  $1 - N_S = 1 - M_S S = 1 + 4 \times 0.775 = 4.10$ . The resistance of this tow-matrix series path is roughly four times that of its matrix alone. The bulk transverse conductivity would be  $[(k_S/k_m) - 1]/M_S v_t = (1 - N_S)^{-1} = (4.10)^{-1} = 0.244$ , or  $k_S/k_m = 0.414$  -- twice the filament conductivity and two fifths that of the matrix.

Referring to equations (A-18) and (A-19), this approximate model indicates two generalizing transverse conductivity variables:  $Y_i \equiv [(k_i/k_m) - 1]/M_i v_t$  and  $N_i \equiv M_i X_i$ , where  $M_i \equiv 1 - k_m/k_{t-i}$  and  $X_i$  is the spacing ratio in the particular transverse direction ( $S$  or  $s$  or  $L$ ). Thus, these variable groupings ought to serve to a "first-order" level of accuracy in correlating data obtained experimentally or by accurate analytical means. Further, if these generalizing variables are



accurate to a "first order" level, then an adjustment factor(s) introduced in some manner into the basic equation  $Y_i = (1 - N_i)^{-1}$  ought to provide a method to improve the accuracy of the model while retaining its comparatively simple, basic form. And, the first-order effects of the key variables could, thereby, remain isolated in relatively uncomplicated variable groups. Successful modification of this basic relationship with an adjustment factor(s) (the latter expressed also in terms of the key variables) should provide a procedure useful as a preliminary design tool.

This approximate model also indicates the importance of the spacing ratio  $X_1$  (S or s or L) on the transverse conductivity. The extent to which the tow (reinforcing elements) shift the transverse conductivity away from that of the matrix can be quite sensitive to the transverse spacing ratio, especially when the spacing ratio is near unity and  $\bar{k}_t = k_t/k_m \gg 1$  (or when the spacing ratio is near zero with  $\bar{k}_t \ll 1$ ). When  $k_t \gg k_m$ , very thin layers of matrix between adjacent tow elements ( $S \approx 1$ ) will drastically lower the conductivity of the tow-matrix series path. Oppositely, when  $k_t \ll k_m$ , a thin layer of tow will create a large reduction in the series conductivity. Any thin layer of tow or matrix (spacing ratios near unity or near zero) could radically alter the transverse conductivity of a two-phase material (see Section B).

Next, this approximate model is applied to three special cases:

(i) Unidirectional sheet tow (the conventional laminate), (ii) unidirectional ribbons of tow in a rectangular array and (iii) rectangular solid chunks of tow in rectangular arrays.

#### b. Unidirectional Sheet Tow (Conventional Laminate).

With the width and length spacing ratios both unity ( $s = L = 1$ ) and alternating parallel layers of tow and matrix, the volume fraction of tow  $v_t$  equals the depth spacing ratio S (equation A-8) and the transverse conductivity  $k_S$  (by equations A-18 and A-19) is given by

$$Y_S = (1 - N_S)^{-1} = (1 - M_S v_t)^{-1} = [k_S/k_m - 1]/M_S v_t$$

or

$$\bar{k}_S = k_S/k_m = (1 - M_S v_t)^{-1} = (1 - N_S)^{-1} \quad (A-20)$$

Again, the generalizing variables are indicated to be  $\bar{k}_S$  or  $Y_S = f(N_S)$ . Applying  $Y_i = (1 - N_i)^{-1}$  to the longitudinal direction (for which  $s = L = 1$ ) yields

$$Y_L = (1 - M_L)^{-1} = (1 - M_L)^{-1} \quad (A-21)$$

or, for the longitudinal relative conductivity

$$\bar{k}_{lg} = k_{lg}/k_m = 1 + M_{lg} v_t / (1 - M_{lg}) = 1 + v_t [(k_{t-lg}/k_m) - 1] \quad (A-22)$$

This is a familiar conductivity expression for two continuous parallel phases (oftentimes referred to as the "rule of mixtures"). If the tow is anisotropic, then a second similar expression would apply to the s-direction.

The anisotropy of this conventional laminate is indicated by examination of the ratio of the transverse to the longitudinal conductivity  $k_{tr}/k_{lg}$ . Letting  $P \equiv (k_{t-lg}/k_m) - 1$  and with  $M \equiv 1 - (k_m/k_{t-tr})$ , then, from equations (A-20) and (A-22)

$$k_{tr}/k_{lg} = (1 - M v_t)^{-1} (1 + P v_t)^{-1} \quad (A-23)$$

This ratio is minimum (maximum anisotropy) for

$$2v_t = M^{-1} - P^{-1} \quad (A-24)$$

The minimum ratio  $k_{tr}/k_{lg}$  is

$$k_{tr}/k_{lg} = 4 MP / (M + P)^2 \quad (A-25)$$

or

$$k_{tr}/k_{lg} = 4 \bar{k}_{t-tr} (\bar{k}_{t-tr} - 1) (\bar{k}_{t-lg} - 1) / (\bar{k}_{t-tr} \bar{k}_{t-lg} - 1)^2 \quad (A-26)$$

where

$$\bar{k}_{t-tr} \equiv k_{t-tr}/k_m \text{ and } \bar{k}_{t-lg} \equiv k_{t-lg}/k_m \quad (A-27)$$

For the special case of isotropic tow,  $k_{t-tr} = k_{t-lg}$ ,  $v_t$   
(for  $\min k_{tr}/k_{lg} = 1/2$ , and

$$(k_{tr}/k_{lg})_{\min} = 4 \bar{k}_t / (\bar{k}_t + 1)^2 \quad (A-28)$$

For the range on  $\bar{k}_t$  from  $10^{-2}$  to  $10^3$ ,  $(k_{tr}/k_{lg})_{\min}$  is 0.039 at  $\bar{k}_t = 10^{-2}$ , unity at  $\bar{k}_t = 1$  and back down to 0.004 at  $\bar{k}_t = 10^3$ .

The individual conductivity levels for minimum  $k_{tr}/k_{lg}$  and isotropic tow ( $v_t = 1/2$ ) are

$$\bar{k}_{lg} = 1 + (\bar{k}_t - 1)/2 = (\bar{k}_t + 1)/2 \quad (A-29)$$

and

$$\bar{k}_{tr} = 2\bar{k}_t / (\bar{k}_t + 1) \quad (A-30)$$

For  $\bar{k}_t \gg 1$ ,  $\bar{k}_{lg} \approx \bar{k}_t/2$  and  $\bar{k}_{tr} \approx 2$ ; the transverse conductivity asymptotically approaches twice the matrix conductivity. When  $\bar{k}_t \ll 1$ ,  $\bar{k}_{lg} \approx 1/2$  and  $\bar{k}_{tr} \approx 2\bar{k}_t$ .

The volume ratio for minimum  $k_{tr}/k_{lg}$  is at or close to  $1/2$  for laminated composites, except for anisotropic tow having values of the tow conductivity in the vicinity of the matrix conductivity.

### c. Unidirectional Tow as Ribbons or Filaments.

A filamentary composite, when compared with a laminate having an equal tow volume ratio  $v_t$  and an equal tow-to-matrix conductivity ratio  $\bar{k}_t$ , will have an equal longitudinal conductivity but a transverse conductivity departing to a greater extent from the matrix conductivity. With the tow continuous in one direction only, a greater amount of tow is now distributed transversely (for the same tow volume) and the matrix gap between tow elements is less. The anisotropy of the fiber composite is thus less than that for a layered composite since the transverse conductivities are closer to the longitudinal conductivities. Equation (A-12) for the approximate model shows that for the tow-matrix series path

$$k_{m-t-S-fiber} / k_{m-t-S-layer} = (1 - N_S)_{layer} / (1 - N_S)_{fiber}$$

Thus, if, for example, the fibers are square in cross section and embedded in a square array, then (by equation A-8),  $S_{\text{fiber}} = (v_t)^{1/2}$  and  $S_{\text{layer}} = v_t$ . With  $v_t = 0.7$  and  $\bar{k}_t/k_m = 50$ , then  $k_{m-t-S-\text{fiber}}/k_{m-t-S-\text{layer}} = 1.74$  or (by equation A-10), the ratio  $k_{S-\text{fiber}}/k_{S-\text{layer}} = 4.81/3.18 = 1.51$ .

The model being used is adapted to a filamentary composite by assuming the filaments (ribbons) are rectangular in cross-section and embedded in a rectangular array. With the length spacing ratio  $L = 1$ , and by use of equations (A-4), (A-6) and (A-8) (and with reference to Figure A-1)

$$v_t = sS = (r/R) S^2 = S^2/\bar{R} \quad (\text{A-31})$$

where

$$\bar{R} \equiv R/r = (r \tan \theta)^{-1} \quad (\text{A-32})$$

is the ratio of the array aspect ratio  $R$  (width-to-depth) to the filament aspect ratio  $r$  (width-to-depth). Thus, the depth spacing ratio  $S$  (a key factor in transverse conductivity) is defined by

$$S = (\bar{R}v_t)^{1/2} \quad (\text{A-33})$$

and by equation (A-18)

$$Y_S = (1 - N_S)^{-1} = [1 - M_S(\bar{R}v_t)^{1/2}]^{-1} \quad (\text{A-34})$$

The generalizing variables are still  $Y_i$  and  $N_i$ . Hence, to a first-order level of accuracy, the transverse conductivity of various types of filamentary laminae or plies (having a single type of tow embedded in a single type of matrix) should be correlated by the two variable groups  $Y_i$  and  $N_i$ .

For a rectangular array, the minimum array angle  $\theta_{\min}$  occurs when the fibers touch in their in-line direction; the depth spacing ratio  $S$  is at its maximum ( $S = 1$ ), and the width spacing ratio (for a given  $v_t$ ) is minimal. With  $S = S_{\max} = 1$ , then

$$s = s_{\min} = v_t$$

$$v_t \bar{R} = 1 \quad (\text{A-35})$$

$$\tan \theta = \tan \theta_{\min} = R_{\max}^{-1} = v_t/r$$

The maximum array angle  $\theta_{\max}$  exists when the tow elements touch laterally ( $s = 1$ ). With  $s = s_{\max} = 1$ , then

$$S = S_{\min} = v_t$$

$$\bar{R} = v_t \quad (A-36)$$

$$\tan \theta = \tan \theta_{\max} = R_{\min}^{-1} = (v_t r)^{-1}$$

For a filament aspect ratio  $r$  of unity, example values of the limits on the array angle and the array aspect ratio  $R$  are as follows:

		Tow Volume Ratio $v_t$				
		0.3	0.4	0.5	0.6	0.7
Square	$\theta_{\min}(\text{deg})$	17	22	27	31	35
Fiber	$R_{\max}$	3.3	2.5	2	1.7	1.4
Square	$\theta_{\max}(\text{deg})$	73	68	63	59	55
Fiber	$R_{\min}$	0.3	0.4	0.5	0.6	0.7
Circular	$\theta_{\min}(\text{deg})$	21	27	32	37	42
Fiber	$\theta_{\max}(\text{deg})$	69	63	57	53	48

For the tow volume ratio  $v_t$  in the range 0.4 to 0.7, the array angles are essentially limited to the approximate range 30 to 60 degrees, with the corresponding range on the array aspect ratio  $R$  being approximately 1/2 to 2.

The approximate effect of the tow aspect ratio  $r$  (filament width to depth) on the transverse conductivity is indicated by this model. For the same tow volume ratio  $v_t$  and array aspect ratio  $R$ , an increase in the tow aspect ratio  $r$  widens and thins the tow filaments while thickening the matrix gap in the tow-matrix series path. Consequently, the depth spacing ratio  $S$  is reduced and the transverse conductivity of the tow-matrix series path is shifted toward the conductivity of the matrix;  $k_{m-t-S}$  decreases when  $\bar{k}_t > 1$  and increases with  $\bar{k}_t < 1$ . On a bulk basis, though there's a compensating effect in that the width of the tow-matrix series path is larger (with a larger tow aspect ratio  $r$ ),

the effect of the change in the series conductivity exceeds the effects of the changes in the width of the two parallel paths and the bulk transverse conductivity  $\bar{k}_S$  also shifts toward the matrix conductivity.

Suppose  $v_t = 0.6$ ,  $\bar{k}_{t-S} = 5$  and  $R = 1(\theta = 45^\circ)$ . With a filament aspect ratio  $r = 3/2$ ,  $\bar{R} = R/r = 2/3$  and  $S = (0.6/1.5)^{1/2} = 0.63$ . Therefore  $\bar{k}_{m-t-S} = (1 - N_S)^{-1} = 2.02$  and  $\bar{k}_S = k_S/k_m = 1 + 0.8 \times 0.6 \times 2.02 = 1.97$ . Decreasing the filament aspect ratio  $r$  to  $2/3$  increases the depth spacing ratio  $S$  to  $(\bar{R}v_t)^{1/2} = (1.5 \times 0.6)^{1/2} = 0.949$ ;  $\bar{k}_{m-t-S} = (1 - 0.8 \times 0.949)^{-1} = 4.15$ ,  $\bar{k}_S = 1 + 0.8 \times 0.6 \times 4.15 = 2.99$ . (The shear analogy [12] [25] for fiber aspect ratios of  $2/3$  and  $3/2$  with  $v_t = 0.6$ ,  $\bar{k}_t = 5$  yields  $\bar{k}_S$  2.00 and 3.01, respectively.)

The influence of the array angle  $\theta$  (or array aspect ratio  $R$ ) on the transverse conductivity is also indicated by the approximate model. Since, by equation (A-31) and (A-32)

$$S = (v_t \bar{R})^{1/2} = (v_t/r \tan \theta)^{1/2}$$

the transverse spacing ratio  $S$  is seen to be influenced approximately inversely as  $(\tan \theta)^{1/2}$ . For  $v_t = 0.6$ ,  $r = 1$  (square filament) and  $\bar{k}_t = k_{t-S}/k_m = 10$ , the model estimates the following influence of the fiber diagonal angle  $\theta$  (or array aspect ratio  $R$ ) on the transverse conductivity of a rectangular in-line array.

	Array Angle $\theta$ (Degrees)	Depth Spacing Ratio $S$	$1 - N_S$	$k_S/k_m$
$v_t = 0.6$	35	0.926	0.167	4.24
$\bar{k}_t = 10$	45	0.775	0.303	2.78
$r = 1$	55	0.648	0.417	2.30

This example illustrates the appreciable rise in transverse conductivity which occurs as the fibers move closer and closer in the  $S$  direction, i.e.  $\theta$  approaching  $\theta_{\max}$  ( $S = 1$ ). For this example, once the fibers touch,  $S = 1$ ,  $\theta = 31^\circ$ ,  $s = v_t = 0.6$ ,  $1 - N_S = 0.1$ , and  $k_S/k_m = 6.4$ . This is the maximum bulk conductivity in the  $S$  direction since the reinforcing elements (with  $S = 1$ ) form continuous paths.

The variable grouping represented by  $\bar{R}$  includes, in this approximate model, the combined effects of the configuration variables. Since, at least for aligned arrays, any packing geometry is likely to show some relationship to a rectangular array, this approximate model suggests that the aspect ratio parameter  $\bar{R}$  incorporated with  $v_t$  as  $\bar{R}v_t$  should be useful --- at least to a first order --- as a generalizing variable to correlate transverse conductivities for various types of filamentary composite materials.

The actual extent to which the bulk transverse conductivity of the composite material  $k_S$  differs from the matrix conductivity  $k_m$  can be defined approximately by the model equations (A-34). Specifically

$$\bar{k}_S - 1 = M_S v_t / [1 - M_S (\bar{R}v_t)^{1/2}] \quad (A-34)$$

where, by equations (A-35) and (A-36), for the physical constraints on fiber position, i.e. touching in the in-line direction,  $S = S_{\max} = 1$ , or touching laterally,  $S = S_{\min}$  ( $s = 1$ ), the parameter  $\bar{R}v_t$  is restricted to the range  $v_t^2 \leq \bar{R}v_t \leq 1$ . This relationship (A-34) is used to illustrate (in Figure A-2) the approximate influence of the fiber diagonal angle  $\theta$  and the tow volume ratio  $v_t$  on the transverse conductivity ratio  $k_S/k_m$  of a filamentary composite having fibers (square in cross-section) embedded in a rectangular array (with a tow conductivity ratio  $\bar{k}_{t-S} = k_{t-S}/k_m = 8$ ). The upper limit occurs when the fibers touch in the transverse direction ( $S = 1$ ); the composite then becomes a laminate and the S-direction conductivity is the conductivity through parallel tow matrix paths (thereby classified longitudinal). The lower limit on the transverse conductivity occurs when the fibers touch laterally ( $s = 1$ ); the filamentary composite is then again a laminate (as with  $s = 1$ ), but now the S-direction conduction is across the layers (a series path through layers of tow and matrix).

For  $\theta \leq 45^\circ$ , the maximum possible tow volume ratio  $v_t$  occurs with  $S = 1$  and is (by equation A-35)

$$v_{\max} = \bar{R}^{-1} = r \tan \theta \quad (\theta \leq 45^\circ)$$

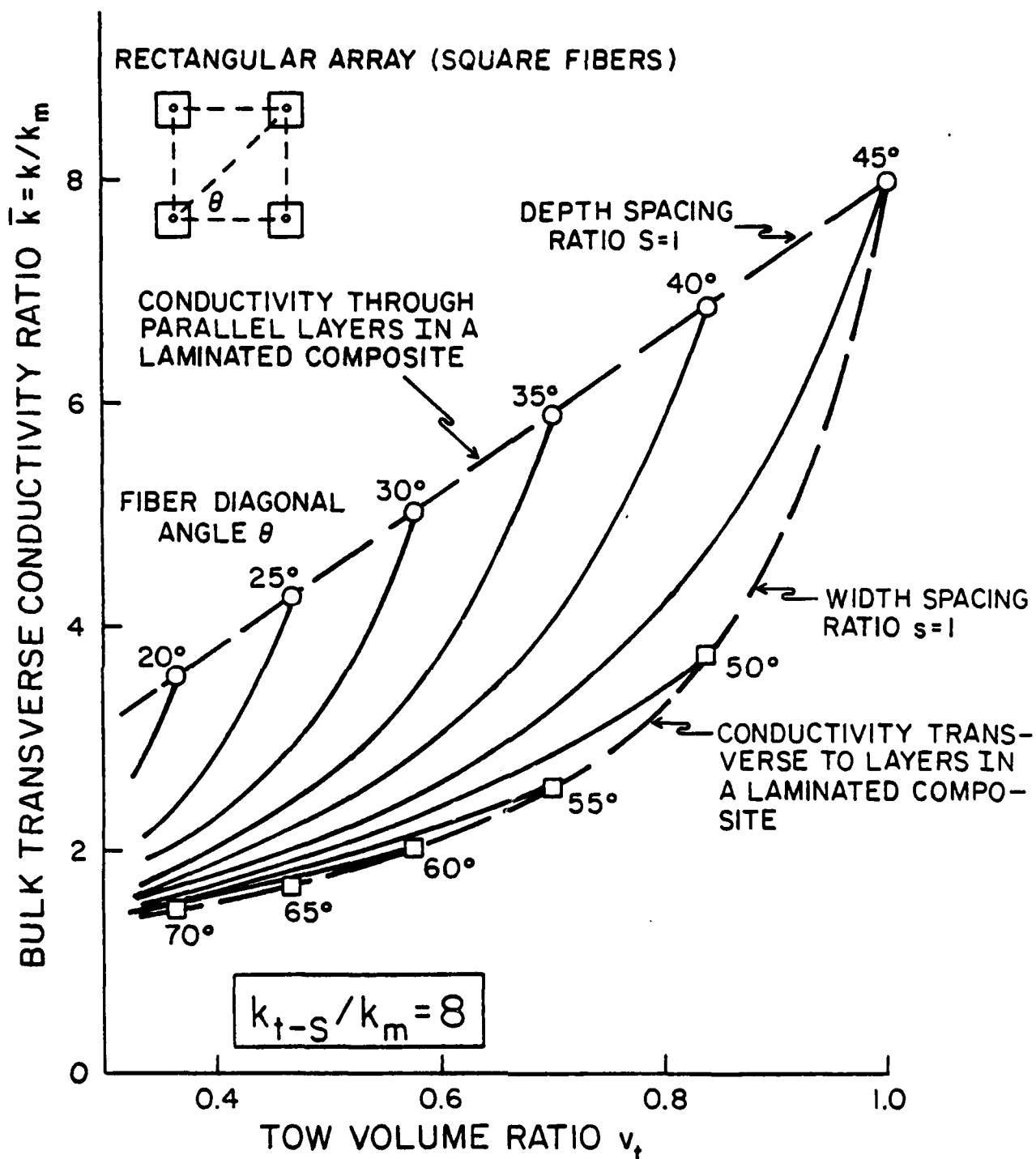


Figure A-2. Use of Approximate Model to Determine the Effect of Fiber Diagonal Angle on the Transverse Conductivity of Square Fibers in A Rectangular Array.



The model equation (A-34) for the transverse conductivity may be rearranged, therefore, to

$$[(\bar{k}_S/k_m)-1]/v_{\max} = M_S \bar{v}/[1 - M_S(\bar{v})^{1/2}] \quad (\theta \leq 45^\circ) \quad (A-37)$$

where  $\bar{v} = v_t/v_{\max}$ . The purpose of this revision is to illustrate, via this approximate model, the usefulness of the relative tow volume  $\bar{v}$  (which is an index to the relative packing density of the fibers). By use of  $\bar{v}$ , equation (A-37) illustrates that one might expect a first-order correlation of the conductivity ratio  $k_S/k_m$  in terms of two independent variables,  $\bar{v}$  and  $\bar{k}_{t-S}$ , rather than the three in equation (A-34),  $v_t$ ,  $\bar{R}$  and  $\bar{k}_{t-S}$ .

The anisotropy of a filamentary composite is also defined approximately by the previous relationships. The longitudinal conductivity is

$$\bar{k}_{lg} = k_{lg}/k_m = 1 + (\bar{k}_{t-lg} - 1) v_t = 1 + P_{lg} v_t \quad (A-38)$$

where  $P \equiv \bar{k}_t - 1$ . For  $\theta \leq 45^\circ$ ,  $v_{\max} = r \tan \theta$ , and by use of equations (A-37) and (A-38), the ratio of the transverse conductivity  $k_S$  to the longitudinal conductivity  $k_{lg}$  becomes

$$k_S/k_{lg} = \left\{ 1 + P_S [1 - (\bar{v})^{1/2} + v_t] \right\} / \left\{ 1 + P_S [1 - (\bar{v})^{1/2}] \right\} (1 + P_{lg} v_t), \quad (A-39)$$

$$(\theta \leq 45^\circ)$$

---

where, again,  $P = \bar{k}_t - 1$ ,  $\bar{v} = v_t/v_{\max}$ ,  $v_{\max} = r \tan \theta$  for  $\theta \leq 45^\circ$ .

---

For  $\theta \geq 45^\circ$ ,  $v_{\max} = \bar{R} = (r \tan \theta)^{-1}$  and by use of equation (A-34)

$$(k_S/k_m) - 1 = M_S v_t / [1 - M_S v_{\max} (\bar{v})^{1/2}], \quad (\theta \geq 45^\circ) \quad (A-40)$$

and, therefore, equations (A-38) and (A-40) yield (for  $\theta \geq 45^\circ$ )

$$k_S/k_{lg} = \left\{ 1 + P_S [1 - v_{\max} (\bar{v})^{1/2} + v_t] \right\} / \left\{ 1 + P_S [1 - v_{\max} (\bar{v})^{1/2}] \right\} \times \quad (A-41)$$

$$\times [1 + P_{lg} v_t]$$

Implicit solutions to the condition of minimum  $k_S/k_{lg}$  (maximum anisotropy) are:

For  $\theta \leq 45^\circ$

$$\left\{ 2 + P_S [2 - (\bar{v})^{1/2}] \right\} / \left\{ 1 + P_S [1 - (\bar{v})^{1/2}] \right\}^2 = 2 (P_{lg}/P_S) (k_S/k_{lg}) \quad (A-42)$$

For  $\theta \geq 45^\circ$

$$\left\{ 2 + P_S [2 - v_{\max}(\bar{v})^{1/2}] \right\} / \left\{ 1 + P_S [1 - v_{\max}(\bar{v})^{1/2}] \right\}^2 = 2 (P_{lg}/P_S) (k_S/k_{lg}) \quad (A-43)$$

If  $\bar{k}_{t-S} \gg 1$ , then the condition of minimum  $k_S/k_{lg}$  for  $\theta \leq 45^\circ$  is defined by

$$(\tan \theta)(\bar{v})^{3/2} = 2[1 - (\bar{v})^{1/2}]^2 \quad (A-44)$$

For  $\bar{k}_{t-S} \ll 1$  and  $\theta \leq 45^\circ$ , the condition of minimum  $k_S/k_{lg}$  is given by

$$2 (P_{lg}/P_S)(\bar{v})^{1/2} = 1 + (P_{lg}/P_S) \bar{v} \tan \theta \quad (A-45)$$

For  $\theta \geq 45^\circ$ , the ratio  $k_S/k_{lg}$  is quite insensitive to the tow volume ratio  $v_+$ , so that equivalent, approximate solutions to equations (A-44) and (A-45) are neither accurate nor needed.

The minimum ratio of the transverse-to-longitudinal conductivity for this model is defined quite accurately for all angles and all tow conductivity ratios by

$$(k_S/k_{lg})_{\min} = [1 + (4/3)(\tan \theta)(\bar{k}_{t-S}-1)/(\bar{k}_{t-S} + 1)] + [1 + (4/9)(\tan \theta)(P_{lg}/P_S)(\bar{k}_{t-S}-1)] \quad (A-46)$$

The ratio of the two transverse conductivities,  $k_S$  and  $k_s$ , is defined by the ratio of equations (A-39) and (A-41), where the angle  $\theta_s$  to be used in equation (A-41) is the complement of the angle  $\theta_S$  in equation (A-39).

Thus, for any angle  $\theta$

$$k_S/k_s = \frac{\left\{ 1 + P_S [1 - v_{\max}(\bar{v})^{1/2} + v_t] \right\}}{\left\{ 1 + P_S [1 - (\bar{v})^{1/2} + v_t] \right\}} \frac{\left\{ 1 + P_S [1 - (\bar{v})^{1/2}] \right\}}{\left\{ 1 + P_S [1 - v_{\max}(\bar{v})^{1/2}] \right\}} \quad (A-47)$$

For  $k_{t-S}$  and  $k_{t-s} \gg 1$

$$k_s/k_S = [1 - v_{\max}(\bar{v})^{1/2} + v_t][1 - (\bar{v})^{1/2}]/[1 - (\bar{v})^{1/2} + v_t] \times [1 - v_{\max}(\bar{v})^{1/2}] \quad (A-48)$$

and for  $\bar{k}_{t-S}$  and  $\bar{k}_{t-s} \ll 1$

$$k_s/k_S = [1 - (\bar{v})^{1/2}]/[1 - v_{\max}(\bar{v})^{1/2}] \quad (A-49)$$

For the limiting case of  $\bar{v} = 1$  (maximum packing of the tow elements), by equation (A-47)

$$k_s/k_S = \bar{k}_{t-s}/(1 + P_S v_t)[1 + P_S(1 - v_t)] \quad (A-50)$$

which for  $k_{t-s} = \bar{k}_{t-s}$  (isotropic tow) reduces to the ratio of the lower to upper bounds  $k^-/k^+$  for the transverse conductivities (Equations I-1 and I-2).

#### d. Rectangular Solid Chunks of Tow Embedded in Rectangular Arrays.

For a three-dimensional distribution of tow in the form of solid rectangular chunks, the departure of the transverse conductivity from the matrix conductivity will exceed the corresponding departure for both the two-dimensional composite (ribbons or filaments) and the one-dimensional composite (the laminate), since (in this configuration) there is no continuous tow direction. Hence, more tow is distributed transversely in this three-dimensional array and the matrix gaps are thinner; the spacing ratio  $S$  or  $s$  (or both) can be greater.

From equations (A-1) through (A-8)

$$S^3 = v_t (R/r)(R'/r) = v_t \bar{R} \bar{R}' \quad (A-51)$$

where

$$\bar{R} \equiv R/r, \bar{R}' \equiv R'/r \quad (A-52)$$

Thus,

$$N_S = M_S (v_t \bar{R} \bar{R}')^{1/3} \quad (A-53)$$

and by equation (A-18), the transverse conductivity in the direction S is

$$Y_S = [(k_S/k_m) - 1]/M_S v_t = [1 - M_S(v_t \bar{R} \bar{R}')^{1/3}]^{-1} \quad (A-54)$$

Since, alternately,  $s^3 = v_t \bar{R}'/\bar{R}^2$  and  $\ell^3 = v_t \bar{R}/\bar{R}'^2$ , equation (A-54) defines also the transverse conductivity ratios  $k_S/k_m$  and  $k_\ell/k_m$ .

For the special case of rectangular solid chunks having dimensions A, a and a' in proportion to the spacing dimensions C, c and c' (the corresponding tow and array dimensions in equal ratios), then  $S = s = \ell$  ( $\bar{R} = 1$ ,  $\bar{R}' = 1$ ) and  $v_t = S^3 = s^3 = \ell^3$ . This special case of geometric similarity includes, of course, the special case of the tow being distributed uniformly as cubes. With geometric similarity between the tow and array configurations in all three directions,

$$Y_i = [(k_i/k_m) - 1]/M_i v_t = (1 - M_i v_t^{1/3})^{-1} \quad (A-55)$$

Or, if the tow material (in addition to the matrix material) is isotropic, then  $M_S = M_s = M_\ell$  in equation (A-55) and the transverse conductivities are equal ( $k_S = k_s = k_\ell$ ).

The Rayleigh-Maxwell equation for the transverse conductivity of spherical bodies dispersed throughout an isotropic, continuous medium is

$$k/k_m = [1 + 2 v_t (\bar{k}_t - 1)/(\bar{k}_t + 2)]/[1 - v_t (\bar{k}_t - 1)/(\bar{k}_t + 2)] \quad (A-56)$$

The transverse conductivity for rectangular chunks dispersed symmetrically ( $\bar{R} = \bar{R}' = 1$ ) as defined by the approximate solution (A-55) is compared in Figure A-3 with the Rayleigh-Maxwell solution (A-56) and with the corresponding two-dimensional solution (all for isotropic tow with  $\bar{k}_t = k_t/k_m = 8$ ).

For the special case of very large tow conductivity relative to the matrix conductivity ( $k_t \gg 1$ ), the asymptotic solutions are displayed in Figure A-4 for symmetrical dispersion of the tow ( $r = R' = 1$ ). The parameter  $[(k_S/k_m) - 1](1 - v_t)$  is used to condense the conductivity range. The Rayleigh solutions yield somewhat higher conductivities than the approximate model. At  $v_t = 0.6$  and  $\bar{k}_t \gg 1$ ,

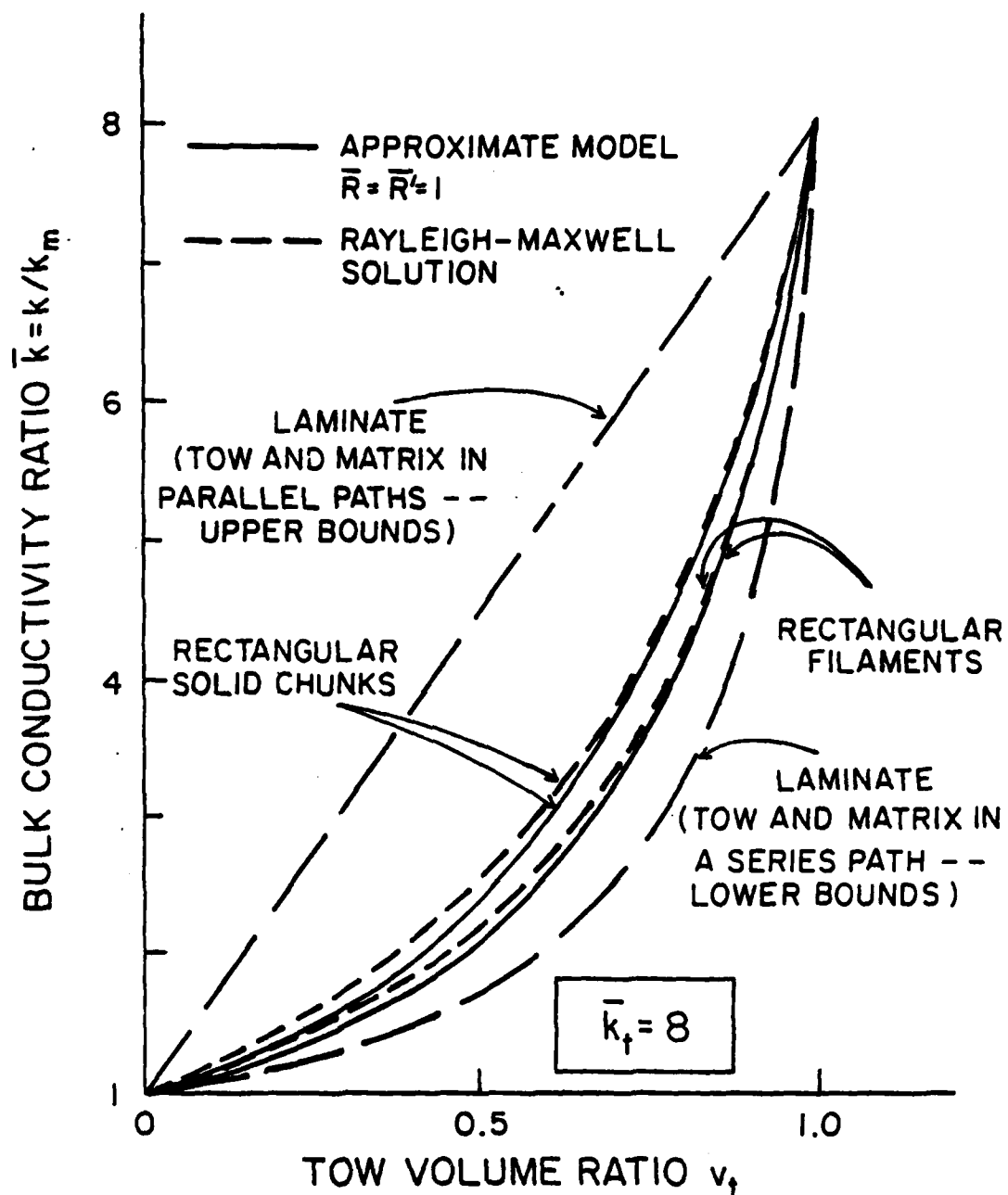


Figure A-3. A Comparison of the Results by the Approximate Model with the Rayleigh-Maxwell Solution.

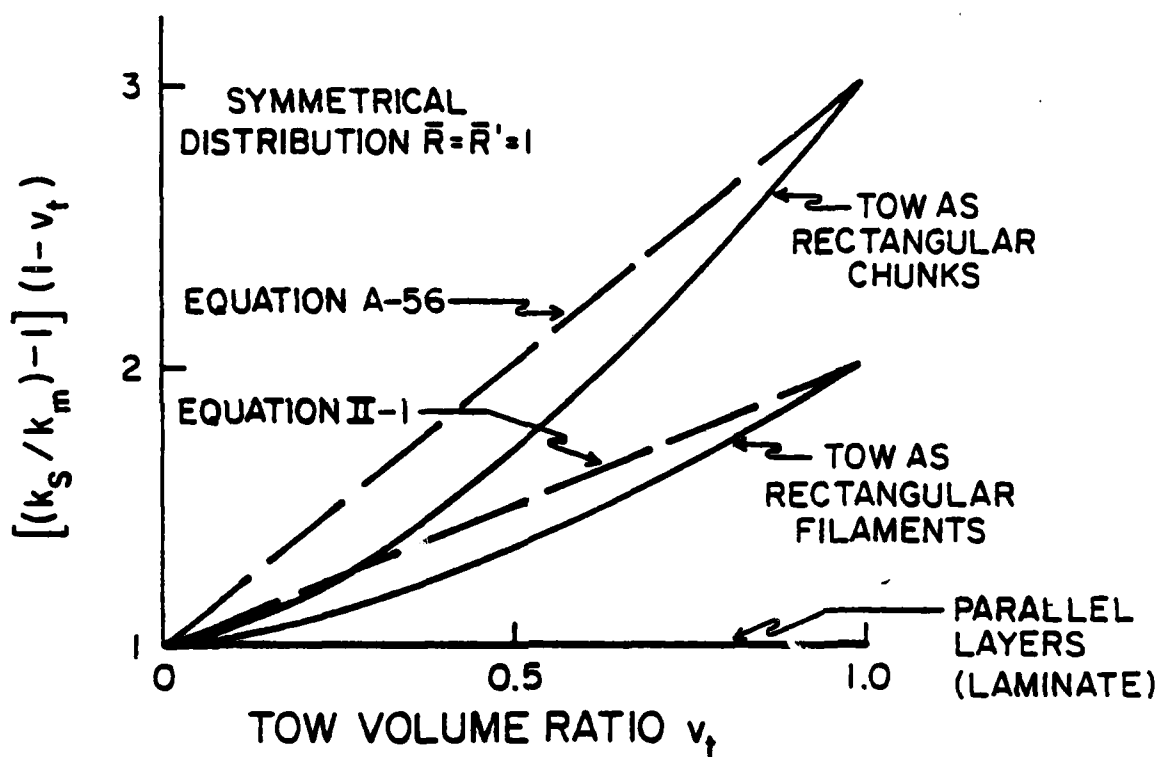


Figure A-4. A Comparison of the Asymptotic Solutions ( $\bar{k}_t \gg 1$ ) for the Approximate Model with the Rayleigh-Maxwell Solutions for Spheres and Cylinders.

$k_s/k_m$  for a cube is 5.5 and 4.8 by the Rayleigh-Maxwell equation and by equation (A-55), respectively. For square filaments and  $v_t = 0.6(\bar{k}_t > 1)$ , the Rayleigh equation (II-1) gives a value of 1.60 versus 1.46 by the two-dimensional model.

## SECTION B

### Approximate Analysis of the Effects of Fiber Packing and Fiber Cross-Sectional Configuration on the Conductivity of A Tow-Matrix Series Path

#### Introduction

As explained and referenced in the Introduction, Section III, estimating the bulk transverse conductivity of multi-phase materials by one-dimensional conduction analysis is a procedure used in the literature a number of times. The most prominent example of its application to conventional composite material is the paper by Springer and Tsai [18].

In the analyses which follow, the conductivity of a tow-matrix series path is studied with respect to the principle variables of tow packing density, tow-to-matrix conductivity ratio, tow cross-sectional shape and tow orientation or alignment. The conductivity of the series path is analyzed assuming one-dimensional conduction. The results are used in Section III to develop approximate models which evaluate the bulk transverse conductivity of a filamentary composite material.

The tow-matrix system is an idealized conventional composite material. The tow (reinforcement) is assumed to be embedded unidirectionally in an isotropic, homogeneous matrix. The tow (as ribbons or filaments) is assumed to be homogeneous, with its length appreciably greater than its cross-sectional dimensions. The tow conductivity might be orthotropic. There are no voids, no interfacial resistances, no cracks, non-uniformities or delaminations.



### One-Dimensional Analysis of the Tow-Matrix Series Path

A tow-matrix series path in a conventional composite material would be, for example (with reference to Figure B-1), an x-direction path of width (a) and of depth C (consisting of tow of depth A and matrix of depth C-A), or a y-direction path of width A and length c.

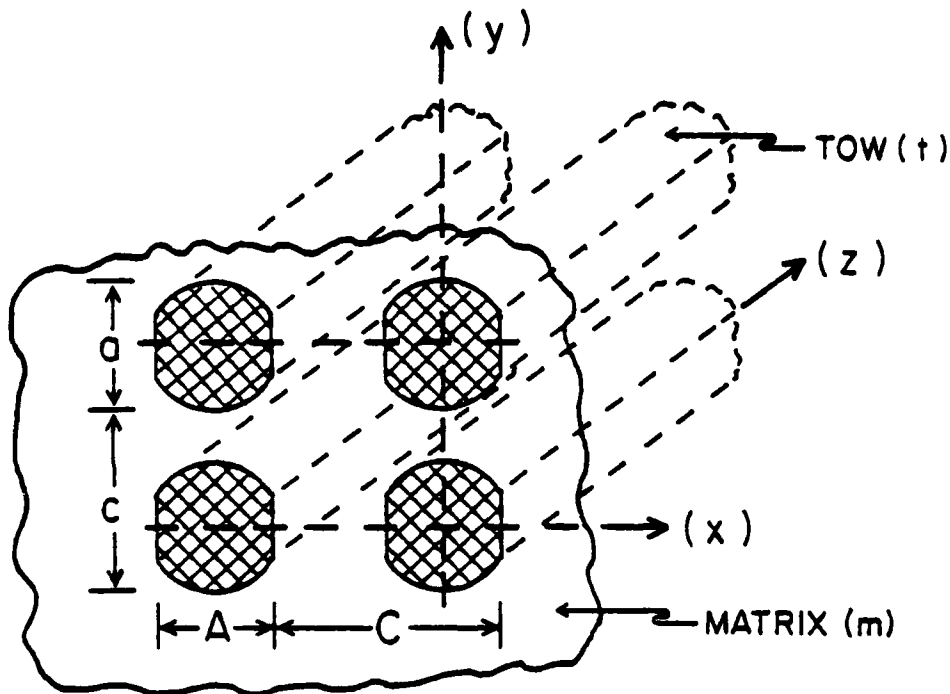


Figure B-1. Schematic of Filamentary Composite Material, Consisting of Continuous Parallel Tow of Arbitrary Cross-Section Embedded in a Matrix.

The thermal resistance of a tow-matrix series path of unit width and of length C is

$$R = R_t + R_m = (2x/k_t) + (C - 2x)/k_m$$

so that the conductivity of the series path  $k_{m-t}$  is

$$k_m/k_{m-t} = (2x/C)(k_m/k_t) + 1 - (2x/C)$$

Or, letting

$$\bar{k}_{m-t} \equiv k_{m-t}/k_m \quad (B-1)$$

$$S \equiv A/C \quad (B-2)$$

$$X \equiv 2x/A \quad (B-3)$$

$$\bar{k}_t \equiv k_t/k_m \quad (B-4)$$

$$M \equiv 1 - (\bar{k}_t)^{-1} \quad (B-5)$$

$$N \equiv MS \quad (B-6)$$

it follows that the conductivity of this tow-matrix series path of unit width located laterally at coordinates (y,z) is defined by

$$\bar{k}_{m-t,y} = (1 - NX)^{-1} \quad (B-7)$$

If, for example, the fiber thickness  $2x$  at (y) equals 0.90 of the fiber spacing distance  $C$ , then  $2x/C = SX = 0.90$  and the tow-matrix series conductivity ratio  $\bar{k}_{m-t} = k_{m-t}/k_m$  equals, by equation (B-7), 5.3 and 0.11 for a tow conductivity ratio  $\bar{k}_t = k_t/k_m = 10$  and 0.1, respectively.

The depth spacing ratio  $S = A/C$  represents the ratio of the maximum fiber thickness to the fiber spacing distance. The corresponding lateral spacing ratio is

$$s \equiv a/c \quad (B-8)$$

The tow volume ratio  $v'_t$  for the tow-matrix series path is defined as the fraction of the path occupied by tow. With reference to Figure B-1

$$v'_t \equiv (\text{Area}_t)/(\text{Area}_{t+m}) = F_A (aA)/(aC) = F_A S \quad (B-9)$$

where  $F_A$  is the ratio of the actual cross-sectional area of the filament to the rectangular area based on the maximum filament thickness and maximum width. If the tow elements are embedded in a rectangular array, the tow-volume ratio  $v_t$  for the entire system would be

$$v_t = (F_A aA)/cC = F_A sS$$

$$v_t = s v'_t$$

Or, if the filaments are in a staggered array (Figure II-15), then

$$v_t = 2F_A aA/cC = 2 F_A sS$$

and

$$v_t = 2sv'_t$$

The bulk (effective overall) conductivity of tow tow-matrix series path  $k_{m-t}$  of width (a) is determined, in this approximate analysis, by evaluation of the total conduction through the series path. Thus, since

$$q_{m-t} = \int_{-a/2}^{a/2} k_{m-t,y} (\Delta T) dy/C = k_{m-t} (a \Delta T)/C$$

it follows that

$$\bar{k}_{m-t} = \int_0^1 \bar{k}_{m-t,y} dY \quad (B-10)$$

where

$$Y \equiv 2y/a \quad (B-11)$$

Or, by equation(B-7), the generalized expression for the conductivity of a tow-matrix series path is

$$\bar{k}_{m-t} = k_{m-t}/k_m = \int_0^1 (1 - NX)^{-1} dY \quad (B-12)$$

where Y and X are the normalized width and depth coordinates, respectively, and  $X = f(Y)$  is set by the shape and packing configuration of filaments.

#### 1. Rectangular Tow Elements.

For tow filaments rectangular in cross-section,  $2x = A$ ,  $X = 1$  and, by equation (B-12)

$$\bar{k}_{m-t} = (1 - N)^{-1} = (1 - MS)^{-1} \quad (B-13)$$

The tow volume fraction for the series path

$$v'_t = F_A S = S \quad (B-14)$$

since  $F_A = 1$  for a tow element rectangular in cross-section.

Representative values of the transverse conductivity ratio for this particular tow-matrix series path and for several tow-matrix combinations used in composites (Figure B-2) range from roughly 1/30 to 10 times the matrix conductivity. These series path conductivities are also the transverse conductivities of a laminated composite.

## 2. Wedge-Type Filaments.

Filamentary tow elements having a sectional configuration approximated by a truncated wedge (Figure B-3) have a normalized thickness  $X$  linearly related to the normalized lateral coordinate  $Y$ ,

$$X = 1 - t Y \quad (B-15)$$

where the filament taper ratio  $t$  defines the proportionate extent to which the area is tapered, i.e.  $t = 1 - (A'/A)$  (Figure B-3). The tow volume ratio  $v'_t$  for this configuration in a series path is

$$v'_t = F_A S = S(1 - t/2) \quad (B-16)$$

From equations (B-12) and (B-15), for this type filament

$$\bar{k}_{m-t} = \int_0^1 [1 - N(1 - tY)]^{-1} dY$$

or

$$\bar{k}_{m-t} = (Nt)^{-1} \ln \left\{ [1 - N(1 - t)] / (1 - N) \right\} \quad (B-17)$$

For  $t = 0$ , the filament is of uniform thickness,  $v'_t = S$ , and equation (B-17) reduces to equation (B-13). For  $t = 1$ ,  $v'_t = S/2$ , the sectional configuration of the filament is a full wedge and

$$\bar{k}_{m-t} = -N^{-1} \ln (1 - N) \quad (B-18)$$

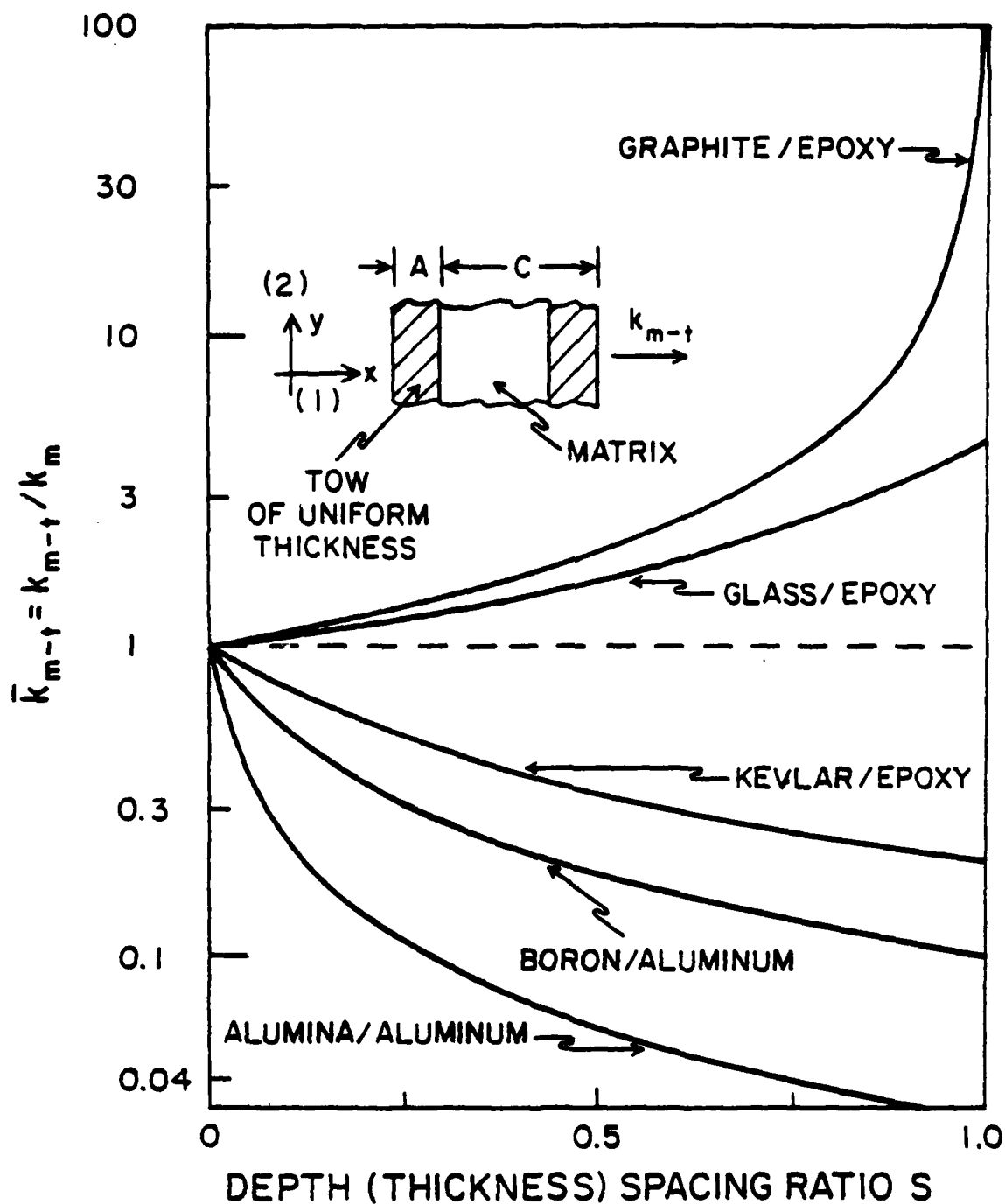


Figure B-2. Representative Conductivities for A Tow-Matrix Series Path Having Tow of Uniform Thickness.

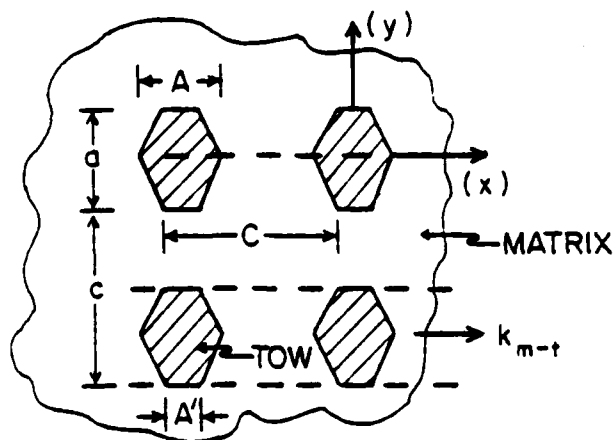


Figure B-3. Wedge-Type Filamentary Tow.

Comparative values of the conductivity for the tow-matrix series path for four wedge-type filament shapes are shown in Figure B-4, with each filament having the same width  $a$  and the same maximum thickness  $A$  (i.e. equivalent width and depth spacing ratios  $s$  and  $S$ ). For a given depth spacing ratio  $S$  and a given tow-to-matrix conductivity ratio  $\bar{k}_t$ , the filament of uniform thickness creates the maximum conductivity departure from that of the matrix, since the average thickness of the matrix gap between the filaments is minimal. Contrariwise, if compared on the basis of equal tow volume fraction, the filament having maximum taper ( $t=1$ ) creates the greatest departure of the conductivity from that of the matrix (Figure B-5), since the greater in-line penetration of tow reduces the effective thickness of the matrix. Fiber shape and its alignment do influence this conductivity to a significant extent. For the example, with  $\bar{k}_t = 10$  and  $v'_t = 0.5 \bar{k}_{m-t}$  for  $t = 0$  (uniform thickness) is about 1.8 (equation B-13). Whereas for  $t = 1$  (full taper),  $S = 2v'_t$  and  $\bar{k}_{m-t}$  is roughly 2.6 (equations B-16 and B-18).

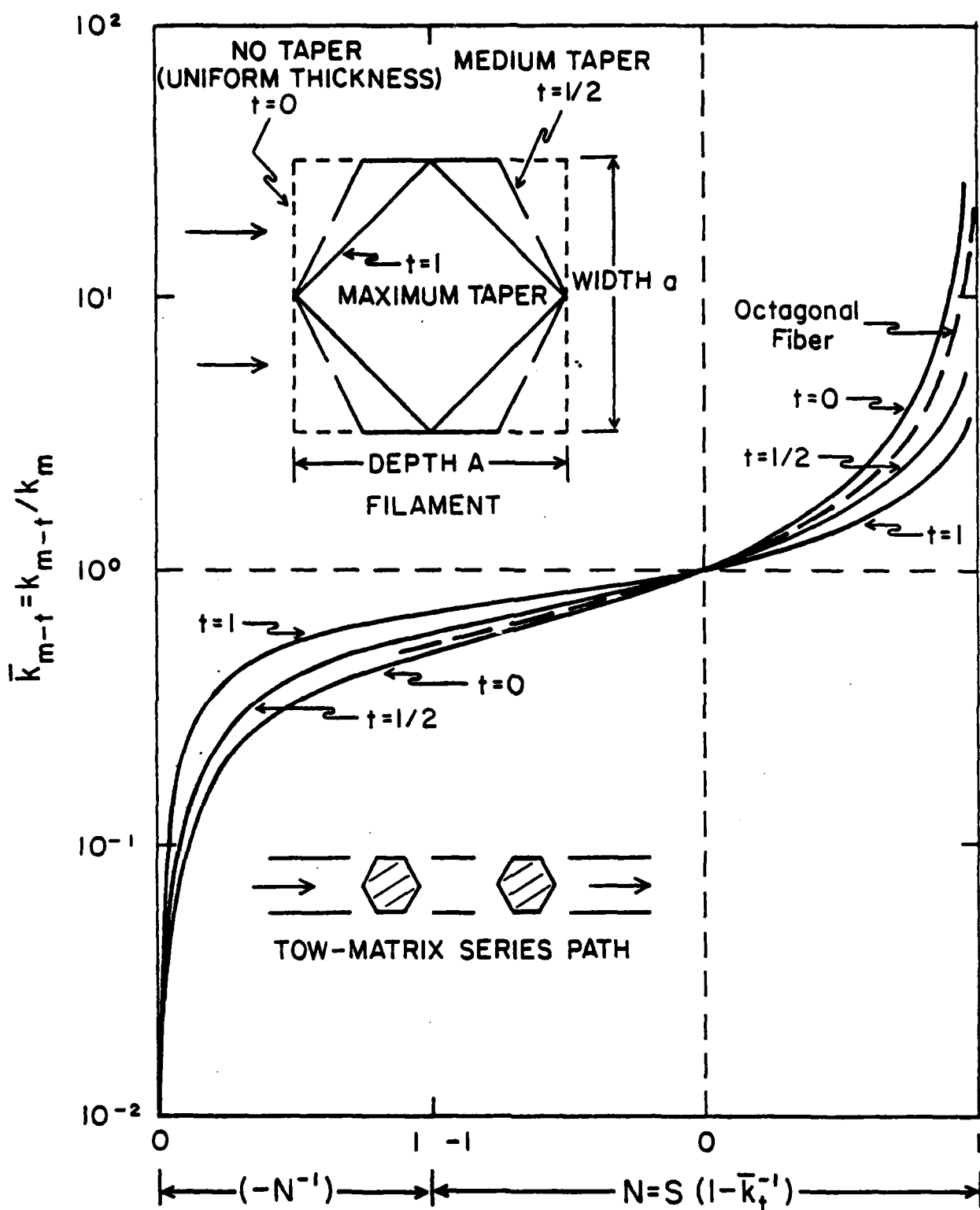


Figure B-4. Conductivities of the Tow-Matrix Series Path for Various Wedge Configurations.

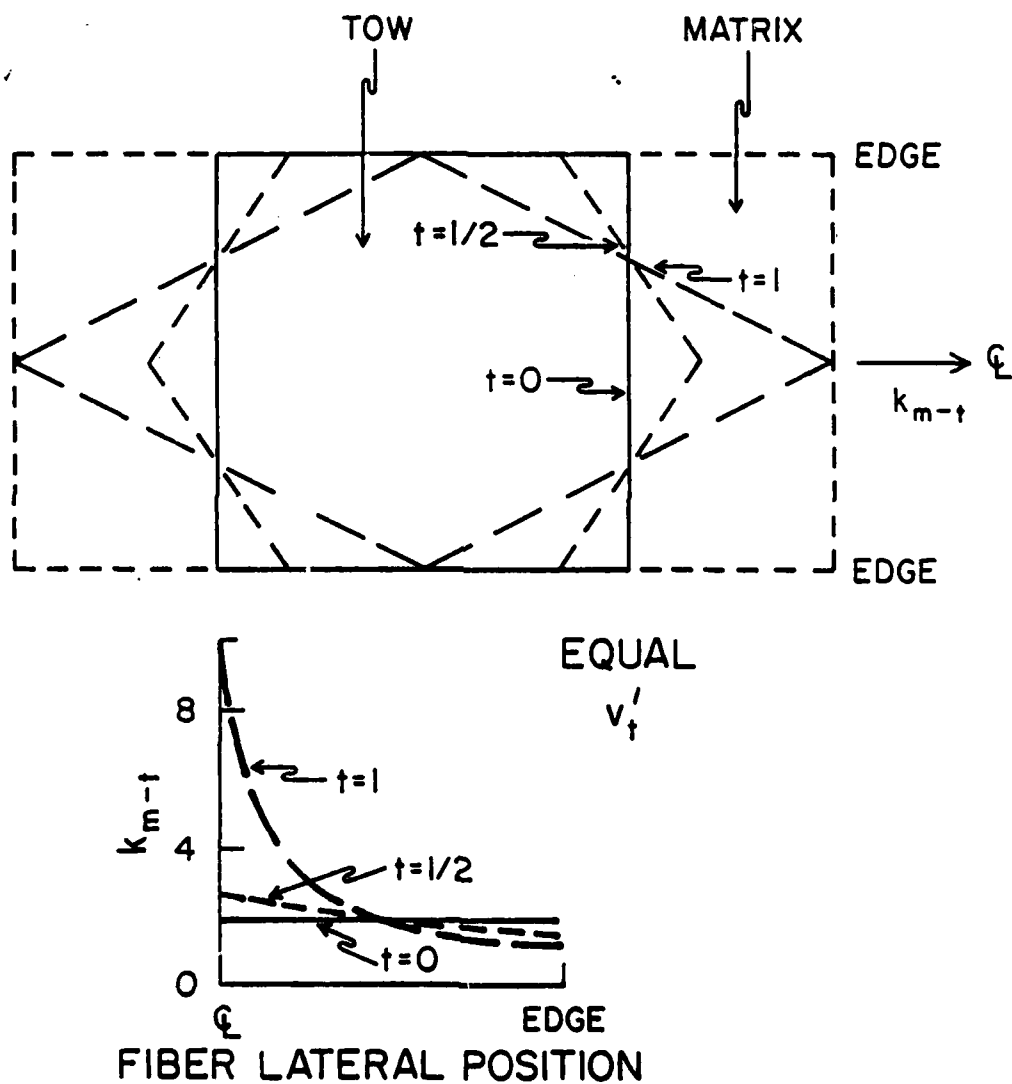


Figure B-5. Illustrating the Influence of the Wedge Taper on the Tow-Matrix Series Conductivity for Equal Tow Volume Ratio  $v_t'$ .



### 3. Octagonal Fibers.

Equation (B-12) applied to an octagonal fiber yields

$$\bar{k}_{m-t} = \int_0^{\sqrt{2}-1} (1-N_t)^{-1} dY + \int_{\sqrt{2}-1}^1 [1-N_t(\sqrt{2}-Y)]^{-1} dY \quad (B-19)$$

$$\bar{k}_{m-t} = (\sqrt{2}-1)(1-N_t) + (N_t)^{-1} \ln \left\{ [1-(\sqrt{2}-1)N_t]/(1-N_t) \right\} \quad (B-20)$$

where for this type filament

$$v_t = F_A sS = 0.8284 sS \quad (B-21)$$

As shown in Figure B-4, this type filament produces series conductivity levels midway between those for a tow of uniform thickness ( $t=0$ ) and the hexagonal shape ( $t = 1/2$ ).

### 4. Circular Fibers.

For a fiber circular in cross-section

$$X^2 + Y^2 = 1$$

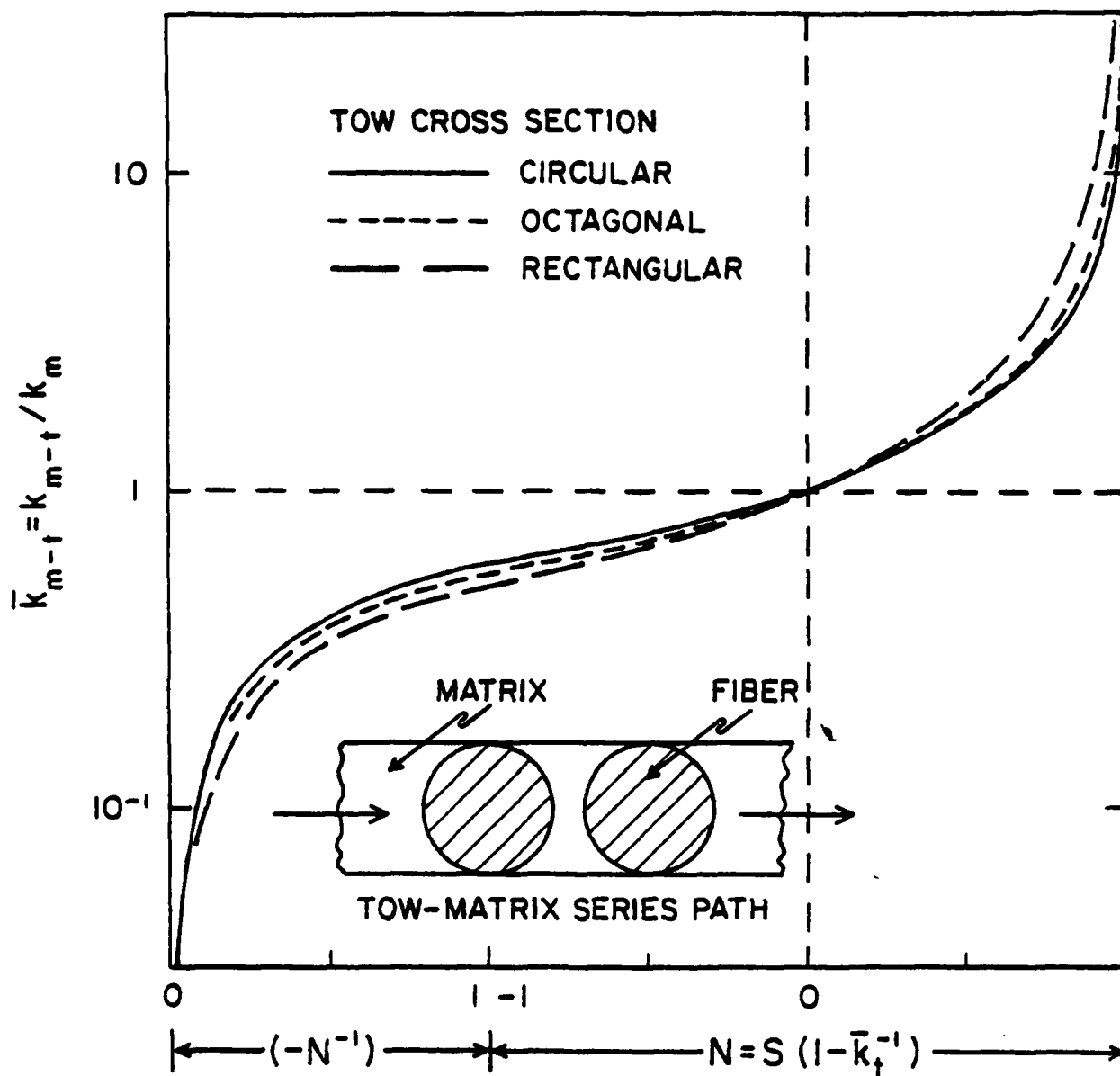
and, therefore, equation (B-12) for  $N \geq -1$  becomes

$$N \bar{k}_{m-t} + \pi/2 = \left(2/\sqrt{1-N^2}\right) \tan^{-1} \left[ (1+N)/\sqrt{1-N^2} \right] \quad (B-22)$$

and for  $N \leq -1$

$$N \bar{k}_{m-t} + \pi/2 = (N^2-1)^{-1/2} \ln \left[ (\sqrt{N^2-1} - N-1)/(\sqrt{N^2-1} + N+1) \right] \quad (B-23)$$

where  $N = MS$ ,  $M = 1 + \bar{k}_{t-1}^{-1}$ ,  $S = A/C$  and  $v_t' = (\pi/4)S$ . The transverse conductivity for this tow-matrix series path is compared in Figure B-6 with the corresponding conductivities for octagonal and rectangular fibers. For a given value of the parameter  $N$  (fixed by  $\bar{k}_t$  and  $v_t'$ ), the series conductivity for the circular fiber departs less from the matrix conductivity than for the octagonal and rectangular fibers. The circular fiber creates less change in the resistance of the series path.



However, more realistically, if the comparison is made on the basis of the same tow volume ratio  $v'_t$  for the series path, then the conductivities for these three fiber shapes are much more nearly alike. Suppose, for example, the rectangular and octagonal fibers have both of their linear dimensions adjusted in proportional amounts to yield the same value of  $v'_t$  as for the circular fiber. Then, by equations (B-21) and (B-9)

$$(\pi/4)^{1/2} (S_{\text{cir}}) = (0.8284)^{1/2} S_{\text{oct}} = S_{\text{rec}} = v'_t$$

Thus, the equivalent depth spacing ratio  $S$  for the rectangular fiber, octagonal fiber and truncated-wedge fiber are:

$$S_{\text{rec-eq}} = 0.886 S_{\text{cir}} \quad (\text{B-24})$$

$$S_{\text{oct-eq}} = 0.974 S_{\text{cir}} \quad (\text{B-25})$$

$$S_{\text{wedge-eq}} (t = 2/3) = 1.085 S_{\text{cir}} \quad (\text{B-26})$$

To illustrate, let the tow-to-matrix conductivity ratio  $\bar{k}_t = k_t/k_m = 50$  and the depth spacing ratio  $S = 0.80$  (the minimum thickness of the matrix gap between fibers being  $1/5$  of the fiber center-to-center distance) for each of these four fiber configurations. For each fiber,  $N = 0.8 (1 - 50^{-1}) = 0.784$ , and by equations (B-17), (B-22), (B-20) and (B-13), the series path conductivities are:

	<u>Wedge (<math>t = 2/3</math>)</u>	<u>Circular</u>	<u>Octagonal</u>	<u>Rectangular</u>
$S$	0.8	0.8	0.8	0.8
$\bar{k}_{m-t}$	2.44	3.08	3.37	4.63

However, using the equivalent spacing ratio  $S_{\text{eq}}$  (assuming a two-dimensional) adjustment, then  $N_{\text{eq}} = (1 - 50^{-1}) S_{\text{eq}}$  and:

	<u>Wedge (<math>t = 2/3</math>)</u>	<u>Circular</u>	<u>Octagonal</u>	<u>Rectangular</u>
$S_{\text{eq}}$	0.868	0.8	0.764	0.709
$\bar{k}_{m-t}$	2.91	3.08	3.14	3.27

Thus, on the basis of equal tow volume ratio, the effect of fiber shape on the series conductivity is not pronounced.

#### The Parameter N

For a given fiber sectional shape and a given packing orientation, the conductivity of tow and matrix elements in series is a function of the parameter  $N \equiv MS$  where  $M \equiv 1 - \bar{k}_t^{-1}$  and  $S$  is the ratio of the maximum fiber thickness to the fiber spacing distance --- the depth spacing ratio in the direction of conduction. It indexes the change in the conduction resistance when tow replaces a portion of the matrix.

With reference to Figure B-1, since

$$R = R_m + R_t$$

and since

$$R_m \propto (C-2x)/k_m$$

$$R_t \propto 2x/k_m$$

$$R_{m\text{-only}} \propto C/k_m$$

it follows that when tow replaces a portion of the matrix in a path of length  $C$ , the fractional change in the matrix resistance is

$$\Delta R/R_{m\text{-only}} = [(2x/k_t) + (C-2x)/k_m - C/k_m]/(C/k_m)$$

$$\Delta R/R_{m\text{-only}} = -(2kx/C)(1 - \bar{k}_t^{-1}) = -N$$

Thus, at a particular lateral position  $y$ , the parameter  $N$  indexes resistance change.

The following several examples illustrate the approximate relative change in the thermal resistance of a tow-matrix series path when  $S = 0.8$  for a circular fiber and  $S = 0.88 \times 0.8 = 0.709$  for a rectangular fiber ( $v'_t = \frac{\pi}{4} \times 0.8^2 = 0.709^2 = 0.503$  for both series paths).

Tow-Matrix System					
	<u>Graphite- Epoxy</u>	<u>Glass- Epoxy</u>	<u>Kevlar- Epoxy</u>	<u>Boron- Alumina</u>	<u>Alumina- Aluminum</u>
Representative Tow-to-Matrix Conductivity Ratio $\bar{k}_t$	200	5	1/5	1/10	1/25
Parameter N (Circular)	0.796	0.64	-3.2	-7.2	-19.2
Parameter N (Rectangular)	0.705	0.567	-2.84	-6.38	17.0
$(R_{t-m}/R_m)$ (Rectangular)	0.295	0.433	3.84	7.38	18.0
$(R_{t-m}/R_m)$ (Circular)	0.313	0.465	3.30	6.01	13.9
$(k_{m-t}/k_m)$ (Circular)	3.2	2.2	0.30	0.17	0.072
$(k_{m-t}/k_t)$ (Circular)	0.016	0.43	1.5	1.7	1.8

For this mid-range volume fraction of tow ( $v_t^* = 0.5$ ), the graphite-epoxy system has a series path resistance of roughly one third the epoxy alone, while glass fibers in epoxy reduce the series resistance to roughly one half of the epoxy alone. Kevlar fibers in epoxy, boron fibers in aluminum and alumina fibers in aluminum create series resistances appreciably above that of the matrix alone.

As illustrated by these examples, the series conductivity is always much closer to the lowest component conductivity. For example, with graphite epoxy and  $v_t' = 0.5$ , the series path  $k_{m-t}$ , though three times that of the matrix only, is less than two per cent of the tow conductivity. Contrariwise, for alumina/aluminum with  $v_t' = 0.5$ ,  $k_{m-t}$  is nearly twice the conductivity of the alumina fibers but only

1/14 of the conductivity of the aluminum matrix.....illustrating, thereby, the dominating influence of the high-resistance component in the series path.

#### Representative Values of the Series Conductivities

Representative values of the series conductivity  $k_{m-t}$  for a tow-matrix series element are summarized in Figure B-7 for a range of tow types, for both resin and metal matrices and for a range on the tow volume fraction  $v'_t$ . The series conductivity of the tow-matrix element ranges from roughly 1/5 to approximately 7 times the conductivity of a resinous base and from about 1/50 to 4 times the conductivity of metal bases.

The anisotropic features of this tow-matrix element are summarized in Figure B-8. The ratio of the bulk transverse to the bulk longitudinal conductivity for this tow-matrix element is shown for representative ranges on tow volume fraction and tow-matrix material combinations. The series conductivity  $k_{m-t}$  is much less than the parallel conductivity for many tow-matrix systems. The ratio of the parallel-path to the series path conductivity lies in the approximate ranges: 0.01 - 0.1 for graphite/resin systems, 0.2 - 0.5 for ceramic/resin combinations, 0.3 - 0.6 for aramid/resin, 0.04 - 1.0 for metal/metal and 0.7 - 1.0 for graphite/metal tow-matrix combinations.

#### Radical Influence of Thin Layers

A conventional composite material consisting of high-conductivity fibers (graphite for example) closely packed in a low-conductivity matrix (epoxy for example) has, nevertheless, quite a low transverse conductivity. Or, a hybrid composite having a thin layer of resin matrix along side a metal-matrix composite can have a drastically reduced transverse conductivity. The explanation lies in the radical effect of a thin layer of low-conductivity material on the overall conductivity of a tow-matrix series path.

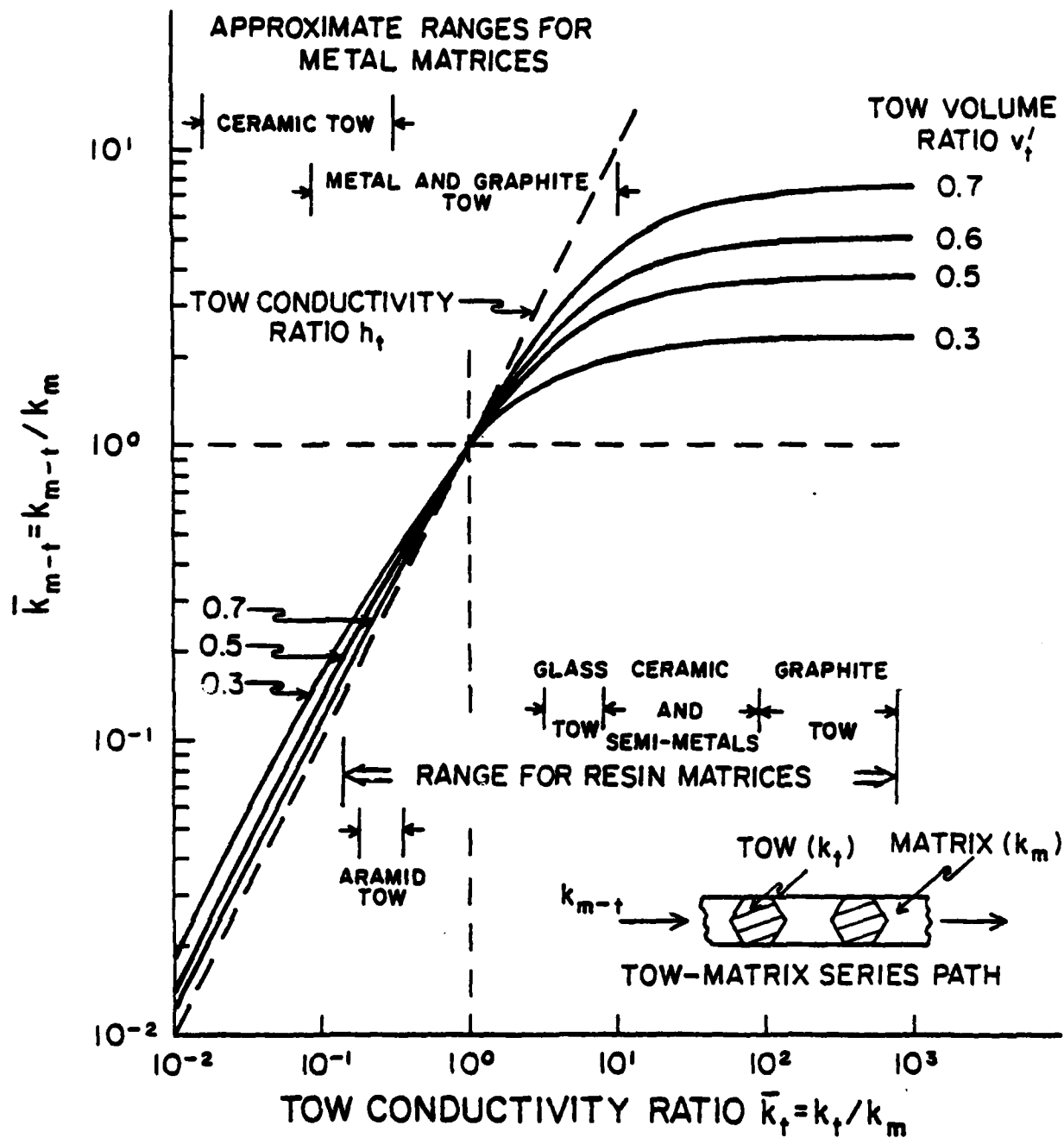


Figure B-7. Representative Values of the Conductivity for A Tow-Matrix Series Path. Isotropic Tow.

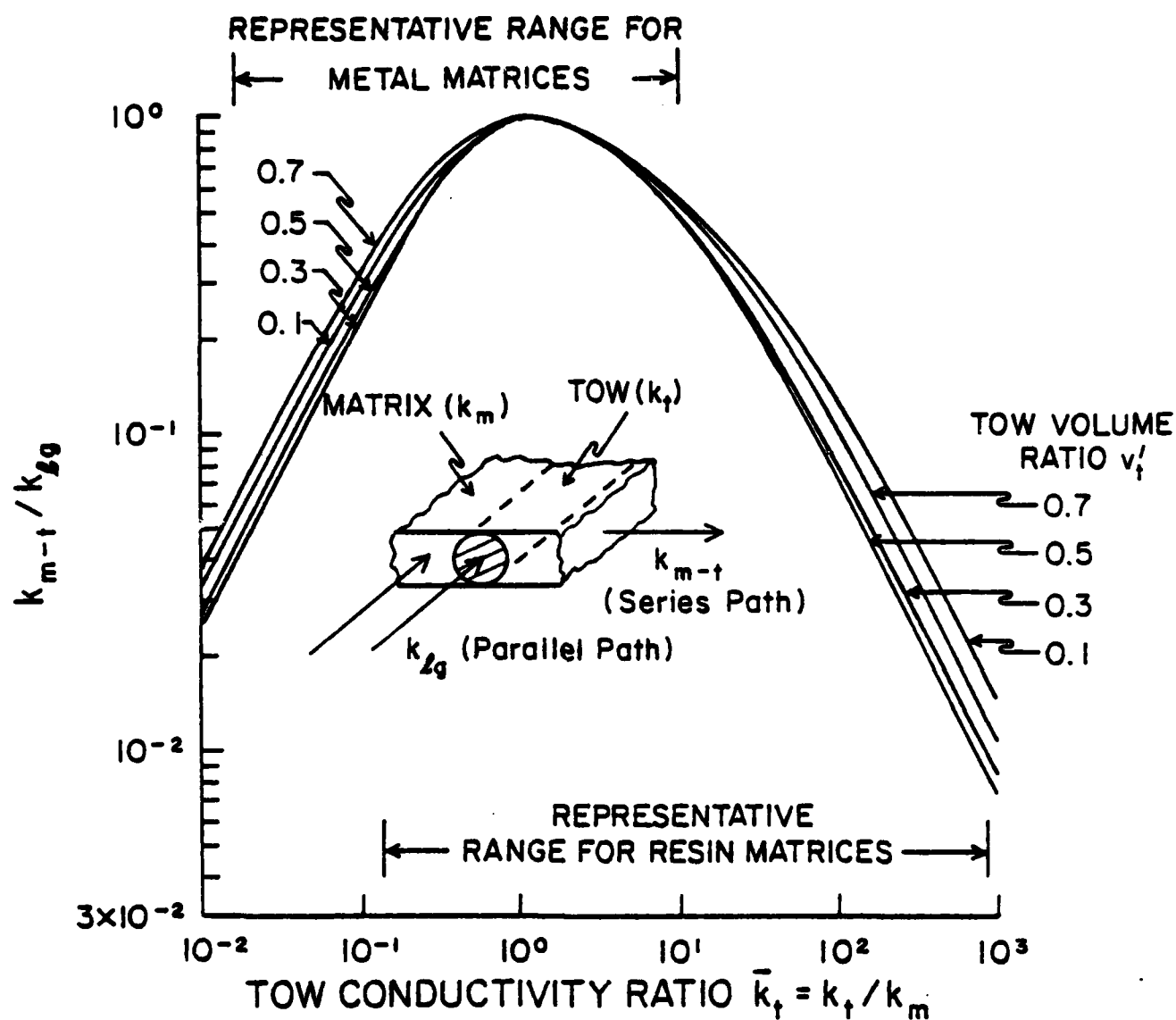


Figure B-8. Illustrating the Anisotropic Conductivity Characteristics of the Tow-Matrix Element. Ratio of the Series Tow-Matrix Conductivity to the Parallel Tow-Matrix Conductivity.



The approximate analysis of the series path showed that the series tow-matrix conductivity is proportional to  $(1-N)^{-1}$  (B-13).

$$\bar{k}_{m-t} = k_{m-t}/k_m \doteq (1-N)^{-1}$$

Therefore

$$dk_{m-t}/k_m = (1-N)^{-2} dN = (1-N)^{-2} M dS \quad (B-27)$$

For a very thin layer of matrix,  $S \doteq 1$  and

$$(1-N)^{-2} M \doteq (1-M)^{-2} M = \bar{k}_t(\bar{k}_t - 1) \doteq \bar{k}_t^2$$

Thus

$$dk_{m-t}/k_t \doteq \bar{k}_t dS \quad (B-28)$$

Suppose, for example,  $\bar{k}_t \doteq 500$  (representative of aluminum in contact with a thin layer of epoxy, or graphite with a thin layer of epoxy).

Therefore,

$$\Delta k_{m-t}/k_t \doteq 500 \Delta S$$

If  $S$  is 0.9999,  $\Delta S = 10^{-4}$  and  $\Delta k_{m-t}/k_t \doteq 0.05$ . A layer of epoxy with  $\Delta S = 10^{-4}$  along side the high conductivity material ( $S = 0.9999$ )

lowers the transverse conductivity  $k_{m-t}$  by 5 per cent. With  $S$  lowered to 0.999,  $k_{m-t}$  falls to two thirds that of the graphite or aluminum.

For a very thin layer of tow along side a matrix,  $S \doteq 0$ , and by equation (B 27)

$$d k_{m-t}/k_m \doteq M dS \quad (B-29)$$

Consequently, a layer of alumina of thickness  $10^{-3}$  times the thickness of an aluminum layer would lower the transverse conductivity by 3 to 5 per cent (below that for aluminum). Or, an aramid material in epoxy of thickness one per cent of the epoxy would produce a comparable reduction.

## REFERENCES

1. Han, L.S. and Cosner, A.A. (1980). Conduction Heat Transfer Analysis in Composite Materials. AFAWL-TR-80-3012.
2. Sendeckyj, G.P. (1974). In "Mechanics of Composite Materials, Volume 2" (G.P. Sendeckyj, ed.), Chapter 3. Academic Press, New York.
3. Hashin, Z. (1970). In "Mechanics of Composite Materials" Pergamon, New York. (F.W. Wendt, H. Leibowitz, and N. Perrone, eds.), pp. 201-242.
4. Nomura, S. and Chou, T.W. (1980). J. Compos. Mater. **14**, 120.
5. i. Beran, M.J. (1965). Il Nuovo Cimento **38**, 771.  
ii. Miller, M.N. (1969). J. Math. Phys. **10**, 1988.
6. Beran, M.J. and Silnutzer, N.R. (1971). J. Compos. Mater. **5**, 240.
7. Elsayed, M.A. and McCoy, J.J. (1973). J. Compos. Mater. **7**, 400.
8. Hale, D.K. (1976). J. Mater. Sci. **11**, 2105.
9. i. Donea, J. (1972). J. Compos. Mater. **6**, 262.  
ii. Elrod, H.G. (1974). J. Heat Transfer **96**, C-1, 05.
10. Rayleigh, Lord (1892). Phil. Mag. **34**, 481.
11. Kerner, E.H. (1956). Proc. Phys. Soc. (London) **B69**, 802.
12. Halpin, J.C. and Tsai, S.W. (1967). Environmental Factors in Composite Materials Design. AFML-TR-67-423.
13. Hermans, J.J. (1967). Proc. Kon. Ned. Akad. Wetensch. Amsterdam **B70**, 1.
14. Hill, R. (1964). J. Mech. Phys. Solids **12**, 199.
15. Behrens, E. (1968). J. Compos. Mater. **2**, 2.
16. Nielsen, L.E. (1974). Ind. Eng. Chem., Fundam. **13**, 17.
17. Chow, T.S. (1980). J. Mater. Sci. **15**, 1873.

#### REFERENCES (Concluded)

18. Springer, G.S. and Tsai, S.W. (1967). J. Compos. Mater. **1**, 166.
19. Zinsmeister, G.E. and Purohit, K.S. (1970). J. Compos. Mater. **4**, 278.
20. Meredith, R.E. and Tobias, C.W. (1960). J. App. Physics **31**, 1270.
21. Foye, R.L. (1966). In "Proceedings of the Tenth National SAMPE Symposium - Advanced Fibrous Reinforced Composites." Vol 10, pp. G-31.
22. Adams, D.F. and Doner, D.R. (1967). J. Compos. Mater. **1**, 152.
23. Tsao, G.T.N. (1961). Ind. Eng. Chem. **53**, 395.
24. Guess, T.R. and Butler, B.L. (1975). Composite Reliability, ASTM STP 580, pp. 229.
25. Halpin, J.C. and Thomas, R.L. (1968). J. Compos. Mater. **2**, 284.

**DATE**  
**ILME**